Universidade do Minho
Escola de Engenharia

Sara Filipa Fontoura Vieira

# Fish sarcoplasmic proteins as biomaterial for biomedical applications

Dissertação de Mestrado

Ciclo de Estudos Integrados Conducentes ao Grau de Mestre em Engenharia Biomédica

Ramo Biomateriais, Reabilitação e Biomecânica

Trabalho efetuado sob a orientação do(s)

**Professor Nuno João Meleiro Alves das Neves**

E co-orientação do

**Doutor Albino Manuel Pereira Martins**

Dezembro de 2016

DECLARAÇÃO

Nome:

Sara Filipa Fontoura Vieira

Endereço eletrónico: saravieira_7@hotmail.com Telefone: 936206565/278713851

Número do Bilhete de Identidade: 144016057

Título da dissertação:

Fish sarcoplasmic proteins as biomaterial for biomedical applications

Orientador:

Professor Nuno João Meleiro Alves das Neves

Co-Orientador:

Doutor Albino Manuel Pereira Martins

Ano de conclusão: 2016

Designação do Mestrado: Ciclo de Estudos Integrados Conducentes ao Grau de Mestre em Engenharia Biomédica

Área de Especialização: Biomateriais, Reabilitação e Biomecânica

Escola de Engenharia

Departamento de Engenharia de Polímeros



Universidade do Minho, ____/____/_____

Assinatura:_____

Effort and hard work construct the bridge
that connects your dreams to reality.

Daisaku Ikeda

## Agradecimentos

Durante este ano muitas pessoas se cruzaram no meu caminho e contribuíram para o progresso da minha tese. Estou profundamente grata a algumas pessoas, que, de certo modo, me guiaram e fizeram parte desta etapa.

Em primeiro lugar, quero agradecer ao meu orientar, Professor Nuno Neves, por me ter concedido a oportunidade de desenvolver este trabalho. Por me ter despertado o espírito crítico no mundo da investigação. Pelo entusiasmo e força que sempre me transmitiu. Por elevar sempre a fasquia em cada desafio que me propunha. Todos estes pequenos detalhes fizeram com que eu crescesse.

Quero agradecer ao meu co-orientador, Albino Martins, por todo o conhecimento transmitido, pelo apoio, e, acima de tudo, pela amizade. Por me ter ensinado a ter paciência e a não desistir à primeira queda. Pelo tempo que dedicou ao meu trabalho e por me ter apresentado o fascinante mundo das células.

Aos meus co-autores, por terem sempre disponibilidade para partilhar conhecimento comigo.

À Iva Pashkuleva e à Ana Carvalho, pelo contributo que deram ao meu trabalho. Pela empatia e pelo sorriso sempre presente na cara cada vez que precisei da ajuda delas.

Aos meus colegas de laboratório, com os quais partilhei grandes gargalhadas e momentos felizes.

À Daniela, que esteve sempre comigo, que deu sempre um apoio especial e disse as palavras certas no momento certo.

Ao Tiago, que sempre esteve disposto a ouvir os meus desabafos.

Aos meus pais e ao meu irmão, que me proporcionaram esta jornada. Que nunca faltaram com nada. Que sempre deram os melhores conselhos. Que nunca me deixaram ir a baixo. Que sempre me ensinaram a lutar pelas coisas. Sem eles, isto seria impossível.

A todos eles, um grande obrigada do fundo do coração!

## Resumo

Em 2014, a captura de peixes e a aquacultura forneceram aproximadamente 167 milhões de toneladas de peixe, das quais 87% foram para consumo humano e 10% destinado a farinhas e óleos de peixes. Os restantes 3% são considerados desperdício, que podem ser utilizados como alimento direto na aquacultura. As proteínas sarcoplasmáticas de peixe são solúveis em água, pelo que grandes quantidades são descartadas juntamente com a água desperdiçada durante a preparação das delícias do mar. As proteínas sarcoplasmáticas constituem cerca de 25-30% das proteínas totais do músculo. Estas proteínas são compostas por proteínas heme e enzimas, que estão associadas com a produção de energia no músculo.

Assim, as proteínas sarcoplasmáticas do bacalhau (*Gadus morhua*) foram isoladas, dando origem a extratos de proteínas sarcoplasmáticas. Tanto os extratos como as membranas foram caracterizados física e quimicamente e a sua citocompatibilidade foi avaliada com fibroblastos do pulmão humano (linha celular MRC-5). Pelo SDS-GE foi possível definir a composição dos extratos das proteínas sarcoplasmáticas. Pelo termograma da calorimetria diferencial de varrimento (DSC) foi possível definir que os extratos desnaturam a 44.12 ± 2.34˚C. Pela dicroísmo circular (CD) verificou-se que a estrutura secundária dos extratos era composta maioritariamente por estruturas α-hélices. Os extratos não apresentaram citotoxicidade para concentrações inferiores a 10 mg/mL durante 72h de cultura. Neste sentido, os extratos foram processados em membranas por spin coating. As membranas compostas por proteínas sarcoplasmáticas foram analisadas através de microscopia eletrónica de varrimento, verificando-se que a superfície era uniforme. Pela análise do espectro de CD, notou-se um aumento na quantidade de estruturas α-hélices. As membranas foram mais estáveis que os extratos, uma vez que temperatura de desnaturação foi superior, como determinado pelo DSC. As membranas foram hidrofóbicas, com uma carga de superfície de -33.4 mV. Por outro lado, apresentaram propriedades mecânicas distintivas, com uma rigidez de 16.57 ± 3.95 MPa e uma tensão de cedência de 23.85 ± 5.97 MPa. Os fibroblastos de pulmão humano cultivados em contacto direto com as membranas demostraram citocompatibilidade até 48h. Com base nestes resultados, as proteínas sarcoplasmáticas de peixe, constituídas maioritariamente por enzimas, podem ser consideradas um potencial biomaterial recuperado das águas residuais dos peixes, com um potencial de interesse para cicatrização de feridas.



**PALAVRAS-CHAVE:** bacalhau, proteínas sarcoplasmáticas, extração, caracterização físico-química, spin coater, membranas.

## ABSTRACT

In 2014, fish captures and aquaculture supplied ca. 167 million tonnes of fish, of which about 87% were used for human food and 10% was destined for fishmeal and fish oil. The remain 3% is waste that can be used as raw material for direct feeding in aquaculture. Fish sarcoplasmic proteins (FSP) are soluble in water. Large quantities of those proteins are discarded as part of the waste water resulting from fish surimi preparation. FSP constitutes around 25-30% of the total fish muscle protein. FSP comprise heme proteins and enzymes, which are associated with the energy-producing metabolism of the muscle.

Herein, FSP from codfish (*Gadus morhua*) were isolated, resulting in FSP extracts. Both FSP extracts and membranes were physicochemically characterized and their cytocompatibility with human lung fibroblasts (MRC-5 cell line) was also evaluated. By SDS-PAGE, it was possible to define the composition of FSP extracts. From the differential scanning calorimetry (DSC) thermograms, it was possible to define that FSP denature at 44.12 ± 2.34˚C. By circular dichroism (CD) spectroscopy, it was possible to defined that the secondary structure of FSP is mainly composed by α-helix structures. For concentrations lower than 10 mg/mL, no cytotoxicity was observed over 72h of culture. Further on, the FSP extracts were processed into FSP membranes by the spin coating.

FSP membranes shown an uniform surface when analyzed by scanning electron microscopy. By CD spectrum, it was verified an increase in the amount of α-helix structures. The FSP membranes were more stable than the FSP extracts, since the denaturation temperature was higher as determined by DSC. FSP membranes were hydrophobic, with a surface zeta potential of -33.4 mV, showing distinctive mechanical properties, with a stiffness of 16.57 ± 3.95 MPa and a yield strength of 23.85 ± 5.97 MPa. Human fibroblasts cultured in direct contact with FSP membranes demonstrate their cytocompatibility until 48h. Based on these results, FSP can be considered a potential biomaterial recovered from the waste water of fish, constituting a pool of enzymes that has potential interest for wound healing applications.



**KEYWORDS:** codfish, sarcoplasmic proteins, extraction, physico-chemical characterization, spin coater, membranes.

## TABLE OF CONTENTS

## LIST OF FIGURES

## LIST OF TABLES

## LIST OF ABBREVIATIONS

**A**

Ala-Trp - alanine-tryptophan

APS – ammonium persulfate

ATPase – adenosine triphosphatase

**B**

BSA – bovine serum albumin

**C**

$\theta$ – contact angle

Caco-2 – human colon epithelial cells

CD – circular dichroism

Cl – chlorine

CRP – C-reactive protein

CRT – cathode ray tube

**D**

$\Delta H$ – denaturation enthalpy

DMEM – Dulbecco's modified eagle's medium

DTT – dithiothreito

DTG – derivate of the TG curve

DSC – differential scanning calorimetry

**E**

$\epsilon$ – Elongation

$E$ – elastic modulus or Young's Modulus

EDL – electric double layer

EDS – energy dispersive X-ray spectroscopy

**F**

$F$ – Force

$f$ – fracture

$\sigma_f$ – fracture strength

FAO – food and agriculture organization

FBS – fetal bovine serum

FSP – fish sarcoplasmic proteins

FTIR – Fourier transform infrared spectroscopy

**G**

G-250 – G-Greenish

GAPDH – glyceraldehyde-3-phospate dehydrogenase

**H**

$\Delta Cp$ – heat capacity differences

HeLa – human cervix epithelial cells

HFIP – 1,1,1,3,3,3-Hexafluoro-2-propanol

**I**

$L_o$ – initial gauge length

IR – infrared

**K**

K – potassium

**M**

MPs – myofibrillar proteins

MRC-5 – human lung fibroblasts

MTS – 3-(4,5-dimethylthiazol-2-yl)-5-(3-carboxymethoxyphenyl)-2-(4-sulfophenyl)-2H-tetrazolium

**N**

N – Newton

NADase – adenine dinucleotidase

NCXs – nanocomplexes

**P**

P – phosphorous

Pa - Pascal

PAGE – Polyacrylamide gel electrophoresis

PBS – phosphate buffer solution

PES - phenazine ethyl sulfate

PMS – phenazine methyl sulfate

PUFAs – polyunsaturated fatty acids

**R**

R-250 – R-reddish

**S**

$\sigma$ – stress

$\varepsilon$ – strain

$\varepsilon_f$ – strain-to-failure

S – sulfur

SDS – sodium dodecyl sulfate

SDS-PAGE – sodium dodecyl sulfate polyacrylamide gel electrophoresis

SEM – scanning electron microscopy

SH – sulfhydryl

SPs – sarcoplasmic proteins

**T**

3D – three-dimensional

$\Delta L$ – total amount of stretch

TEER – transepithelial electrical resistance

TEMED – tetramethylethylenediamine

TG – thermogravimetry

TGA – thermogravimetric analysis

TGase – transglutaminase

TMAO – trimethylamine oxide

TCPS – tissue culture polystyrene

**U**

$u$ – ultimate point

$\varepsilon_u$ – ultimate strain

$\sigma_u$ – ultimate strength

U2OS – human bone epithelial cells

**Y**

$y$ – yield point

$\varepsilon_y$ – yield strain

$\sigma_y$ – yield strength

# CHAPTER 1

Introduction

## 1.1 FISHING IN THE WORLD

The ocean is a vast and rich repository of natural resources. Seafood occurs in various forms (fish, shellfish and seaweed) and is used as food for human beings, once it is a rich source of nutrients [1]. The main seafood consumed daily by human is fish, which is also the main source of protein from the sea. Fish are the most diverse group of vertebrates, with over 32000 different species [1]. Fish are aquatic vertebrates, grouped in marine pelagic, marine demersal, diadromous and fresh water. The pelagic fish lives near to the surface water column of the sea; demersal fish live at the bottom of the sea; diadromous fish are fish which migrate between the sea and fresh water; and fresh water fish live in rivers, lakes and ponds.

The growth in the supply of fish for human consumption has outpaced the population growth in the past five decades, increasing at an average annual rate of 3.2 % in the period 1961– 2013 (double of the population growth) (Figure 1.1) [2]. According to the Food and Agriculture Organization (FAO), in 2014, capture fisheries and aquaculture supplied about 167 million tonnes of fish, of which about 146 million tonnes were used as food for people [2]. The remaining 21 million tonnes is destined for non-food products, where 76% was reduced to fishmeal and fish oil, and the rest being largely used for a variety of purposes, including as raw material for direct feeding in aquaculture. This reduces the fish-derived waste.

Fish consumption (Kg) *per capita* in some European countries and its forecast to 2025 is represented in Table 1.1. The countries whose consumption was less than 20 Kg/ *capita* were not presented in the Table 1.1, which are Austria, Bulgaria, Czech Republic, Estonia, Germany,

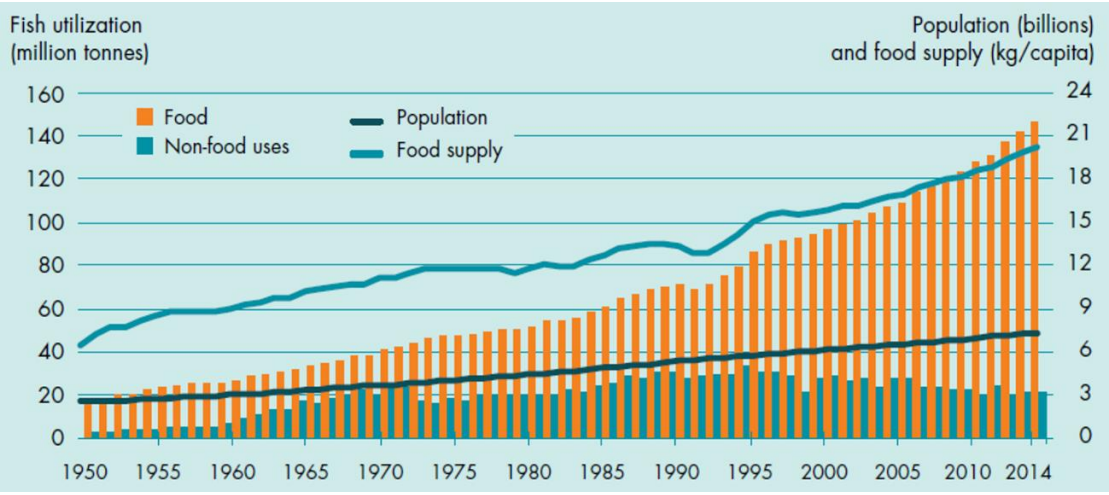


**Figure 1.1 –** World fish use and supply. Adopted from [2].

**Table 1.1 –** Fish consumption (Kg) *per capita* for some European countries from 2010 to 2025. Adopted from [3].

| Eropean country | 2010 | 2015 | 2020 | 2025 |
|---|---|---|---|---|
| Belgium-Luxembourg | 22 | 23 | 23 | 23 |
| Cyprus | 24 | 24 | 23 | 23 |
| Denmark | 25 | 26 | 27 | 28 |
| Finland | 35 | 35 | 36 | 36 |
| France | 32 | 32 | 32 | 33 |
| Greece | 26 | 26 | 27 | 27 |
| Ireland | 21 | 21 | 21 | 21 |
| Italy | 25 | 26 | 27 | 28 |
| Latvia | 37 | 38 | 38 | 38 |
| Malta | 31 | 32 | 33 | 34 |
| Norway | 45 | 45 | 45 | 45 |
| Portugal | 59 | 59 | 58 | 58 |
| Spain | 39 | 39 | 39 | 39 |
| Sweden | 28 | 27 | 27 | 27 |
| United Kingdom | 24 | 25 | 25 | 25 |

Hungary, Lithuania, Netherlands, Poland, Romania, Slovakia, and Slovenia. Portugal is the European country with higher fish consumption, despite a slight decrease compared to previous years [3].

## 1.2 HEALTH BENEFITS OF FISH CONSUMPTION

Fish has long been recognized as a health promoting food. In 2013, fish accounted for about 6.7% of all protein consumed, 17% of the world population's intake when considering animal protein [2]. Fish is easily digested and has an excellent nutritional value. The nutritional composition of some fishes is shown in Table 1.2. Fish provides high quality proteins containing all essential amino acids, unsaturated essential fats (e.g. long-chain omega-3 fatty acids), vitamins (D, A and B) and minerals (including calcium, iodine, zinc, phosphorous, magnesium, iron and selenium), particularly if eaten whole. Specifically, omega 3 long-chain polyunsaturated fatty acids have a role in the prevention and modulation of certain diseases, providing health benefits [4, 5]. They are involved in the prevention of cardiovascular diseases (e.g. restenosis, and cardiac arrhythmias) and decreases hypertension (high blood pressure); they help in fetal and infant central nervous system development and visual acuity, reduce tendency to have aggression behavior and depression; and they act against inflammatory and auto-immune disorders (e.g. rheumatoid arthritis, psoriasis, ulcerative colitis and asthma).

**Table 1.2 -** Compositional data of fish fillet from different species. Adapted from [6].

| Components \ Fish species | **Sea bass** | **Atlantic cod** | **Pacific cod** | **Cusk** | **Eel** | **White halibut** | **Mackerel** | **Monkfish** | **Red fish** | **Yellowfin tuna** | **Salmon** |
|---|---|---|---|---|---|---|---|---|---|---|---|
| | *Morone saxiatilis* | *Gadus morhua* | *Gadus macrocephalus* | *Brosme brosme* | *Anguilla anguilla* | *Hippoglossus hippoglossus* | *Scomber scombrus* | *Lophius piscatorius* | *Sebastes marinus* | *Thunnus albacares* | *Salmo salar* |
| Moisture (g/100 g) | 79 | 81 | 81 | 76 | 68 | 78 | 64 | 83 | 79 | 71 | 59 |
| Raw protein (g/100 g) | 18 | 18 | 18 | 19 | 18 | 21 | 19 | 15 | 19 | 23 | 20 |
| Total lipids (g/100 g) | 2 | 0.5 | 0.4 | 0.7 | 12 | 2.3 | 14 | 1.5 | 1.6 | 15 | 6 |
| Calcium (mg/100 g) | 15 | 16 | 7 | 10 | 20 | 3 | 12 | 8 | 107 | 16 | 12 |
| Magnesium (mg/100 g) | 40 | 32 | 24 | 31 | 20 | 26 | 76 | 21 | 30 | 50 | 29 |
| Phosphorous (mg/100 g) | 198 | 203 | 174 | 204 | 216 | 164 | 217 | 200 | 216 | 191 | 200 |
| Potassium (ng/100 g) | 256 | 413 | 403 | 392 | 272 | 268 | 314 | 400 | 273 | 444 | 490 |
| Sodium (mg/100 g) | 69 | 54 | 71 | 31 | 51 | 80 | 90 | 18 | 75 | 37 | 44 |
| Zinc (mg/100 g) | 0.4 | 0.5 | 0.4 | 0.3 | 1.6 | 0.4 | 0.6 | 0.3 | 0.5 | 0.52 | 0.69 |
| Copper (mg/100 g) | 0.03 | 0.03 | 0.03 | 0.02 | 0.02 | 0.03 | 0.07 | 0.03 | 0.03 | 0.06 | 0.3 |
| Manganese (mg/100 g) | 0.12 | 0.02 | 0.01 | 0.02 | 0.04 | 0.01 | 0.02 | 0.02 | 0.02 | 0.02 | 0.02 |
| Selenium (mg/100 g) | 375 | 32 | 37 | 37 | 7 | 37 | 44 | 36 | 43 | 36 | 37 |
| Iodine (mg/100 g) | | 187 | | | | 74 | 109 | 27 | 70 | | 45 |
| Eicosapentaenoic acid (g/100 g) | 0.169 | 0.064 | 0.08 | Total PUFA | 0.084 | 0.526 | 0.898 | Total PUFA | 0.08 | 0.037 | 0.32 |
| Docosahexaenoic acid (g/100 g) | 0.585 | 0.12 | 0.135 | 0.28 | 0.063 | 0.393 | 1.401 | 0.61 | 0.211 | 0.181 | 1.12 |
| Cholesterol (mg/100 g) | 80 | 39 | 37 | 41 | 51 | 42 | 33 | 33 | 42 | 45 | 26 |

Evidences suggest that the benefits of fish consumption are not limited to the well-appreciated effects of omega-3 fatty acids [7]. Proteins, peptides and amino acids, together with vitamins, are bioactive constituents that may also be important on disease prevention by controlling circulating levels of cholesterol, lipoproteins and triglycerides, increasing endogenous antioxidants and lowering blood pressure. In particular, specific amino acids could be implicated in reducing inflammation.

Fish proteins are associated with a risk reduction of type 2 diabetes, namely by the regulation of insulin sensitivity and glucose homeostasis [8]. The consumption of cod proteins improves insulin sensitivity [9] and reduces the circulation levels of C-reactive protein (CRP) [10, 11], in insulin-resistant men and women. Dietary cod proteins, when compared with casein and soy protein, fully prevented the development of skeletal muscle insulin resistance [12]. The effect of dietary cod protein allows normalizing the activation status of the PI3-kinase/Akt pathway, coupled to an increased translocation of GLUT4 to the T-tubules in obese rats [13].

Dietary cod protein also suppresses the non-esterified fatty acid and triacylglycerol contents in serum, and decreases the hepatic triacylglycerol and fatty acid desaturase indices [14]. The high non-esterified fatty acid content in blood is associated with a risk factor for developing type-2 diabetes. Fish protein, when compared with casein, was reported to lower blood pressure and allows lowering liver cholesterol and phospholipid concentrations [15-17]. It was also demonstrated a beneficial metabolic effect of cod-scallop in diet, namely in aorta atherosclerosis, body weight, visceral adipose tissue, serum glucose and leptin levels, reduction [18]. Dort *et al.* (2012) also demonstrated that cod protein, when compared with casein, reduces inflammation, and promotes skeletal muscle mass and myofiber recovery during the regeneration process, following muscle injury in rats [19].

## 1.3 STRUCTURE OF FISH MUSCLE

Muscle from aquatic beings shares many properties and general structural features with muscles from terrestrial animals [20]. As all vertebrates, fish muscle can be divided into three basic types: skeletal, smooth and cardiac [21]. Skeletal muscles compose the major component of fish muscle and, being voluntary, fish use them to move their bones and fins. Smooth muscles are involuntary and linked to the operation of internal organs, such as stomach and intestines. Heart muscle is also known as cardiac muscle. A fish fillet (or fish flesh) is the largest lateral

skeletal muscle present in both sides of the body, from the head to the tail, which is normally white [20, 22]. The subcutaneous muscles, localized along the lateral line, are red or dark muscles, as represented in Figure 1.2.

White and red muscle can be differentiated according to its chemical composition, physiological importance and nutritional value [6]. While the white muscle gives energy from anaerobic glycolysis for rapid and sudden movements, the red muscle is used for continuous swimming motion. This type of muscle is supplied with blood and rich in myoglobin – which gives the color – and the energy provided from lipids and carbohydrates. Most of the species have more abundant white than red muscle. Compared to the white muscle, the red muscle contains more mitochondria and less sarcoplasmic reticulum, and also comprises larger concentrations of lipid, B vitamin, glycogen, and nucleic acids [20]. Red muscle is richer in enzymes involved in carbohydrates and the enzymes of the tricarboxylic acid cycle, pentose phosphate shunt, electron transport, glycogen synthesis and liposis. On the other hand, white muscle possesses higher contents of adenosine triphosphatase (ATPase) activity, glycolytic acids, and water.

A white fish muscle, illustrated in Figure 1.3, is composed by myocommata (or myosepta), which is a thin connective tissue membrane, that divides the fish muscles into segments called myotomes (or myomers) [20, 22]. In the cross section, the myocommata between the myotomes curves in a complex manner (Figure 1.3).

The structural components of fish muscle are illustrated in Figure 1.4. Each myotome is composed of muscle fibers parallel to the long axis of the fish [20, 22]. All the components of a cell and 1000 - 2000 elongated bundles of myofibrils make a muscle fiber. These muscle fibers have a diameter ranging from 0.02 - 1 mm and a length of 20 mm. Each fiber is surrounded by a

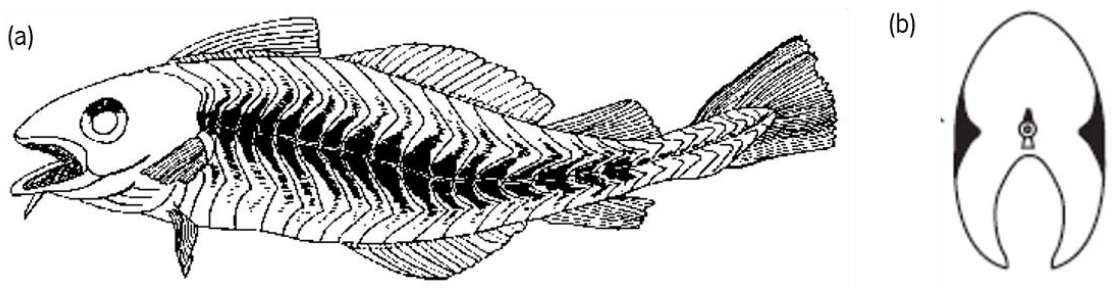


**Figure 1.2 –** Muscle of codfish with skin removed (a) and a cross section (b) to show dark muscle. Adapted from [23].

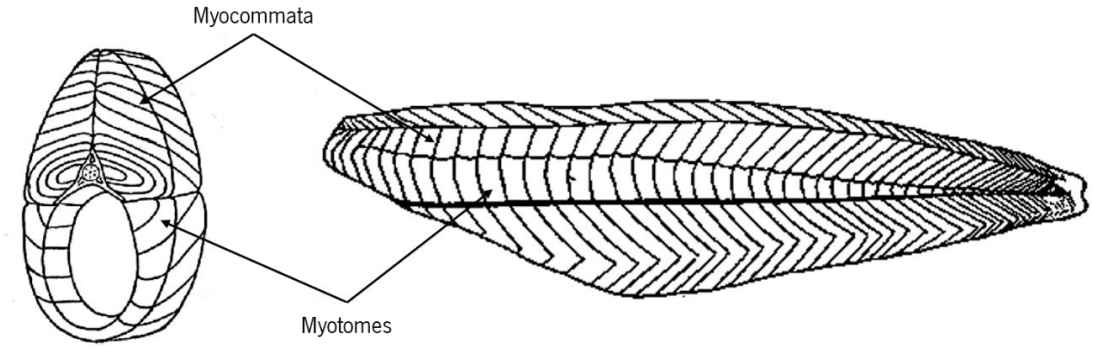


**Figure 1.3 -** Fish muscle division into myotomes and myocommata. Adapted from [22, 24].

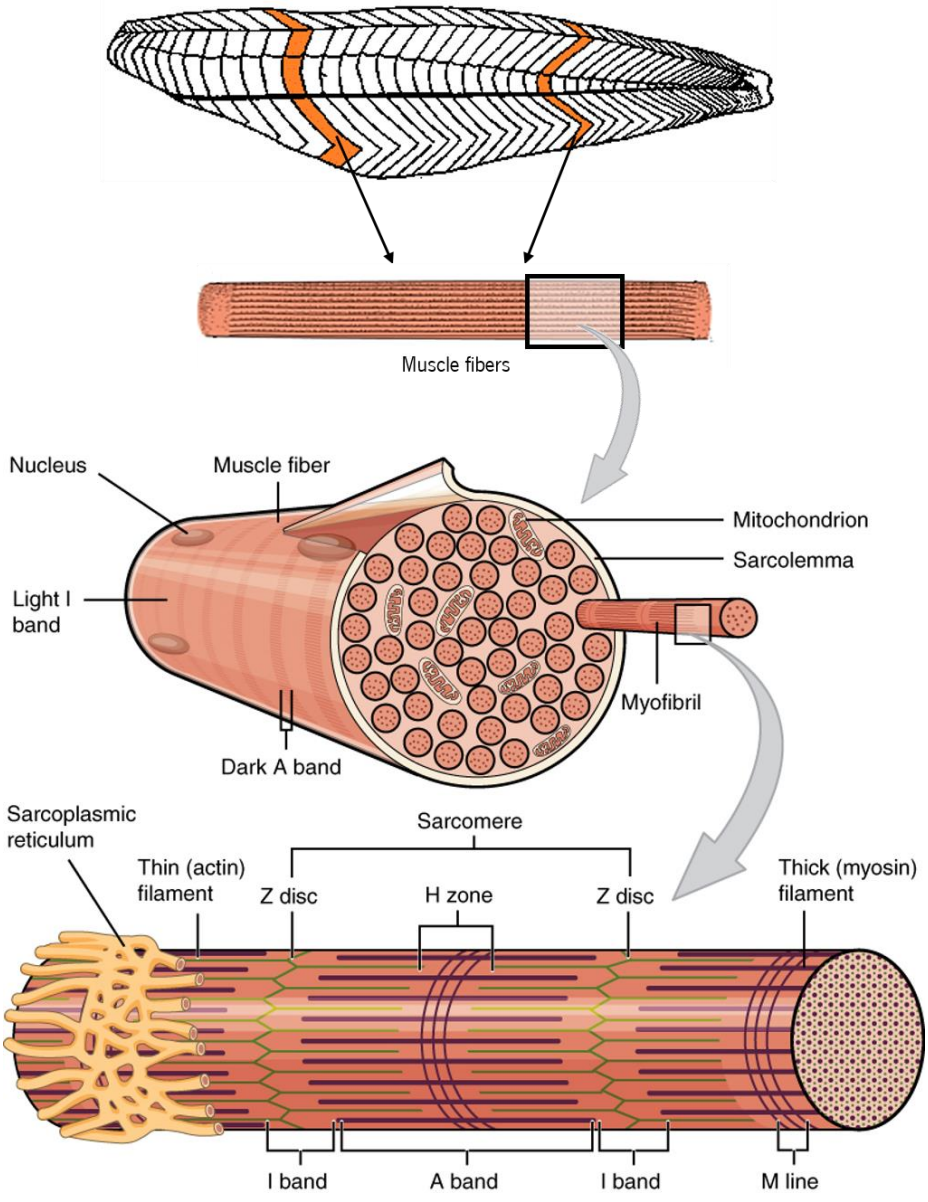


**Figure 1.4 -** Structure of fish muscle. Adapted from [20, 23, 25, 26].

membrane named sarcolemma, which contains thin collagenous fibrils. The junction between the fine fibrils and myocommata originates the myotome-myocommata junction. The myofibrils are segmented into sarcomeres and the space between myofibrils is filled by sarcoplasmic proteins [23]. A sarcomere is composed of thin and thick filaments, showing alternate arrangements of anisotropic (A) and isotropic (I) bands bordered by Z-lines. The thick filaments are composed of myosin molecules and the thin filaments consist of double helical strings of actin. During muscle contraction, this filaments overlap and slide over one another. The thick filaments of a vertebrate contain 200-400 molecules of myosin. Tropomyosin and troponin, which are thin filaments, are others proteins involved in the contractile mechanism.

## 1.4 COMPOSITION OF FISH MUSCLE

Water, proteins and lipids are the main chemical components of fish, which comprises about 98% of the total mass of the flesh. The other components with a minor percentage, such as vitamins, carbohydrates and minerals, have an important role in biochemical process of live fish. Among all nutrients, the protein content is high in many different types of fish.

### 1.4.1 Water

The principal component of the edible portions of fish is water (up to 80%). The average percentage of moisture in raw edible flesh varies between 74.3% and 82.8% [20].

### 1.4.2 Nonprotein nitrogenous constituents

The nonprotein nitrogen content of fish muscle is mainly composed by free amino acids, small peptides, trimethylamine oxide (TMAO) and its degradation products (i.e. urea, triethylamine, creatine, creatinine), and adenosine nucleotides [6, 20, 25]. Glycine, taurine, alanine and lysine amino acids are generally present in relatively higher amounts. TMAO, a water soluble nitrogenous compound [27], is the most important of the amines in marine fish, because when reduced it contributes to fishy odors.

### 1.4.3 Lipids

Lipids in fatty fish are mostly localized subcutaneously, while in lean fish they are deposited in the liver, muscle tissue and in mature gonads [20]. Fish lipids have a high content of long-chain,

highly unsaturated fatty acids of the *n*- 3 series (eicosapentaenoic acid 20:5 and docosahexaenoic acid 22:6), normally named as polyunsaturated fatty acids (PUFAs) [6]. The amounts of lipids in fish may vary from 0.2% to 23.7%, depending of fish characteristics [20].

### 1.4.4 Vitamins

The vitamin content in fish varies according to its specie [6]. The liver of fish is a rich source of fat-soluble vitamins, such as vitamin A, D, E and K. Thiamine, riboflavin, and niacin (water-soluble vitamins) are present in relatively large amounts in the fishes' muscle. B vitamins are also present.

### 1.4.5 Minerals

Fishes are good sources of several minerals, including macroelements (i.e. sodium, potassium, magnesium, calcium, iron, phosphorus) and microelements (i.e. iodine, fluorine, selenium, manganese, cobalt). Indeed, fish is the predominantly source of selenium and iodine [6]. All these minerals are important in human nutrition [20].

### 1.4.6 Fish muscle proteins

The muscles contain several classes of proteins which perform different functions in an aquatic organism. The amount of protein from different fishes depends on several factors, such as specie, nutritional state, stage of the reproductive cycle and specific properties of the different parts from an organism [25]. All proteins in a fish are composed by chains of chemical units – amino acids – linked together to make a long molecule (polypeptide) [21, 23]. This polypeptides chains are normally folded upon itself to constitute the secondary (internal structural features), tertiary (gross shape of the unit or subunits), and quaternary (presence of subunits) structures of the native protein [27]. Denaturation occurs when the long amino acids' chain, that comprises the protein, experiences an unfolding state, exposing the other regions of a protein. This can lead to protein–protein interactions, termed "aggregation," which under proper conditions was result in the formation of a gel.

The proteins of fish muscle are rich in amino acids, that have a high biological value [6], and can be divided into three major classes, based on their solubility in aqueous solutions in connective tissue (stroma) proteins, myofibrillar proteins or sarcoplasmic proteins [20, 23]. Solubility of fish muscle protein is also affected by the pH [28]. The selective solubility of proteins

according to pH and salt concentration is a fundamental step to recover the different proteins from minced fish muscle.

#### 1.4.6.1 Connective tissue (stroma) proteins

The stroma proteins, also called connective-tissue proteins, constitute only 3% of the total protein content, being completely water insoluble [20, 21, 29, 30]. The connective tissues are responsible for the integrity of the fish fillet. Collagen is the major protein of connective tissues [27, 31]. Collagen can be also found in fish skin. The connective tissue proteins consist not only of collagen, but also of elastin and other denatured muscle proteins. Collagen fibrils can be found in the membrane that encloses each muscle fiber (called endomysium) and the membrane that surrounds the muscle bundles (called perimysium) [23, 31]. Collagenous microfilaments are observed in the junction between the muscle fibers and the connective tissue sheets, which connect the collagen fibers of the myocommata with the basal lamina and the sarcolemma in the invagination near to the base of the muscle fiber. The contents of fish collagens vary according to the specie, anatomic location, age, season and nutritional status.

#### 1.4.6.2 Myofibrillar proteins

The myofibrillar proteins (MPs) constitute approximately 70 - 80% of the total amount of protein and are related with muscle contraction [30, 32]. MPs are composed by structural proteins (myosin and actin (F and G types)) and regulatory proteins (tropomyosin, troponin and actinin) [20, 23]. Myosin comprises 50 - 58% of the myofibrillar proteins and the actin constitutes about 20%. MPs are soluble in the presence of neutral salt solutions (ionic strengths 0.3 to 0.6) [20, 23]. Within this ionic strength, the thick filaments depolymerize (and other minor proteins constituents solubilize as well) and the sarcomeres disassembly [27]. However, myofibrillar proteins are water insoluble in typical physiological ionic strength of the fish muscle [23].

The thermal stability of seafood myofibrillar protein, namely the heat-induced denaturation, is also affected by the pH and the ionic strength. Extreme pH and high temperature cause protein denaturation resulting in lower solubility.

The myosin molecule (Figure 1.5) consists of two heavy chains (200 and 240 kDa) associated noncovalently with two pairs of light chains (16 to 28 kDa). The myosin molecule is comprised of two globular heads (2 nm x 160 nm) attached to a tail (19 nm). The myosin heavy chain (globular protein) is 60% α-helix and 15% β-sheet structure [27]. Fish myosins possess ATPase activity regulated by the presence of $Ca^{2+}$ and $Mg^{2+}$ [32]. Compared with meat, fish myosins

are more unstable, and, consequently, more sensitive to denaturation, coagulation, degradation or chemical changes, resulting in changes in the overall physical properties of the muscle tissues. However, the instability of myosin varies among each fish' specie.

Actin (Figure 1.5) is a globular monomer (G-actin) with a molecular weight of 43 kDa [27]. The G-actin has the property of being polymerized in the presence of neutral salts forming the filamentous actin, commonly referred as fibrous actin (F-actin). Tropomyosin (with 68 kDa) and troponin regulate muscle contraction. Myosin and actin, under specific conditions, are able to develop a gel-like texture [33]. MPs have highly reactive surfaces once the protein is unfolded, which then interact to form intermolecular bonds. Thereafter, a three-dimensional gel network is formed, when a sufficient number of bonds exists [27].

#### 1.4.6.3 Sarcoplasmic proteins

Sarcoplasmic proteins (SPs) are proteins of the sarcoplasm, components of the extracellular fluid and proteins contained in small particles of the sarcoplasm [20]. SPs are soluble in water or in low ionic strength solutions, and constitute around 25-30% of the total fish muscle protein, depending on the specie considered [20, 23, 29, 30]. Since they are completely soluble in water, they can be isolated from fish muscle by simply pressing the fish muscle tissue or by extraction with a low ionic strength saline solution [34]. Although the SPs are soluble in water, they easily lose solubility when heated [35]. The SPs have a very low capacity of absorbe water in their

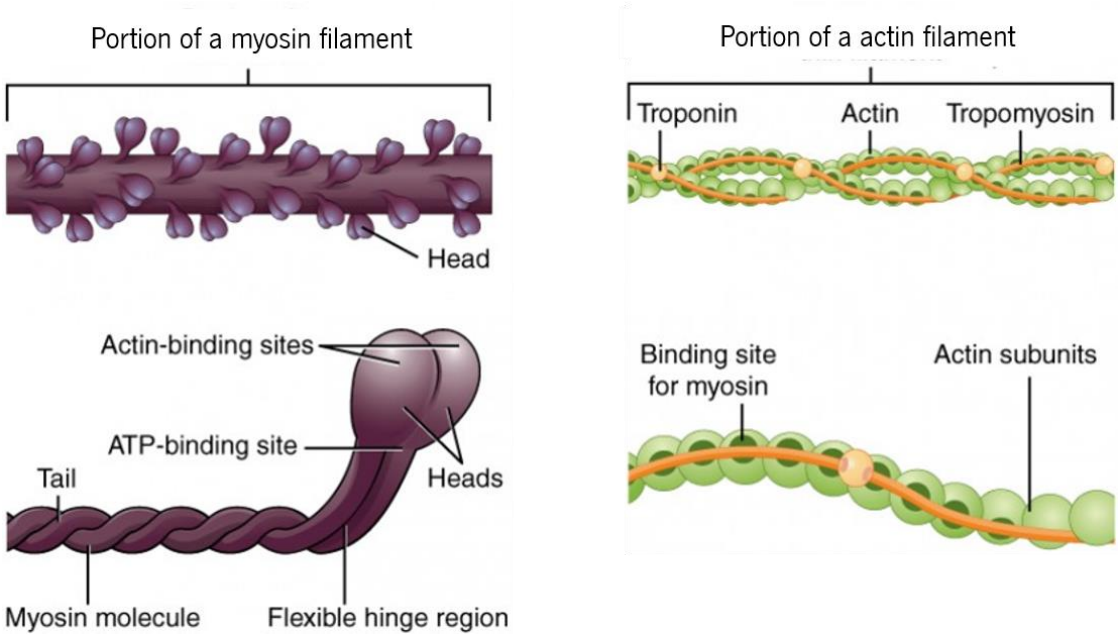


**Figure 1.5 –** Myosin and actin molecule. Adapted from [26].

structure [22]. SPs have relatively low molecular weights, globular- or rod-like conformations, and low viscosity [36]. SPs comprise several types of proteins, including heme proteins and enzymes, which are associated with the energy-producing metabolism of the muscle, such as the glycolysis (i.e. the anaerobic energy conversion from glycose to ATP), the citrate cycle and the oxidative phosphorylation [37]. These proteins can be used to identify different fish species, when separated by electrophoresis [38].

The heme proteins that comprise the SPs are responsible for the pigmentation, i.e. for the color characteristics of fish muscle [20, 29]. Hemoglobin (66.5 kDa) and myoglobin (18 kDa) are the heme (iron-containing) proteins from the blood and the red muscle cells, respectively [27]. These proteins contain 0.30% to 0.35% of the iron present in the heme prosthetic group [20, 29]. Hemoglobins are composed by four chains of two different types of polypeptides, whereas the myoglobin contains only one type of polypeptide chain. The heme proteins influences postharvest color change and lipid oxidation [27, 29]. This protein fraction also contains several compounds that are involved in physiological events such as respiration, intracellular digestion, cell growth, cell division and secondary metabolism [29] (e.g. catalyze the degradation of nitrogenous compounds) [20].

SPs also include hydrolytic enzymes (i.e. proteinases, peptidases, lipases, phospholipases and glycogen hydrolases), oxidoreductase enzymes (i.e. polyphenol oxidase, lipoxygenases, peroxidase, catalase, superoxide dismutase, lactic dehydrogenase, oactate dehydrogenase, glyceraldehyde-3-phospate dehydrogenase (GAPDH), glutamate dehydrogenase and uricase) and other enzymes such as transferases, transaminases, phosphorylases, phosphofructokinase, transglutaminase (TGase), glutathione S-transferase, enolase, carnosinase, arginase, nicotinamide adenine dinucleotidase (NADase), ATPase, adenosine deaminase, trimethylamine demethylase and thiaminase [20, 29]. Proteinases comprise cathepsins, alkaline proteases, collagenase, pepsins, trypsin and chymotrypsin and lipolytic enzymes such as lipases and phospholipases.

Calcium-binding proteins, namely parvalbumins and calmodulins, are present in significant amount in fish sarcoplasmic proteins, representing 20–30% of the sarcoplasmic fraction, which have the same function as the troponin and tropomyosin complex [20, 29]. Parvalbumins are proteolytic enzymes, heat-stable, water-soluble, acidic and with a low molecular weight around 12 kDa. They are associated with fast nerve impulse-activated skeletal muscle. It should be noted that fish from Arctic and Antarctic waters also have antifreezing proteins in their blood, that lower the freezing temperature with no significant effect on its osmotic pressure [20, 29].

## 1.5 PHYSICOCHEMICAL PROPERTIES OF FISH SARCOPLASMIC PROTEINS

Nakagawa *et al.* (1988) reported that fish ordinary muscle was generally rich in three glycolytic enzymes, with molecular weight of 43 kDa, 40 kDa and 35 kDa [37], which were identified as creatine kinase, aldolase and GAPDH, respectively [38]. A phosphorylase was reported to have a molecular weight of 94 kDa [39]. Recently, two proteinase inhibitors, also glycolytic enzymes, with a molecular mass of 47 and 52 kDa were found in sarcoplasmic protein fraction from common carp (*Cyprinus carpio*) [40]. The presence in fish muscle of other enzymes such as cathepsin A and D, a sub-endopeptidase, a calcium-dependent cysteine proteinase known as calpain and its specific inhibitor, calpastatin, and even a trypsin inhibitor was reported by Toyohara *et al.* (1983) [41]. Jiang *et al.* (1990) reported milkfish muscle proteases A (15.6 kDa) and C (35.6 kDa) as cathepsin A and protease B, named trypsinlike enzyme, with a molecular weight of 33 kDa [42]. Soluble phospholipase, a lipolytic enzyme, has been isolated from Pollack muscle (*Pollachius sirens*) with a molecular weight of 13.7 kDa [43]. Three peroxidase from freshwater crayfish (*Genus orconectes*) were purified with molecular weights of 33 kDa, 76 kDa and 147 kDa [44]. TGase was described to have a molecular weight of 80 kDa in an isolate from carp [45]. Fructose-bisphosphate aldolase A (39.6 kDa), glycogen phosphorylase (97.2 kDa), beta-enolase (47.1 kDa), triosephosphate isomerase B (26.5 kDa), phosphoglucomutase (60.8 kDa) and phosphoglycerate kinase (44.1 kDa) are also involved in SPs fraction of Atlantic Mackerel (*Scomber scombrus*) [46]. Table 1.3 summarizes the proteins that comprise the SPs and their molecular weight (MW).

The native structure of SPs is strongly dependent on several chemical forces (i.e. hydrophobic, ionic, hydrogen and disulfide bonds). The conformational changes of SPs as a function of pH (2-12) were studied by Tadpitchayangkoon *et al.* (2010) [47]. According to a solubility study, the isoelectric point (pI) of striped catfish (*Pangasius hypophthalmus*) SPs was 5.0. Moreover, more than 1/3 of SPs are soluble at the pI while approximately 2/3 of SPs are insoluble. The authors noticed that the solubility increased gradually as the pH shifted away from the pI. The SPs distinctively exhibited molecular weights of 11, 13, 27, 31, 36, 38, 43, 50, 61 and 97 kDa. Typically, independently of the pH, the SPs bands of 11, 13, 27, 36, 43, 50 and 97 kDa appeared. At pH between 6 and 12, the detergent sodium dodecyl sulfate polyacrylamide gel electrophoresis (SDS-PAGE) patterns of SPs were similar. The most abundant sarcoplasmic protein of striped catfish had a molecular weight of 43 kDa, presumably creatine kinase, being less soluble at acidic pH. The proteins with molecular weight of 38 and 43 kDa are less soluble at extreme acid and

alkali pH, being soluble at pH 5-5.5. A protein with a molecular weight of 61 kDa disappeared at pH 2–4. Myoglobin (17kDa) was more soluble at pH 2–5.5 and was not extracted at pH 6–12. In short, SPs from striped catfish became more soluble through alkaline than acidic extraction. Total sulfhydryl (SH) content of SPs was higher at pH 6 and decreased when pH shifts away from 6, which indicated that thiol oxidation of SPs occurred during acidic (pH 2-4) and alkaline (pH 10-12) extraction. Alkaline extraction induced SPs unfolding by exposing the buried hydrophobic clusters, while acid extraction appeared to promote hydrophobic interactions of SPs, leading to lower hydrophobicity.

The patterns of differential scanning calorimetry and endothermic transition (i.e. protein denaturation) of SPs changed with pH. In the native state (at pH 7), SPs exhibited both major

**Table 1.3 -** Some SPs and respective molecular weights.

| **Proteins** | | **MW (kDa)** | **Reference** |
|---|---|---|---|
| Heme proteins | Myoglobin | 18 | [27] |
| | Hemoglobin | 66.5 | [27] |
| Enzymes | Peroxidase | 147, 76 and 33 | [44] |
| | Glycogen phosphorylase | 97.2 | [45] |
| | Phosphorylase | 94 | [39] |
| | TGase | 80 | [45] |
| | Phosphoglucomutase | 60.8 | [45] |
| | Proteinase inhibitors | 52 and 47 | [40] |
| | Beta-enolase | 47.1 | [45] |
| | Creatine kinase | 43 | [37, 38] |
| | Aldolase | 40 | [37, 38] |
| | Phosphoglycerate kinase | 44.1 | [45] |
| | Fructose-bisphosphate aldolase A | 39.6 | [45] |
| | Protease C | 35.6 | [42] |
| | GPDH | 35 | [37, 38] |
| | Protease B (trypsinlike) | 33 | [42] |
| | Triosephosphate isomerase B | 26.5 | [45] |
| | Protease A | 15.6 | [42] |
| | Phospholipase | 13.7 | [43] |
| | Parvalbumins | 12 | [20, 29] |

exothermic and endothermic peaks, with thermal denaturation at 67.7 and 85.8˚C. At extreme acidic pH (2-3), the proteins conformation was destroyed (complete unfolding), while in extreme alkaline pH some SPs were stable. Denaturation patterns of sarcoplasmic proteins at pH 5.5–8 were highly linked to protein aggregation and improved rheological properties, forming a viscoelastic gel network at T<59˚C. In contrast, negatively charged proteins at pH 10–12 were unlikely to aggregate and form an elastic gel network, due to strong intermolecular electrostatic repulsion, requiring higher temperatures to initiate the aggregation. At pH 7.0 the SPs had a predominant α-helix conformation, and did not shown major β-sheet conformation [48]. The α-helix was converted to a β-sheet conformation following an acidic extraction (pH 3); in contrast, with an alkaline treatment (pH 11), the secondary structure of SPs did not disrupt the α-helix conformation.

High-pressure processing is a technology for food preservation, which improves the food quality. The SPs have been associated as markers of product quality, in terms of color and water-holding [46]. Some studies demonstrated the influence of high pressure on the aggregation of SPs in fish products [46, 49, 50]. Villamonte *et al.* (2016) determined the effect of high pressure processing on the structure of SPs isolated from hake (*Merluccius merluccius*) [49]. The solubility of SPs decreases with pressure, indicating that proteins were denatured. After a treatment at 200 MPa, approximately 87% of the SPs were present in the soluble fraction. In contrast, with a treatment at 600 MPa, only 20% of SPs remained soluble. On the other hand, the turbidity of SPs increased after pressure treatment, proving the protein aggregation. The SPs from hake showed 12 major SDS-PAGE bands at 78, 73, 63, 48, 42, 37, 32, 30, 22, 19, 12 and 7 kDa. By increasing the pressure, the solubility of five proteins (with 78, 73, 63, 58, 37, 32, 22 and 12 kDa) was effected. The surface hydrophobicity of SPs increased with the pressure. Native SPs had a dominante α-helix conformation. When a pressure of 400 MPa is applied a conformational transition to β-sheet and β-turn is observed. The protein aggregation is associated with the disruption of α-helix structures and the formation of β-sheet structures. Another study also related the denaturation of sarcoplasmic protein from cod (*Gadus morhua*) muscle at 300 MPa [50].

Surimi gel is a concentrate of MPs, when subjected to a subsequent thermal treatment acquires the product name of kamaboko. Both are considered a viscoelastic gel system [27]. SPs may impact gel formation and texture properties of protein gels, although there was no absolute agreement on the role of SPs on the gelation of MPs. Some enzymes present in SPs, such as heat-stable proteinases, has an ability to cleave and weaker the protein structures, contributing

negatively on the gelation of myofibril proteins [27]. However, other enzymes such as TGase do promote protein crosslinking, which results in stronger gels.

Some authors defend that higher concentrations of MPs for making protein gels is preferred, since it improves gelation properties of fish protein gels [51-53]. Parker and Matak (2015) reported that SPs may disrupt the formation of a gel network made of MPs and interfere with TGase activity, an enzyme that enhances the formation of a gel network made of MPs [51]. Nakagawa *et al.* (1989) studied the effect of the remaining glycolytic enzymes on kamaboko gel strength, after washing the minced fish muscle with various concentrations of NaCl [52]. Independently of the fish specie and the storage period, the remaining enzymes decreased with the increase of NaCl concentration in the washing solution. The gel strength of red sea bream (*Pagrus major*) and Pacific mackerel (*Scomber japonicas*) became higher when decreased of the remaining enzymes (and the decrease of SPs), indicating that these enzymes interact with MPs, reducing the gel-forming ability of fish muscle [53]. However, the authors were aware of the involvement SPs in gelation and they suggested that this may be partly due to the fishes' species, and to the preparation method of kamaboko. Kudo *et al.* (1973) concluded that washing with cold water fish mince from different species an effective method to remove water-soluble proteins, resulting in a firmer gel compared with gels from unwashed minced fish [54].

Recent studies indicate that SPs contribute positively in the gelation of MPs, namely SPs from milkfish (*Chanos chanos*) [55], rockfish (*Sebastes flavidus*) [56] and carp (*Cyprinus carpio*) [57]. Benjakul *et al.* (2004) claimed that the sarcoplasmic fraction from bigeye snapper (*Priacanthus tayenus*) muscle had cross-linking activity toward myosin heavy chain [58]. The addition of small amounts of these proteins into the gel increases the denaturation temperature of myosin and actin, increasing the breaking force (strength of the gels) [56]. Jafarpour and Gorzyca (2009) verified that the addition of SPs also improved the breaking distance and textural quality of threadfin bream kamaboko gel [57]. These properties were directly proportional to the concentration of SPs. The whiteness of surimi decreased in 33% with the addition of 5% of SPs from carp (*Cyprinus carpio*). However, based on scanning electronic microscopy (SEM) micrographs, no specific physical interactions between the added SPs and the MPs were observed in the gel network. The authors reported nine proteins bands in freeze-dried SPs, with approximately 10, 23, 26, 27, 38, 43, 50, 60 and 90 KDa.

Hemung and Chin (2013) produced MPs gels and investigated the effects of SPs from red sea bream (*Pagrus major*) on the properties of these gels [59]. A reduction of shear stress upon

addition of SPs was observed. The authors suggested that the addition of these proteins into MPs resulted in the formation of more compact protein complexes, which might not be easily destructed by shearing force. However, fish SPs did not inhibit crosslinking of myofibrillar proteins. The analysis of protein content of the SPs solution resulted in 10 major bands, with molecular weights around 30-40 kDa. The interactions between the two groups of proteins resulted in an increased thermal stability of the gels. The breaking force of fish myofibrillar gel was not affected by the addition of lower concentrations of SPs, but higher SPs concentrations resulted in significantly decreased. A smoother structure was observed when SPs were added to the gel, which may be able to absorb more water into the structure.

Yongsawatdigul and Hemung (2010) denoted that the adjustment of pH near to the isoelectric point of SPs (pH 5) appeared to unfold the secondary structure of threadfin bream gels, due the destabilization of electrostatic and hydrophobic interactions [60]. Based on Fourier transform infrared spectroscopy (FTIR) spectrum, a decrease in β-structure occurred to a greater extent in acidic pH than in alkaline condition, which means that the gels were more prone to unfold at extreme acidic pH than alkaline condition. Most proteins in SPs probably unfolded at either pH 3 or 12. When pH was adjusted to 7, the proteins underwent refolding and aggregation, leading to a reduced protein solubility. The lyophilizing only reduced overall protein solubility, but did not affect the water extractability of individual components of SPs. SPs are hydrophobic when compared to other proteins. These proteins had a greater emulsifying property at pH 3 and 12. Other studies also reported the emulsifying properties of sarcoplasmic proteins [49, 61].

As SPs class consist of many individual proteins, the differences between published results can be related with differences in the composition of SPs. Based on this principle, Morioka *et al.* (1997) explored the effect of SPs with different composition on the gel strength of myofibrillar gel [62]. They reported that the high gel strength was related with the high amount of heat-coagulable proteins in SPs, namely the 94, 64 and 40 kDa components.

SPs are able to form a weak gel against stretching force but highly resistant to punching force. The puncture force and the jelly strength was highly correlated with the heat-coagulability of SP [63]. Proteins with molecular weights of 94, 55, 43, 40, 35, 26, 25 and 23 kDa are heat-coagulable compounds. A good correlation between these two properties was observed in components with high amount of 94 and 40 kDa. The relative amount of 26 kDa component also showed good correlation with the strength of SPs gel. Karthikeyan *et al.* (2004) fractionated the SPs from oil sardine (*Sardinella longiceps*) and studied the influence of their properties on the

gelation behavior of washed sardine meat [64]. It was found that SPs coagulated with the increase of temperature; for instance, at 40˚C nearly 9% of proteins were coagulated and 91% of proteins were in the supernatant. Each fraction had a different composition and thermal stability, suggesting that specific properties of each fraction influence their conformation. The authors also reported that interactions between fractions altered the usual properties and gel forming ability.

## 1.6 APPLICATIONS OF FISH SARCOPLASMIC PROTEINS

### 1.6.1 Fish muscle proteins as edible films

Over the last years, fish proteins have been proposed as biopolymer films to protect and preserve food, pharmaceuticals and other products, mainly due to their advantages over synthetic polymers, such as biodegradability and environmental characteristics. Cuq *et al.* (1995) demonstrated that MPs from Atlantic sardines (*Smdina pilchardus*) had the capacity to form transparent and resistant film [65]. These authors developed a series of studies on the production of edible films from fish MPs [66-69]. Several studies described the production of edible films based on MPs from different sources [70-73]. Generally, these films are stable when immersed in water for 24h, showing that the protein network is able to remain intact [71].

Only few studies with fish SPs demonstrated the film-forming potential due to the poor functional properties [74]. Iowata *et al.* (2000) and Tanaka *et al.* (2001) demonstrated that SPs from blue marlin (*Makaira mazara*), despite their low molecular weight, are also able to form flexible films [74, 75]. In these studies, glycerol was added to the SPs and the solution was heated at 70˚C during 15 minutes. The plasticizer improves the workability of the film, to reduce its brittleness [65]. When glycerol is incorporated into fish SPs films, direct interactions are more difficult due to the distance between protein chains, although the movements of protein chains are accelerated on fish sarcoplasmic proteins (FSP) films plasticized with glycerol [75]. The SPs are generally composed by globular proteins, which have to be thermally denatured to form a continuous matrix [74]. Heat modifies the 3D structure of the globular proteins, causing exposure of the SH groups. As a consequence, S-S bonds were generated between adjacent proteins, reducing the exposure of hydrophobic moieties during drying [76], causing the insolubility of the film due to the interaction of protein molecules [74]. SPs film without glycerol had tensile strength between 3 and 5.5 MPa, and elongation at break between 40 and 75% [75]. No differences were observed in the effect of SPs concentrations on the tensile strength of films. However, the elongation at break increased

with increasing FSP concentration. With the addition of glycerol, the tensile strength decreased and the elongation at break increased. Edible FSP films without plasticizer had slightly better water vapor barrier capacity [74]. This property is important to protect and preserve the food, since it acts as a gas barrier preventing e.g. oxidation.

As the SPs also have the capacity to form a continuous matrix, Paschoalick *et al.* (2003) hypothesized supposed that edible films can be produced by a mixture of SPs with MPs. This premise avoid the washing process of the muscles [77]. The presence of SPs caused little alterations on the functional properties of edible films. However, the color, the opacity, the water vapor permeability, and the mechanical and viscoelastic properties were in the order same of magnitude of those based on the MPs of Nile Tilapia (*Oreochromis niloticus*). Other studies also reported the development of homogeneous, colorless, resistant and workable films by casting technique of myofibrillar and sarcoplasmic fraction from Thai and Nile Tilapia muscle [73, 78, 79].

### 1.6.2 Fish muscle proteins as eco-friendly material

The possibility to substitute petroleum-derived synthetic polymers, which cause severe environmental pollution and toxicity, and degrade slowly under environmental conditions, is highly appealing. Recently, Sett *et al.* (2016) proposed a mixture of FSP from codfish (*Gadus morhua*) with nylon 6 as a substitute of traditional synthetic polymers [80]. The authors produce nanofibers with different ratios of FSP/nylon 6, using solution blowing. According to energy dispersive X-ray spectroscopy (EDS), the elements phosphorous (P), sulfur (S), chlorine (Cl) and potassium (K) are unique markers of FSP in the blend. It is important to emphasized that P and K were present in higher quantities than S and Cl. As the weight ratio of FSP in nanofibers increase, the weight percentages of the atomic markers also increase. This shows that the solutions were homogeneous without the presence of any undissolved protein. The average fiber diameter and porosity increased with the increase of FSP ratio. Compared with pure nylon 6 nanofibers, the increase of FSP ratio caused a decreased in the rupture stress. However, as indicated by the increasing strain at rupture of samples with increasing FSP ratio, the presence of protein in the fibers provided stretchability. There was no difference in Young's modulus and the yield stress between pure nylon 6 nanofibers and FSP-based nanofibers was up to 50%. Thus, biodegradable FSP can be used as an interesting eco-friendly material.

### 1.6.3 Fish muscle proteins in biomedical applications

Codfish protein hydrolysates have shown to have bioactive properties, such as anticancer [81] and antioxidant characteristics [82-84]. On the other hand, Ren *et al.* (2008) produced FSP hydrolysates from grass carp with antioxidant activity [85]. In this way, Stephansen *et al.* (2014) developed and characterized a bioactive electrospun nano-microfiber mesh based on FSP from codfish (*Gadus morhua*) as a drug delivery system [86]. FSP micro-nanofibers had an interesting morphology, containing fiber diameters ranging from hundreds of nanometers to few microns. During the FSP dissolution in 1,1,1,3,3,3-Hexafluoro-isopropanol (HFIP) and the freeze drying process, the protein composition was preserved, as demonstrated by SDS-PAGE. The gel also revealed that the majority of the proteins showed molecular weights around 30-40 kDa. This was supported by amino acid analysis, which demonstrated very similar amino acid compositions for FSP extract, freeze fried FSP and FSP fibers (Table 1.4).

FSP fibers were immersed in gastric buffer and intestinal buffer, and low molecular weights compounds were observed. Degradation results point out that these FSP fibers were not

**Table 1.4** - Amino acid composition (mol %) in FSP extract, freeze dried FSP, and FSP fibers. Kindly provided by Karen Stephansen. Unpublished data.

| Amino acid | FSP extract | Freeze dried FSP | FSP fiber |
|---|---|---|---|
| Glycine | 11.13 ± 0.04 | 10.66 ± 0.07 | 10.62 ± 0.06 |
| Alanine | 10.45 ± 0.07 | 9.91 ± 0.04 | 9.92 ± 0.07 |
| Aspartic acid | 10.33 ± 0.10 | 10.43 ± 0.06 | 10.48 ± 0.08 |
| Glutamic acid | 9.68 ± 0.18 | 9.76 ± 0.05 | 9.84 ± 0.04 |
| Lysine | 8.01 ± 0.12 | 8.00 ± 0.03 | 7078 ± 0.04 |
| Leucine | 7.48 ± 0.07 | 7.68 ± 0.11 | 7.73 ± 0.21 |
| Valine | 6.31 ± 0.14 | 6.36 ± 0.02 | 6.55 ± 0.05 |
| Serine | 5.39 ± 0.17 | 5.11 ± 0.16 | 5.08 ± 0.07 |
| Phenylalanine | 4.41 ± 0.03 | 4.21 ± 0.05 | 4.26 ± 0.07 |
| Threonine | 4.40 ± 0.04 | 4.74 ± 0.03 | 4.83 ± 0.03 |
| Isoleucine | 4.34 ± 0.16 | 4.40 ± 0.16 | 4.46 ± 0.09 |
| Histidine | 4.11 ± 0.21 | 4.03 ± 0.30 | 3.72 ± 0.34 |
| Proline | 3.95 ± 0.02 | 4.04 ± 0.03 | 4.12 ± 0.10 |
| Arginine | 3.79 ± 0.02 | 3.98 ± 0.03 | 3.96 ± 0.03 |
| Methionine | 2.23 ± 0.10 | 2.59 ± 0.09 | 2.61 ± 0.11 |
| Tyrosine | 2.22 ± 0.04 | 2.36 ± 0.03 | 2.28 ± 0.01 |
| Cysteine | 1.80 ± 0.09 | 1.74 ± 0.12 | 1.81 ± 0.09 |

solubilized in the enzyme-free solutions over a period of 24h. This property makes the FSP fibers a very interesting carrier material, since many fibers made of natural biopolymers present high dissolution and degradation rates in aqueous environment needing modifications, e.g. crossinliking, frequently with toxic agents to become insoluble. In the presence of enzymes, the FSP fibers degraded slowly. Stephansen *et al.* (2014) noticed that the degradation mechanism of FSP and FSP fibers was different [86]. The FSP proteins have a folded state and, when processed by electrospinning, they have an unfolded state with higher predisposition to degradation (cleavage sites were available for the enzymes). The degradation products from FSP fibers had inhibitory properties, probably due to proline, against dipeptidyl peptidase-4 (DPP-IV), an enzyme with an essential role in glucose metabolism and linked to type 2 diabetes, making FSP fibers an attractive device for the delivery of antidiabetic drugs like insulin. It was proved that FSP fibers can be a carrier system, due the incorporation and release of Alanine-Tryptophan (Ala-Trp) into FSP fibers. Ala-Trp was uniformly distributed throughout the fiber and the release by diffusion was composed of a burst release within one minute followed by a slower, although still fast, release.

Stephansen *et al.* (2015) proposed the intestinal delivery of insulin using FSP nanofibers [87]. In this study, the FSP and insulin were dissolved in HFIP and processed into FSP-Ins nanofibers. The insulin was successfully incorporated (≈99%), uniformly distributed throughout the whole fibers, without modifying their morphology. Insulin was released from FSP-Ins fibers gradually, reaching a plateau after 3h in physiological conditions. The FSP fibers protected physically the insulin, minimizing the degradation of this molecule in the gastrointestinal tract over 8h. When encapsulated into fibers, insulin permeated through the Caco-2 cells (tumoral cell line) monolayer, according to a concentration gradient-driven flux. The contact and direct interaction between the fibers and the tumoral cells monolayer decreased the transepithelial electrical resistance (TEER), which modify the tight junction structure, namely the claudins and zonula occludens proteins. As a consequence, the permeation of insulin increases locally at the gap junctions. Interestingly, the change in tumoral monolayer integrity was reversible. The FSP-Ins fiber had a high cellular compatibility (>90%) for 4h of exposure, demonstrating that the decrease in TEER was not due to cell death. In the release studies, the authors noticed that the release of insulin from FSP fibers was dependent on the physiological environment [87]. The surfactants affected the insulin release, because they interact with the FSP-Ins fibers, and this interaction depend on the properties of the surfactant. In order to elucidate this mechanism, Stephansen *et al.* (2016) investigated the interactions of insulin-loaded electrospun FSP fibers with four different

bile salts present in the human intestinal fluid [88]. The results point out that the insulin release was dependent on bile salts concentration as biological anionic surfactants (sodium taurocholate, sodium taurodeoxycholate, sodium glycocholate and sodium glycodeoxycholate). Increasing surfactants concentrations leads to increased insulin release. In this environment, the fibers were physically stable and remained non-dissolved. In the presence of synthetic anionic surfactant (sodium dodecyl sulfate), the release of insulin was similar to the previous surfactants, although the fibers degraded for higher concentrations. The insulin release profile was not affect by the presence of neutral surfactants (Triton X-100). When incubated with cationic surfactant (benzalkonium chloride), approximately 1% of the incorporated insulin was released from FSP-Ins fibers. When this surfactant interacts with FSP-Ins fibers, it stabilizes the fiber structure, preventing insulin release. The organization of the surfactant molecules in solution did not affect the behavior of the surfaces with respect to fiber interactions. Small molecules such as Bovine Serum Albumin (BSA), interact with the fibers, change their properties, increasing the insulin release. Thus, the maximum insulin release is altered according to the type and the amount of surfactant present in the physiological environment. It was known that porosity of the fibers affects *in vitro* release of incorporated compounds and only compounds localized at the fibers surface will be released. Before incubation in a buffer containing the surfactant, the inner structure of the FSP-Ins fibers became more porous. The increment of porosity is correlated with the insulin release. The different properties of the surfactants result in different contact angles and required time for complete liquid drop absorption. The FSP-Ins fibers are hydrophobic in contact with the buffer. Despite the complexity of the FSP matrix, the hydrophobic regions were homogeneous. With the addition of synthetic and biological anionic surfactants, the contact angle increased, whereas it decreases with the addition of neutral and cationic surfactants. The authors hypothesized a decrease in the amount of hydrophobic regions, due to changes in the surface properties of the FSP-Ins fibers. Thus, it is important to taking into account that the surfactants in solution interact with FSP-Ins fibers, influencing the release, the fiber stability, porosity, and the fiber surface properties when used for Tissue Engineering, wound healing, drug delivery, and other biomedical applications.

Polysaccharide and proteins are natural “building blocks” of living systems, which perform essential and specialized functions. In this way, Stephansen *et al.* (2015) reported nanocomplexes (NCXs) obtained by electrostatic self-assembling complexation, formed between sarcoplasmic proteins isolated from codfish and alginate (FSP-Alg) [89]. Under physiological conditions, FSP had a negative surface density. The FSP-Alg NCXs when incubated in water for 72h present a decrease

in particle size, while may cause a rearrange of FSP and alginate inside the NCXs. However, the NCXs are stable, as well as in different buffers that simulate physiological relevant environments. SDS-PAGE suggested that NCXs consisted of a mixture of all FSP, rather than specific proteins of either high or low molecular weight. When FSP and NCXs were exposed to pepsin, the degradation of proteins was initiated quickly. But, when exposed to pancreatin, the degradation was slower, and the remaining products presented a molecular weight around 6, 14 and 36 kDa. The individual compounds alginate and FSP did not compromise the metabolic activity of HeLa and U2OS cell lines (tumoral cells). But when they are combined in NCXs, for high concentrations, the cell viability was compromised. The ease, by which the NCXs were formed, together with the distinct stability of the particles, makes the use of NCXs in, for instance biomedical, food or biotechnological applications, appealing.

## 1.7 PURPOSE OF THE WORK

The FSP from codfish, a natural source, are easily accessible and available in large quantities, comprising peptides and proteins with low molecular weights [86]. FSP micro-nano fibers have shown bioactive properties, with capacity to incorporate and release macromolecules. FSP are degradable by proteolytic enzymes and biocompatible, when in contact with cells [87]. As the FSP are water soluble, they become part of the waste water of surimi preparation from fish (e.g. hake, cod and Alaska Pollock), which is discarded [27, 90, 91]. The washing step is essential for improving the quality of surimi gel, because SPs compounds can lead to deterioration during surimi storage, due the retention of heme proteins which introduces ferric iron, promoting the oxidation of residual lipids [27, 29]. In fact, the amount of total sarcoplasmic proteins being lost is estimated to be at least 5000 tons as a dry base per year [92]. Although these proteins are nutritionally equivalent to the MPs of the muscle, and have been considered a potential source of enzymes, there has been little incentive to recover them [93].

On the other hand, large quantities of water are necessary for processing of seafood products [92]. In contrast, water drained from codfish salting has high content of chloride, being ecotoxic waste [94]. The proteins and peptides that constitute the FSP mixture, and others essential free amino acids, are also found in the waste water from salting codfish [95-97]. Putting it into numbers, 155 L of water by the sixth day of the salting process comprised 820 g of free amino acids and 570 g of muscle proteins. It was demonstrated that amino acids mixtures extracted from this

wastewater were transported across the intestinal epithelial cell layer *in vitro*, and it can have potential applications in human and animal food, cosmetics and pharmaceutical formulations [98]. Therefore, the development of new technologies enabling for a more efficient utilization of this marine resource, such as the full utilization of seafood and a cost reduction of waste water treatment, is of critical importance. These figures and facts make the FSP a potential biomaterial for biomedical applications.

In the present study, FSP from codfish (*Gadus morhua*) were isolated and processed into FSP membranes, by the spin coating technique, as a substrate. Both FSP extracts and membranes were physicochemically characterized to evaluate the secondary structure and the thermal degradation. The morphology, the surface charge density and the mechanical properties of FSP membranes were also analyzed. Cytocompatibility with human lung fibroblasts (MRC-5 cell line) was evaluated by MTS assay for FSP extracts and FSP membranes (in direct contact).

## 1.8 REFERENCES

[1] K. Se-Kwon, V. Jayachandran, Introduction to Seafood Science, in: S.-K. Kim (Ed.), Seafood Science: Advances in Chemistry, Technology and Applications, CRC Press2014, pp. 1-13.
[2] FAO, The State of World Fisheries and Aquaculture. Contributing to food security and nutrition for all, Rome, 2016.
[3] FAO, Future Prospects for Fish and Fishery Products, Rome, 2007.
[4] I.H. Pike, Health benefits from feeding fish oil and fish meal. The role of long chain omega-3 polyunsaturated fatty acids in animal feeding, IFOMA, 1999.
[5] K.S. Sidhu, Health benefits and potential risks related to consumption of fish or fish oil, Regulatory Toxicology and Pharmacology 38(3) (2003) 336-344.
[6] J. Oehlenschläger, H. Rehbein, Basic Facts and Figures, Fishery Products, Wiley-Blackwell2009, pp. 1-18.
[7] I.-J. Jensen, M. Walquist, B. Liaset, E.O. Elvevoll, K.-E. Eilertsen, Dietary intake of cod and scallop reduces atherosclerotic burden in female apolipoprotein E-deficient mice fed a Western-type high fat diet for 13 weeks, Nutrition & Metabolism 13(1) (2016) 8.
[8] H.O. Bang, J. Dyerberg, A. Nielsen, Plasma lipid and lipoprotein pattern in Greenlandic Wesy-Cast eskimos, The Lancet 297(7710) (1971) 1143-1146.
[9] V. Ouellet, J. Marois, S.J. Weisnagel, H. Jacques, Dietary cod protein improves insulin sensitivity in insulin-resistant men and women, Diabetes Care 30(11) (2007) 2816-2821.
[10] V. Ouellet, S.J. Weisnagel, J. Marois, J. Bergeron, P. Julien, R. Gougeon, A. Tchernof, B.J. Holub, H. Jacques, Dietary Cod Protein Reduces Plasma C-Reactive Protein in Insulin-Resistant Men and Women, Journal of Nutrition 138(12) (2008) 2386-2391.
[11] A.D. Pradhan, J.E. Manson, N. Rifai, J.E. Buring, P.M. Ridker, C-reactive protein, interleukin 6, and risk of developing type 2 diabetes mellitus, Jama-Journal of the American Medical Association 286(3) (2001) 327-334.

[12] C. Lavigne, F. Tremblay, G. Asselin, H. Jacques, A. Marette, Prevention of skeletal muscle insulin resistance by dietary cod protein in high fat-fed rats, American Journal of Physiology - Endocrinology And Metabolism 281(1) (2001) E62.
[13] F. Tremblay, C. Lavigne, H. Jacques, A. Marette, Dietary Cod Protein Restores Insulin-Induced Activation of Phosphatidylinositol 3-Kinase/Akt and GLUT4 Translocation to the T-Tubules in Skeletal Muscle of High-Fat-Fed Obese Rats, Diabetes 52(1) (2003) 29.
[14] H. Maeda, R. Hosomi, M. Koizumi, Y. Toda, M. Mitsui, K. Fukunaga, Dietary cod protein decreases triacylglycerol accumulation and fatty acid desaturase indices in the liver of obese type-2 diabetic KK-Ay mice, Journal of Functional Foods 14 (2015) 87-94.
[15] D. Ait-Yahia, S. Madani, J.-L. Savelli, J. Prost, M. Bouchenak, J. Belleville, Dietary fish protein lowers blood pressure and alters tissue polyunsaturated fatty acid composition in spontaneously hypertensive rats, Nutrition 19(4) (2003) 342-346.
[16] A. Shukla, A. Bettzieche, F. Hirche, C. Brandsch, G.I. Stangl, K. Eder, Dietary fish protein alters blood lipid concentrations and hepatic genes involved in cholesterol homeostasis in the rat model, British Journal of Nutrition 96(4) (2006) 674-682.
[17] X. Zhang, A.C. Beynen, Influence of dietary fish proteins on plasma and liver cholesterol concentrations in rats, British Journal of Nutrition 69(3) (1993) 767-777.
[18] I.-J. Jensen, M. Walquist, B. Liaset, E.O. Elvevoll, K.-E. Eilertsen, Dietary intake of cod and scallop reduces atherosclerotic burden in female apolipoprotein E-deficient mice fed a Western-type high fat diet for 13 weeks, Nutrition & Metabolism 13(1) (2016) 8.
[19] J. Dort, A. Sirois, N. Leblanc, C.H. Côté, H. Jacques, Beneficial effects of cod protein on skeletal muscle repair following injury, Applied Physiology, Nutrition, and Metabolism 37(3) (2012) 489-498.
[20] V. Venugopal, F. Shahidi, Structure and composition of fish muscle, Food Reviews International 12(2) (1996) 175-197.
[21] B.-N. Ahn, S.-K. Kim, Muscle Proteins of Fish and Their Functions, Marine Proteins and Peptides, John Wiley & Sons, Ltd2013, pp. 641-645.
[22] E. Dunajski, Texture of Fish Muscle, Journal of Texture Studies 10(4) (1980) 301-318.
[23] R. Tahergorabi, S.V. Hosseini, J. Jaczynski, Seafood proteins, in: G.O.P.a.P.A. Williams (Ed.), Handbook of Food Proteins, Woodhead Publishing2011, pp. 116-149.
[24] J.-H. Cheng, D.-W. Sun, Z. Han, X.-A. Zeng, Texture and Structure Measurements and Analyses for Evaluation of Fish and Fillet Freshness Quality: A Review, Comprehensive Reviews in Food Science and Food Safety 13(1) (2014) 52-61.
[25] Z.E. Sikorski, The Contents of Proteins and Other Nitrogenous Compounds in Marine Animals, in: Z.E. Sikorski, B.S. Pan, F. Shahidi (Eds.), Seafood Proteins, Springer US, Boston, MA, 1995, pp. 6-12.
[26] OpenStax, Introduction, Anatomy & Physiology, OpenStax, 2016.
[27] J. Yongsawatdigul, P. Carvajal, T. Lanier, Surimi Gelation Chemistry, Surimi and Surimi Seafood, Second Edition, CRC Press2005, pp. 435-489.
[28] Y.-C. Chen, J. Jaczynski, Protein Recovery from Rainbow Trout (*Oncorhynchus mykiss*) Processing Byproducts via Isoelectric Solubilization/Precipitation and Its Gelation Properties As Affected by Functional Additives, Journal of Agricultural and Food Chemistry 55(22) (2007) 9079-9088.
[29] N.F. Haard, B.K. Simpson, B.S. Pan, Sarcoplasmic Proteins and Other Nitrogenous Compounds, in: Z.E. Sikorski, B.S. Pan, F. Shahidi (Eds.), Seafood Proteins, Springer US, Boston, MA, 1995, pp. 13-39.
[30] K. Hashimoto, S. Watabe, M. Kono, K. Shiro, Muscle protein-composition of sardine and mackerel, Bulletin of the Japanese Society of Scientific Fisheries 45(11) (1979) 1435-1441.

[31] Z.E. Sikorski, J.A. Borderias, Collagen in the Muscles and Skin of Marine Animals, in: Z.E. Sikorski, B.S. Pan, F. Shahidi (Eds.), Seafood Proteins, Springer US, Boston, MA, 1995, pp. 58-70.
[32] Z.E. Sikorski, The Myofibrillar Proteins in Seafoods, in: Z.E. Sikorski, B.S. Pan, F. Shahidi (Eds.), Seafood Proteins, Springer US, Boston, MA, 1995, pp. 40-57.
[33] A.P. Stone, D.W. Stanley, Mechanisms of fish muscle gelation, Food Research International 25(5) (1992) 381-388.
[34] Z.E. Sikorski, A. Kołakowska, Changes in Proteins in Frozen Stored Fish, in: Z.E. Sikorski, B.S. Pan, F. Shahidi (Eds.), Seafood Proteins, Springer US, Boston, MA, 1995, pp. 99-112.
[35] Z.E. Sikorski, B.S. Pan, The Effect of Heat-Induced Changes in Nitrogenous Constituents on the Properties of Seafoods, in: Z.E. Sikorski, B.S. Pan, F. Shahidi (Eds.), Seafood Proteins, Springer US, Boston, MA, 1995, pp. 84-98.
[36] A. Asghar, K. Samejima, T. Yasui, R.L. Henrickson, Functionality of muscle proteins in gelation mechanisms of structured meat products, C R C Critical Reviews in Food Science and Nutrition 22(1) (1985) 27-106.
[37] T. Nakagawa, S. Watabe, K. Hashimoto, Electrophoretic Analysis of Sarcoplasmic Proteins from Fish Muscle on Polyacrylamide Gels, Nippon Suisan Gakkaishi 54(6) (1988) 993-998.
[38] T. Nakagawa, S. Watabe, K. Hashimoto, Identification of Three Major Components in Fish Sarcoplasmic Proteins, Nippon Suisan Gakkaishi 54(6) (1988) 999-1004.
[39] M. Toyohara, M. Murata, M. Ando, S. Kubota, M. Sakaguchi, H. Toyohara, Texture Changes Associated with Insolubilization of Sarcoplasmic Proteins During Salt-vinegar Curing of Fish, Journal of Food Science 64(5) (1999) 804-807.
[40] S. Siriangkanakun, E.C.Y. Li-Chan, J. Yongsawadigul, Identification and characterization of alpha-l-proteinase inhibitor from common carp sarcoplasmic proteins, Food Chemistry 192 (2016) 1090-1097.
[41] H. Toyohara, Y. Makinodan, K. Tanaka, S. Ikeda, Detection of Calpastatin and a Trypsin Inhibitor in Carp Muscle, Agricultural and Biological Chemistry 47(5) (1983) 1151-1154.
[42] S.T. Jiang, C.Y. Tsao, Y.T. Wang, C.S. Chen, Purification and characterization of proteases from milkfish muscle (*Chanos chanos*), Journal of Agricultural and Food Chemistry 38(7) (1990) 1458-1463.
[43] M.A. Audley, K.J. Shetty, J.E. Kinsella, Isolation and properties of phospholipase a from Pollock muscle, Journal of Food Science 43(6) (1978) 1771-1775.
[44] R.H. Ilgner, A.E. Woods, Purification, physical properties and kinetics of peroxidases from freshwater crayfish (genus Orconectes), Comparative Biochemistry and Physiology Part B: Comparative Biochemistry 82(3) (1985) 433-440.
[45] H. Kishi, H. Nozawa, N. Seki, Reactivity of Muscle Transglutaminase on Carp Myofibrils and Myosin B, Nippon Suisan Gakkaishi 57(6) (1991) 1203-1210.
[46] M. Pazos, L. Méndez, J.M. Gallardo, S.P. Aubourg, Selective-Targeted Effect of High-Pressure Processing on Proteins Related to Quality: a Proteomics Evidence in Atlantic Mackerel (*Scomber scombrus*), Food and Bioprocess Technology 7(8) (2014) 2342-2353.
[47] P. Tadpitchayangkoon, J.W. Park, J. Yongsawatdigul, Conformational changes and dynamic rheological properties of fish sarcoplasmic proteins treated at various pHs, Food Chemistry 121(4) (2010) 1046-1052.
[48] P. Tadpitchayangkoon, J.W. Park, S.G. Mayer, J. Yongsawatdigul, Structural Changes and Dynamic Rheological Properties of Sarcoplasmic Proteins Subjected to pH-Shift Method, Journal of Agricultural and Food Chemistry 58(7) (2010) 4241-4249.

[49] G. Villamonte, L. Pottier, M. de Lamballerie, Influence of high-pressure processing on the physicochemical and the emulsifying properties of sarcoplasmic proteins from hake (*Merluccius merluccius*), European Food Research and Technology 242(5) (2016) 667-675.
[50] K. Angsupanich, D.A. Ledward, High pressure treatment effects on cod (*Gadus morhua*) muscle, Food Chemistry 63(1) (1998) 39-50.
[51] I. Paker, K.E. Matak, Impact of sarcoplasmic proteins on texture and color of silver carp and Alaska Pollock protein gels, LWT - Food Science and Technology 63(2) (2015) 985-991.
[52] T. Nakagawa, F. Nagayama, H. Ozaki, S. Watabe, K. Hashimoto, Effect of Glycolytic Enzymes on the Gel-forming Ability of Fish Muscle, Nippon Suisan Gakkaishi 55(6) (1989) 1045-1050.
[53] G. Kudo, M. Okada, D. Miyauchi, Gel-Forming Capacity of Washed and Unwashed Flesh of Some Pacific Coast Species of Fish, 35(12) (1973) 10-15.
[54] G. Kudo, M. Okada, D. Miyauchi, Gel-Forming Capacity of Washed and Unwashed Flesh of Some Pacific Coast Species of Fish, Marine Fisheries Review 35(12) (1973) 10-15.
[55] W.-C. Ko, M.-S. Hwang, Contribution of Milkfish Sarcoplasmic Protein to the Thermal Gelation of Myofibrillar Protein, Fisheries science 61(1) (1995) 75-78.
[56] Y.S. Kim, J. Yongsawatdigul, J.W. Park, S. Thawornchinsombut, Characteristics of sarcoplasmic proteins and their interaction with myofibrillar proteins, Journal of Food Biochemistry 29(5) (2005) 517-532.
[57] A. Jafarpour, E.M. Gorczyca, Characteristics of Sarcoplasmic Proteins and Their Interaction with Surimi and Kamaboko Gel, Journal of Food Science 74(1) (2009) N16-N22.
[58] S. Benjakul, W. Visessanguan, C. Chantarasuwan, Cross-linking activity of sarcoplasmic fraction from bigeye snapper (*Priacanthus tayenus*) muscle, LWT - Food Science and Technology 37(1) (2004) 79-85.
[59] B.-O. Hemung, K.B. Chin, Effects of fish sarcoplasmic proteins on the properties of myofibrillar protein gels mediated by microbial transglutaminase, LWT - Food Science and Technology 53(1) (2013) 184-190.
[60] J. Yongsawatdigul, B.-O. Hemung, Structural Changes and Functional Properties of Threadfin Bream Sarcoplasmic Proteins Subjected to pH-Shifting Treatments and Lyophilization, Journal of Food Science 75(3) (2010) C251-C257.
[61] B.-O. Hemung, S. Benjakul, J. Yongsawatdigul, pH-dependent characteristics of gel-like emulsion stabilized by threadfin bream sarcoplasmic proteins, Food Hydrocolloids 30(1) (2013) 315-322.
[62] K. Morioka, T. Nishimura, A. Obatake, Y. Shimizu, Relationship between the Myofibrillar Protein Gel Strengthening Effect and the Composition of Sarcoplasmic Proteins from Pacific mackerel, Fisheries science 63(1) (1997) 111-114.
[63] K. Morioka, Y. Shimizu, Relationship between the Heat-Gelling Property and Composition of Fish Sarcoplasmic Proteins, Nippon Suisan Gakkaishi 59(9) (1993) 1631-1631.
[64] M. Karthikeyan, S. Mathew, B.A. Shamasundar, V.P. Rakash, Fractionation and Properties of Sarcoplasmic Proteins from Oil Sardine (*Sardinella longiceps*): Influence on the Thermal Gelation Behavior of Washed Meat, Journal of Food Science 69(3) (2004) 79-84.
[65] B. Cuq, C. Aymard, J.-L. Cuq, S. Guilbert, Edible Packaging Films Based on Fish Myofibrillar Proteins: Formulation and Functional Properties, Journal of Food Science 60(6) (1995) 1369-1374.
[66] B. Cuq, N. Gontard, J.L. Cuq, S. Guilbert, Rheological Model for the Mechanical Properties of Myofibrillar Protein-Based Films, Journal of Agricultural and Food Chemistry 44(4) (1996) 1116-1122.
[67] B. Cuq, N. Gontard, J.-L. Cuq, S. Guilbert, Stability of Myofibrillar Protein-Based Biopackagings During Storage, LWT - Food Science and Technology 29(4) (1996) 344-348.

[68] B. Cuq, N. Gontard, J.-L. Cuq, S. Guilbert, Functional Properties of Myofibrillar Protein-based Biopackaging as Affected by Film Thickness, Journal of Food Science 61(3) (1996) 580-584.

[69] B. Cuq, N. Gontard, J.-L. Cuq, S. Guilbert, Selected Functional Properties of Fish Myofibrillar Protein-Based Films As Affected by Hydrophilic Plasticizers, Journal of Agricultural and Food Chemistry 45(3) (1997) 622-626.

[70] E.S. Monterrey, P.J.d.A. Sobral, Caracterização de propriedades mecânicas e óticas de biofilmes a base de proteínas miofibrilares de tilápia do nilo usando uma metodologia de superfície-resposta, Food Science and Technology (Campinas) 19 (1999) 294-301.

[71] E.S. Monterrey-Quintero, P.J.d.A. Sobral, Preparo e caracterização de proteínas miofibrilares de tilápia-do-nilo para elaboração de biofilmes, Pesquisa Agropecuária Brasileira 35 (2000) 179-189.

[72] P.J.D.O.A. Sobral, Influência da espessura de biofilmes feitos à base de proteínas miofibrilares sobre suas propriedades funcionais, Pesquisa Agropecuária Brasileira 35 (2000) 1251-1259.

[73] P.J.d.A. Sobral, J.S. Santos, F.T. García, Effect of protein and plasticizer concentrations in film forming solutions on physical properties of edible films based on muscle proteins of a Thai Tilapia, Journal of Food Engineering 70(1) (2005) 93-100.

[74] K.I. Iwata, S.H. Ishizaki, A.K. Handa, M.U. Tanaka, Preparation and characterization of edible films from fish water-soluble proteins, Fisheries Science 66(2) (2000) 372-378.

[75] M. Tanaka, K. Iwata, R. Sanguandeekul, A. Handa, S. Ishizaki, Influence of plasticizers on the properties of edible films prepared from fish water-soluble proteins, Fisheries Science 67(2) (2001) 346-351.

[76] M.B. Perez-gago, J.M. Krochta, Denaturation Time and Temperature Effects on Solubility, Tensile Properties, and Oxygen Permeability of Whey Protein Edible Films, Journal of Food Science 66(5) (2001) 705-710.

[77] T.M. Paschoalick, F.T. Garcia, P.J.A. Sobral, A.M.Q.B. Habitante, Characterization of some functional properties of edible films based on muscle proteins of Nile Tilapia, Food Hydrocolloids 17(4) (2003) 419-427.

[78] P.J.d.A. Sobral, F.T. García, A.M.Q.B. Habitante, E.S. Monterrey-Quintero, Propriedades de filmes comestíveis produzidos com diferentes concentrações de plastificantes e de proteínas do músculo de tilápia-do-nilo, Pesquisa Agropecuária Brasileira 39 (2004) 255-262.

[79] F.T. García, P.J.d.A. Sobral, Effect of the thermal treatment of the filmogenic solution on the mechanical properties, color and opacity of films based on muscle proteins of two varieties of Tilapia, LWT - Food Science and Technology 38(3) (2005) 289-296.

[80] S. Sett, K. Stephansen, A.L. Yarin, Solution-blown nanofiber mats from fish sarcoplasmic protein, Polymer 93 (2016) 78-87.

[81] L. Picot, S. Bordenave, S. Didelot, I. Fruitier-Arnaudin, F. Sannier, G. Thorkelsson, J.P. Bergé, F. Guérard, A. Chabeaud, J.M. Piot, Antiproliferative activity of fish protein hydrolysates on human breast cancer cell lines, Process Biochemistry 41(5) (2006) 1217-1222.

[82] A.T. Girgih, R. He, F.M. Hasan, C.C. Udenigwe, T.A. Gill, R.E. Aluko, Evaluation of the in vitro antioxidant properties of a cod (*Gadus morhua*) protein hydrolysate and peptide fractions, Food Chemistry 173 (2015) 652-659.

[83] K.H. Sabeena Farvin, L.L. Andersen, H.H. Nielsen, C. Jacobsen, G. Jakobsen, I. Johansson, F. Jessen, Antioxidant activity of Cod (*Gadus morhua*) protein hydrolysates: In vitro assays and evaluation in 5% fish oil-in-water emulsion, Food Chemistry 149 (2014) 326-334.

[84] K.H. Sabeena Farvin, L.L. Andersen, J. Otte, H.H. Nielsen, F. Jessen, C. Jacobsen, Antioxidant activity of cod (*Gadus morhua*) protein hydrolysates: Fractionation and characterisation of peptide fractions, Food Chemistry 204 (2016) 409-419.

[85] J. Ren, M. Zhao, J. Shi, J. Wang, Y. Jiang, C. Cui, Y. Kakuda, S.J. Xue, Optimization of antioxidant peptide production from grass carp sarcoplasmic protein using response surface methodology, LWT - Food Science and Technology 41(9) (2008) 1624-1632.

[86] K. Stephansen, I.S. Chronakis, F. Jessen, Bioactive electrospun fish sarcoplasmic proteins as a drug delivery system, Colloids and Surfaces B: Biointerfaces 122 (2014) 158-165.

[87] K. Stephansen, M. García-Díaz, F. Jessen, I.S. Chronakis, H.M. Nielsen, Bioactive protein-based nanofibers interact with intestinal biological components resulting in transepithelial permeation of a therapeutic protein, International Journal of Pharmaceutics 495(1) (2015) 58-66.

[88] K. Stephansen, M. Garcia-Diaz, F. Jessen, I.S. Chronakis, H.M. Nielsen, Interactions between Surfactants in Solution and Electrospun Protein Fibers: Effects on Release Behavior and Fiber Properties, Molecular Pharmaceutics 13(3) (2016) 748-755.

[89] K. Stephansen, M. Mattebjerg, J. Wattjes, A. Milisavljevic, F. Jessen, K. Qvortrup, F.M. Goycoolea, I.S. Chronakis, Design and characterization of self-assembled fish sarcoplasmic protein–alginate nanocomplexes, International Journal of Biological Macromolecules 76 (2015) 146-152.

[90] G.M. Pigott, Surimi: The “high tech” raw materials from minced fish flesh, Food Reviews International 2(2) (1986) 213-246.

[91] G.M. Hall, N.H. Ahmad, Surimi and fish-mince products, in: G.M. Hall (Ed.), Fish Processing Technology, Springer US, Boston, MA, 1997, pp. 74-92.

[92] E. Okazaki, A study on the recovery and utilization of sarcoplasmic protein of fish meat discharged during the leaching process of surimi processing, Bulletin of the National Research Institute of Fisheries Science 0(6) (1994) 79-160.

[93] T.C. Lanier, Functional Food Protein Ingredients from Fish, in: Z.E. Sikorski, B.S. Pan, F. Shahidi (Eds.), Seafood Proteins, Springer US, Boston, MA, 1995, pp. 127-159.

[94] M. Meneses, J.C. Pasqualino, R. Céspedes-Sánchez, F. Castells, Alternatives for Reducing the Environmental Impact of the Main Residue From a Desalination Plant, Journal of Industrial Ecology 14(3) (2010) 512-527.

[95] V. Ferraro, I.B. Cruz, R.F. Jorge, F. Xavier Malcata, P.M.L. Castro, M.E. Pintado, Characterisation of high added value compounds in wastewater throughout the salting process of codfish (*Gadus morhua*), Food Chemistry 124(4) (2011) 1363-1368.

[96] V. Ferraro, I.B. Cruz, R. Ferreira Jorge, M.E. Pintado, P.M.L. Castro, Solvent extraction of sodium chloride from codfish (*Gadus morhua*) salting processing wastewater, Desalination 281 (2011) 42-48.

[97] V. Ferraro, R.F. Jorge, I.B. Cruz, P.M.L. Castro, M.E. Pintado, Recovery of free amino acids and muscle proteins from codfish (*Gadus morhua L.*) salting wastewater by sorption on Amberlite XAD16, Journal of Chemical Technology & Biotechnology 89(5) (2014) 671-681.

[98] V. Ferraro, R.F. Jorge, I.B. Cruz, F. Antunes, B. Sarmento, P.M.L. Castro, M.E. Pintado, In vitro intestinal absorption of amino acid mixtures extracted from codfish (*Gadus morhua L.*) salting wastewater, International Journal of Food Science and Technology 49(1) (2014) 27-33.

# CHAPTER 2

## Materials and Methods

## 2.1 MATERIALS

### 2.1.1 Codfish

The order Gadiformes is restricted to the cods, hakes, grenadiers, and their more immediate relatives [1]. Cod is included into Gadidae family, which means that these group of fishes live on continental shelves around the North Atlantic. Gadidae family is divided into three subfamilies that are rather different from each other. Codfish belongs to Gadinae subfamily, which is characterized by fishes having three dorsal fins and two anal fins, all separated from each other, and are inserted into Gadus genus. The specific features of Gadus are the lower jaw shorter than upper, palatine teeth lacking, the chin barbell well developed, first anal fin base short, and pelvic fins with a slightly elongated filament. The lateral line is pale and continuous for at least mid-length of third dorsal fin, interrupted to end of caudal peduncle. Gadus have a lateral line pores present on head and scales overlapping. The Gadus genus includes three species: *macrocephalus*, *morhua*, and *ogac* (Figure 2.1). To distinguish this species, it is evaluated the predorsal distance – distance between mouth and the first dorsal fin –, the spots in the body, and the format of head.

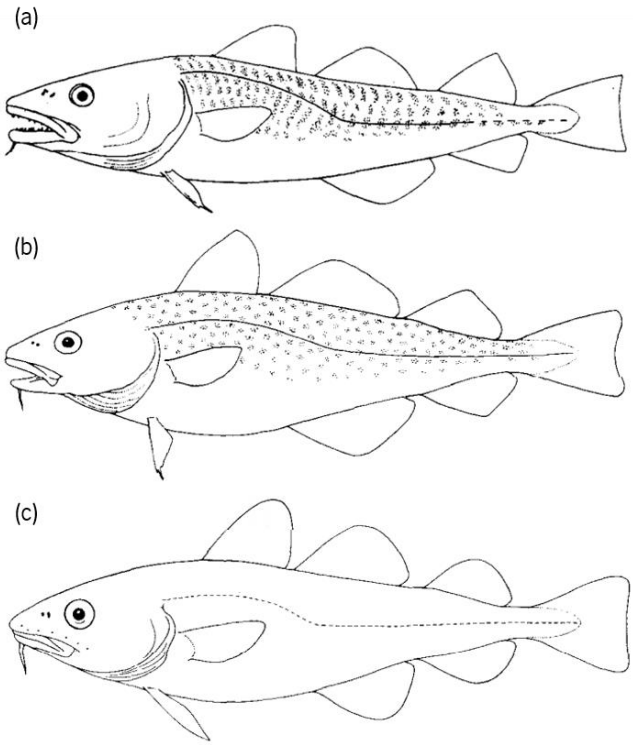


**Figure 2.1** - Anatomical features of (a) *Gadus macrocephalus*; (b) *Gadus morhua*; and (c) *Gadus ogac*. Adopted from [1].

*Gadus morhua*, also known as Atlantic cod, was the fish selected for this work. The head is relatively narrow and can have variables colors, such as brownish to greenish or grey dorsally and on upper side. The ventral skin is pale. The *Gadus morhua* can be found in Cape Hatteras to Ungava Bay along the North American coast; east and west coasts of Greenland, extending for variable distances to the north, depending upon climate trends; around Iceland; coasts of Europe from the Bay of Biscay to the Barents Sea, including the region around Bear Island (Figure 2.2). *Gadus morhua* is generally considered a demersal fish, although its habitat may become pelagic under certain hydrographic conditions, when feeding or spawning. The prey distribution is the factor that generally determines the presence of cod. Larger fish are found in colder waters in most areas (0-5˚C). *Gadus morhua* lives in almost every salinity – from nearly fresh to full oceanic water –, and in a wide range of temperatures nearly -20˚C. This species is mostly found within the continental shelf areas from 150-200 m.

It is one of the world's most fecund fishes, with an average production of 1 million eggs per female. The growth rate is rather high, the females growing slightly faster than the males. Three-year-old fish average 56 cm (males) and 59 cm (females); 5-year olds, 81 cm (males) and 85 cm (females). The species lives up to 20 years.

The body musculature of codfish, reaching from head to tail, is called fish muscle [2]. The muscle consists of segments (myotomes) lying between connective tissue layers (myocommata). The muscle fibers within the myotomes are longitudinally oriented. Proteins are the most important part of fish muscle tissue and can be dived into three major groups according to their water solubility characteristics: myofibrillar, sarcoplasmic and stroma proteins [3].

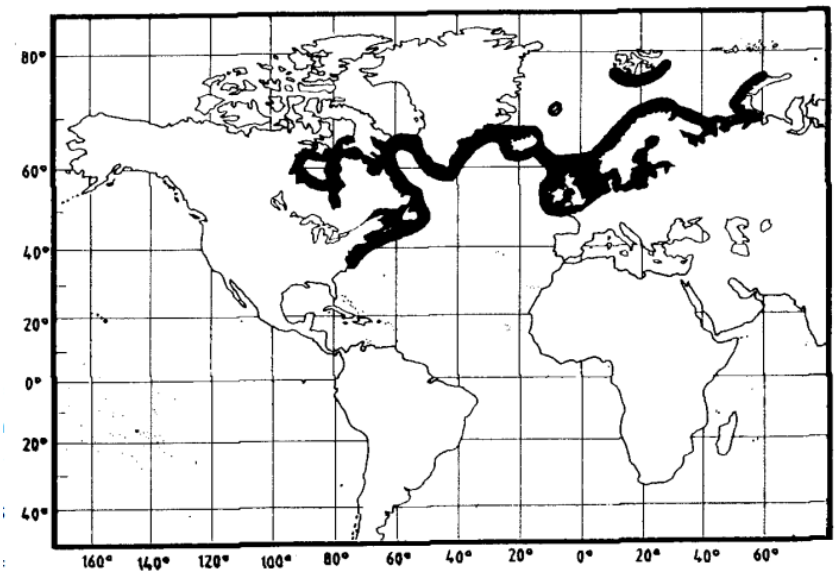


**Figure 2.2 -** Geographical distribution of *Gadus morhua* (darker region). Adopted from [1].

### 2.1.2 HFIP

1,1,1,3,3,3-Hexafluoro-2-propanol (HFIP) (Figure 2.3), also called hexafluoroisopropanol, is a highly polar water-white solvent used as solvent and synthetic intermediate [4]. This fluorinated alcohol is transparent to UV light, thermally stable, and miscible with water and many organic solvents. It is a volatile and polar reagent, with high density, low viscosity, and low surface tension and refractive index. The Table 2.1 presents some properties of HFIP. HFIP exhibits strong hydrogen bonding and will associate with and dissolve most molecules with groups such as oxygen, double bonds, or amine groups. HFIP is capable to dissolve some polar polymers, whose are not soluble in common organic solvents. On the other hand, HFIP is used to solubilize peptides and to monomerize β-sheet protein aggregates [5]. Stephansen *et al.* (2014) showed by SDS-PAGE that the protein composition of codfish sarcoplasmic proteins was preserved during dissolution in HFIP [6].

## 2.2 METHODS

### 2.2.1 FSP extraction

Fish muscle protein consists of three kinds of proteins: sarcoplasmic proteins, myofibrillar proteins and stroma proteins; and these three protein fractions can be differentiated by their solubility. To recover high quantities of protein from fish muscle, the pH shift process was used [7]. The pH shifting process uses isoelectric solubilization/precipitation to obtain high amount of proteins by exposure to acidic or pH conditions. This method separates the protein from the insoluble fractions of the fish, such as cell membrane lipids. Most of protein is solubilized at extreme acidic and alkaline pH, and precipitated at its isoelectric point. However, the solubility of muscle protein is pH-dependent on fish species due to variation in muscle composition.

Fish sarcoplasmic proteins can be extracted using different types of buffer solution. Hashimoto *et al.* (1979) studied the sarcoplasmic proteins extracted from sardine and mackerel

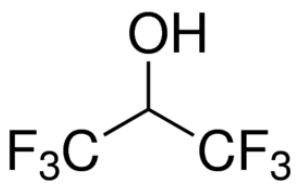


**Figure 2.3 -** Molecular structure of HFIP. Adopted from [4].

[8]. The authors mixed 20 grams of muscle with 200 mL of phosphate buffer (15.6 mM $Na_2HPO_4$, 3.5 mM $KH_2PO_4$) pH 7.5, and homogenized fully with an Ultra-Turrax homogenizes. The homogenate was centrifuged at 5000 g for 15 minutes. To the residue was added 200 mL of the same buffer, and the mixture homogenized and centrifuged again. These two supernatants were combined and added trichloroacetic acid up to 5%. The resulting precipitate was collected by filtration and used as the sarcoplasmic protein fraction. Some modifications of this method are described by others authors [9]. For example, Ren *et al.* (2008) included the freeze drying of sarcoplasmic protein solution [10].

Smith (2010) proposes to extract proteins from muscles with an extraction buffer comprising 0.15 M sodium chloride, and 0.05 M sodium phosphate, at pH 7.0 and a ratio 1:3 (fish:extraction buffer) for 1 minute in a blender [11]. The muscle homogenates were put into a centrifuge tube and centrifuged at 2000 g for 15 minutes at room temperature. The supernatant was collected and filtered with a Whatman No. 1 filter paper. The filtered solution was the fish muscle proteins.

Hashimoto *et al.* (2004) extracted sarcoplasmic protein fraction from bonito and cod muscle. Homogenized muscle samples were defrosted and blend mixed with a buffer solution (0.05 M NaCl, 0.05 M potassium phosphate, 5 mM EDTA), at a 1:4 ratio (muscle:buffer solution) and pH 7.0, during 4 minutes at maximum speed at 2-4˚C [12]. The suspension was mixed with a propeller at 30 rpm for 4 h followed by filtration through a strainer at 4˚C. The suspension was centrifuged at 7000 g for 30 min. The supernatant (sarcoplasmic protein fraction) was collected. The extracted sarcoplasmic protein fraction was dialyzed against deionized water for 24 hours twice to remove the low-molecular weight substances, and freeze-dried.

Stephansen *et al.* (2015) extracted sarcoplasmic proteins from cod muscle. Initially, the muscle was stored vacuum packed at -30˚C until use [13]. The tissue samples were partly defrosted and cut into small pieces. A buffer solution (50 Mm Tris-HCL, pH 7.4, 1 mM EDTA) was added and the mixture was kept on ice and homogenized at 8000 g for 3 x 30 seconds with 2

**Table 2.1 -** Typical physical properties of HFIP. Adopted from [4].

| Property | Value |
|---|---|
| Molecular weight | 168.05 |
| Boiling point | 58.2˚C |
| Melting point | -3.3˚C |
| Density, 25˚C | 1.596 g/mL |

minutes between each homogenization, followed by centrifugation (11,200 g, 20 minutes at 3˚C). The supernatant was transferred to a dialysis tube (6-8 kDa MWCO) and dialyzed against water. Dialysis was performed for 48 hours with change of water four times. The dialysis solution was centrifuged (11200 g, during 20 minutes at 3˚C) and the supernatant freeze dried. The freeze dried protein was stored at -20˚C until.

Fish sarcoplasmic proteins were extracted according to the procedure described by Stephansen *et al.* (2014) with some alterations [6]. A similar extraction was done by Kim *et al.* [14]. Codfish (*Gadus morhua*) from the Norway Sea (Northeast Atlantic) was obtained from MAKRO, Braga. Fresh cod muscle was separated from bones and skin. Codfish muscle was filleted and frozen at -20°C until further use. The freezing process becomes the codfish more rigid, thus the cutting is easier. The frozen fillet was defrosted – but not completely –, cut into small pieces, added to centrifuged tubes and centrifuged for 20 minutes at 3°C with 18000 g (5810R, Eppendorf, Germany). To purify the proteins by removing salts and others small proteins, a dialysis was accomplished. Thus, the supernatants were collected and transferred to the dialysis tubes with cutoff of 3.5-5 kDa. The pH of the codfish muscle pieces and of the supernatant was monitored with pH meter (PHS 3BW, SCANSCI). The dialysis was performed against ultra-pure water at 4°C under stirring. The ultra-pure water was changed 5 times a day with a minimum of 2h between, during 3 days. The supernatant was transferred to balloons, frozen at -80°C, freeze dried (CryoDos -80, Telstar, London) and the product, which were fish sarcoplasmic proteins (FSP), was stored at -20°C. This procedure was done three times for different cod fishes to assure the reproducibility, resulting in three bathes.

### 2.2.2 FSP characterization/separation by electrophoresis

Electrophoresis consists of the movement of charged molecules, namely proteins, in response to an applied electric field, resulting in their separation. There are a several range of sizes and shapes of proteins and their charge come from the dissociation constants of constituent amino acids. As a result, proteins can be separate based on characteristic migration rate [15].

Polyacrylamide gel electrophoresis (PAGE), which the gel works as a size-selective sieve during separation, covers a protein size range of 5-250 kDa. The gel is vertically mounted between two buffer chambers and the gel is the only electrical path between the two buffers. Thus, the proteins are forced to migrate through the gel, in response to an electric field, and the smaller proteins travel longer than larger proteins due the gels pore structure.

To ensure that all proteins enter the gel matrix at the same time, a discontinuous system should be used. This system is composed by two sections: a large pore-size stacking gel on top of a small pore-size separation gel. In this system, proteins first migrate quickly through the large-pore stacking gel and then are slowed as they enter the small pore-size separation gel (or resolving gel). Due to decreased speed, the proteins stack on top of separation gel, forming a tight band that improves the resolution. Ions present in the electrophoresis buffer also migrate through the gel, tightening the protein bands.

Polyacrylamide is ideal for protein separation because is stable, chemically inert, electrically neutral, hydrophobic, transparent for optical detection, the matrix does not interact with the solutes and has low affinity with common protein stains. Free radical polymerization between acrylamide and a co-monomer bis-acrylamide (crosslinker) produces a solid polyacrylamide gel. The addition of a catalyst such as ammonium persulfate (APS) with tetramethylethylenediamine (TEMED) promotes the polymerization. Total monomer concentration and weight percentage of crosslinker characterize the polyacrylamide gels in terms of pore size. By optimizing these two parameters it is possible to obtain the best separation and resolution for the proteins of interest. For example, a high monomer concentration leads to a smaller average pore size. Typical gel used in protein electrophoresis are made with a gradient of monomer concentration though the gel, as reported before, due the range of molecular weights of proteins. These gels give a good resolution of both high and low molecular weight bands on the same gel. In general, the compositions are between 3-8% for stacking gel and 5-15% for separation gel. The selection of gels' composition is based on the optimum resolution of proteins present in a sample. Separation of proteins in a polyacrylamide gel is influenced by the pH and ionic composition of the selected buffer system.

The solubilization of the protein sample is of utmost importance in PAGE, because the breaking of interactions (disulfide bonds, hydrogen bonds, van der Waals forces, ionic interactions and hydrophobic interactions) prevents the protein aggregation or precipitation. Detergent sodium dodecyl sulfate (SDS) was incorporated in sample buffer – creating a SDS-PAGE –, promoting the denaturation and dissociation of proteins. SDS is negatively charged and binds non-covalently to proteins, giving (i) an overall negative charge to the proteins, masking the intrinsic charge of them; (ii) a similar charge/mass ratio for all proteins in a mixture; and (iii) a long shape of proteins instead of complex tertiary conformation. The rate at which SDS-bound protein migrates throughout the gel depends mainly on its size. As a result, the molecular weight can be estimated. On the other hand, SDS is an anionic detergent which rapidly solubilize proteins, through disrupt hydrophobic

interactions between and within proteins. To achieve complete protein unfolding, dithiothreitol (DTT) - a thiol reducing agent - is added to the protein sample, which disrupts intramolecular and intermolecular disulfide bonds, maintaining proteins in their fully reduced states. Protein standards are well-characterized or recombinant proteins solutions that are loaded at same time as protein samples into a gel. Protein standards allow to monitor their separation in the size range of interest, as well as estimate the size and concentration of the proteins separated by the gel.

In technical terms, in PAGE separations, the gel between the glass plates is placed in the chamber between two electrodes. Then, the tank is filled with running buffer and the proteins sample and protein standards are loaded into the wells. Electrophoresis is initiated by programming the power supply (regulated direct current) and the running conditions, which provide an optimum resolution, are selected. The driving force behind protein separation is the differential electrical potential applied across the electrodes. This leads to an electric current flow through the gel, which has an intrinsic resistance. A scheme of SDS-PAGE is illustrated in Figure 2.4.

Following electrophoretic separation, the proteins cannot be seen into the gel by naked eye, whereby is essential to use protein stains. In this step, the proteins into the gel are fixed by a methanol and acetic acid solution and exposed to a dye solution. There are several total protein staining techniques: coomassie blue, fluorescent, silver, negative and stain-free technology. The commonly used stain is the coomassie (brilliant) blue, which is anionic protein dye. There are two variants of this dye: R-250 (R-reddish), which offers shorter staining times, and G-250 (G-Greenish), which is more sensitive. Then, the gel is washed to remove the excess dye. The gel is ready to qualitative analysis.

SDS-PAGE was performed for the three different batches of FSP extracts to analyze the

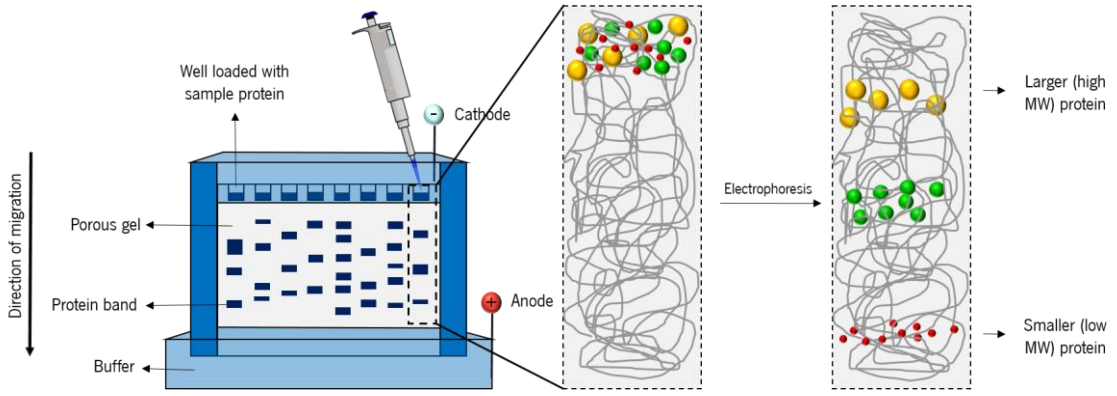


**Figure 2.4 -** Schematic representation of electrophoretic protein separation in a polyacrylamide gel. Adapted from [15].

molecular weight and protein composition. Glass plates and comb (14 wells) were cleaned with ethanol. The spacers were cleaned only with water. Casting stand was assembled and the comb was placed. It was marked at ≈ 10 mm below the bottom of the well and the comb was removed. It was used a handcast gel composed by 4% acrylamide as stacking gel and 9% acrylamide as separation gel. APS (10% w/v) was prepared freshly. All reagents were added by the order presented in Table 2.2 and mixed gently. It is important to mix the solution before adding APS. The TEMED and APS should be added at the end, because they are catalysts and the polymerization starts. The separation solution was mixed again and poured in between the glass plates until the mark. To prevent dehydration and to keep oxygen out of the system, as it inhibits polymerization an overlay made of ultra-pure water was added on top of the separation solution. After 45-65 minutes the gel was polymerized. It was possible to see a line between the separation gel and the ultra-pure water. The stacking gel was prepared in same order as the first gel, according to Table 2.2. The ultra-pure water was removed and the excess adsorbed with filter paper without touching the gel. Staking solution was poured between the glass plates until the top of the short plate was reached. The comb was carefully inserted, avoiding air bubbles formation. After 30 minutes, the gel was polymerized and the comb was gently and slowly removed. The wells were rinsed with ultra-pure water to remove some unpolymerized material.

The three different batches of FSP extracts at 1 mg/mL were dissolved in ultra-pure water. While the gel polymerizes, the protein sample and standard were prepared: 6 µL of each protein sample was added to Eppendorf tubes together with 24 µL of loading buffer (15 mM Tris-HCl pH 6.8, 2.5% -SDS, 25% glycerol, 0.1% bromophenol blue, 5% DTT); 5 µL of protein standard were added to Eppendorf tubes with 24 µL of loading buffer and 1 µL of ultra-pure water; as blank 24 µL of loading buffer and 6 µL of ultra-pure water were mixed per each free well. All mix samples were heated for 30 minutes at 65°C, after one denaturation process of 5 minutes at 95°C.

The electrophoresis system was assembled with the polyacrylamide gel and the running buffer (250 Mm Tris, 1.92M glycine and 1% SDS) was added to reservoirs. In the upper reservoir

**Table 2.2 –** Composition of 15 mL separation gel and 5 mL stacking gel.

| Reagent | Separation gel (9%) (mL) | Stacking gel (4%) (mL) |
|---|---|---|
| Ultra-pure water | 5.09 | 3.233 |
| Separation gel buffer | 5.00 | - |
| Stacking gel buffer | - | 1.00 |
| Polyacrylamide | 4.66 | 0.667 |
| TEMED | 0.25 | 0.10 |
| APS | 0.10 | 0.03 |

the wells should be submerged by running buffer. In the bottom reservoir it is important to avoid the bubbles formation between bottom edges of glass plates. If bubbles exist, they should be removed with the help of a syringe with running buffer. When the running buffer is injected of syringe, the bubbles run until the surface and disappear. 30 µL of each protein, protein standards, and the marker were loaded. The lid was placed and connected to the power supply. A constant voltage of 150 V was applied until the bromophenol blue reached the bottom of the gel (≈ 5 hours). After electrophoresis was completed, the power supply was turned off and disconnected the electrical leads. The gel was gently removed from the glass plates. The gel was stained with coomassie blue (0.125% coomassie blue R-250, 50% methanol, 10% acetic acid) during overnight. This staining solution was prepared by dissolving the coomassie blue R-250 in methanol and water, during 6 hours; and more 1h to mix with ultra-pure water. Then, it was filtered and protected from the light. The gel was placed into distaining solution I (29% methanol, 5% acetic acid) during 24h. The distaining solution I was removed and the distaining solution II (5% methanol, 7% acetic acid) was added to gel overnight. At this point, the gel could be visualized in a scanner.

### 2.2.3 Production of FSP membranes by spin coating technique

Spin coating technique is a reliable, simple and rapid process to produce uniform thin films over flat substrates. A machine used for this technique is called spin coater or spinner and it is shown in Figure 2.5. The substrate is held over a chuck by the influence of a vacuum. The technique is based on the deposition of a small amount of a polymeric solution onto the center of a substrate's surface and then spin the substrate at high speed. The continued action of spinning, called centrifugal force, causes the spreading of the polymeric solute in direction the edge of the

**Figure 2.5 -** Spin coater machine (left) and chuck detail (right).

substrate – and the excess of solution spreads out -, producing a very uniform thin film of material over the substrate surface. Normally, the solvent is volatile and evaporates at the same time [16-18].

One of the advantages of spin coating is repeatability. Furthermore, spin coating is a low cost technique that allows an easy control and management of chemicals and substrates. On the other way, it is possible to produce films at faster rates over any substrate, with a firm control over the morphologies and properties of the produced films. Spin coating does not dependent of external variables. The thickness of the film can be easily altered by changing of associated parameters, such as the spinning speed or the viscosity of the solution. However, spin coating also have some drawbacks. One of them is the substrate sizes, because large substrates cannot be spun at a sufficiently high rate in order to allow the film thinning [17, 18].

The physics theory of spin coater follows mathematical models and the process can be described in detail into four distinct stages (Figure 2.6) [17, 18]:

a) Dispense stage

As seen previously, the spin coating process starts with a dispensing stage, where an excess of polymeric solution is deposited onto the center of the substrate surface, depicted as in Figure 2.6-a. There are two methods of dispensing: static and dynamic. Static dispensing consists in simply depositing a small amount of polymeric solution on the substrate surface. In dynamic dispensing, the solution is deposited as the substrate is spinning at low speed (usually around 500 rpm). The common method provides the less waste of material, once it is used less solution to cover whole substrate surface.

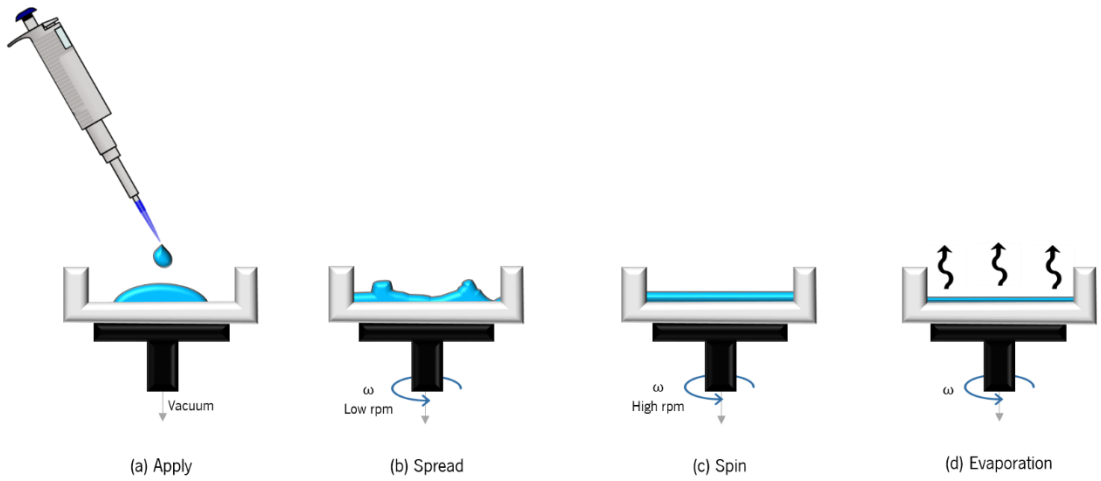


**Figure 2.6 -** Schematic representation of the spin coating technique stages. Adapted from [17, 19].

b) Substrate acceleration stage

In this step, the centrifugal force is generated by rotation of the substrate and the liquid flow radially outward. This stage is characterized by aggressive solution expulsion from the substrate surface due the rotational motion (Figure 2.6-b). Spiral vortices may be observed due to twisting motion caused by inertia at the top of the solution layer, while the substrate below rotates faster and faster. When the puddle is thin enough, it co-rotates with the substrate surface. At this moment, no fluid thickness difference is observed, because the substrate reaches the desired speed and the solution is thin enough that the viscous shear drag exactly balances the rotation accelerations. Typical spin speeds for this stage of spin coating range from 1500-6000 rpm, depending on the properties of the solution and of the substrate.

c) Spin

In the third stage, the substrate is spinning at a constant rate ($\omega$), when fluid viscous forces dominated fluid thin behavior. The excess of liquid flows to the edge of the substrate in the form of droplets, which produces an uniform thin fluid, after suffering gradual fluid thinning (Figure 2.6-c). As the fluid thickness is reduced, this event is less pronounced. It is important to mention that the thickness around the edge of the substrate can be different, because a small bead may be formed due to surface tension, solution viscosity, or rotation rate.

d) Evaporation

At this last stage, the substrate is still spinning at constant rate and any evaporation of a volatile solvent is the primary phenomenon of fluid thinning behavior (Figure 2.6-d). At this point, as the solvents are being evaporated, the viscosity of the remaining solution will rise, keeping the coating in place. The film drying stage begins.

The drying rate of the solution is defined by the nature of the solvent, in terms of volatility, as well as the environment conditions around the substrate during the spinning process. When the spinning stops, some materials or applications was require a further treatment. Stages c) and d) are two process that occur at the same time and this stages are the most important determining the final thickness.

The polymeric solution properties such as viscosity, surface tension, drying rate, together with the fume exhausting, and the selected parameters for the spinning (rotational speed, acceleration, spinning time, dispense solution) will affect the final thickness of the film [16-18].

The distribution of solution and the thickness of the resulting films are controlled by various factors. Emslie *et al.* (1958) [20] studied the physics of the subtract rotation (rpm) and they notice that the normal flow condition is a balance between the rotational accelerations and the viscous drag felt within the solution. The local shear rate is proportional to the radius of the substrate, i.e., the flow will be faster at larger radius. In the central region of the substrate, the rotational acceleration is lower, whereby the fluid flow is slower. This result in gradually thinner coating along the radius. The speed of the spinning step generally defines the final film thickness. The higher the angular speed and longer the spinning, the thinner is the film. On the other hand, the solvent evaporation is facilitated by the quick substrate spinning. This phenomenon occurs uniformly over the top surface of the solution [21], producing evaporative cooling. Faster evaporation rate provides a slightly thicker film. The relative humidity affects the drying rate: variations of only a few percent in the relative humidity can result in huge changes in the final film thickness.

In short, the rotation affects the viscous flow rate and the evaporation rate. In other words, the thickness of the film depends on the concentration of the solution and the solvent. Solutions with higher viscosity and/or large substrates require a big puddle to assure full coverage of the substrate during the high acceleration stage [17, 18].

In this study, we will use spin coating technique to produce a membrane as a substrate to cell culture. Spin coated FSP membranes were prepared from 100 mg/mL solutions of FSP dissolved in HFIP, stirring overnight. Polystyrene petri dishes (85 mm diameter) were the substrate, that were placed on the stage of a spin coater (WS-650Hzb-23NPPB-UD-3, Laurell Technologies). Then, the protein solution was applied to the center of the substrate surface with a pipet. The volume of a solution puddle ranges between 0.5-1.5 mL. The substrate was then spun at 1000 rpm for 5 seconds. The FSP membranes were dried at room temperature. Then, the FSP membranes were detached and stored until further characterization. For each batch of FSP extracts was produced the respective batch of FSP membranes.

### 2.2.4 Physical characterization

#### 2.2.4.1 Scanning electron microscopy

Scanning electron microscopy (SEM) is a technique that allows to analyze in detail the surface sample by scanning a focused energetic electron beam [22, 23]. SEM allows studying surface morphology, identifying small areas with high spatial resolution, that cannot be observed by optical microscopy.

SEM equipment is under vacuum and the sample should be dry. The sample should be electrically conductive, at least at the surface, to prevent accumulation of electrostatic charges at the sample's surface, and be properly grounded. Non-conductive specimens accumulate charge when bombarded with the electron beam and, therefore, need to be coated with a thin coating of electrically conductive materials, such as gold or carbon.

Briefly, the primary electrons – emitted from an electron gun - will interact with atoms of a sample's surface and various signals will be emitted. The electrons are accelerated to energy of 0.2–40 keV and spatially focused by one or two condenser lenses in a spot with 0.4–5 nm of diameter. Then, the electron beam passes through scanning coils (or deflector plates), in the electron column, to achieve deflation in the $x$ and $y$ directions for scanning. When the primary electron reaches the sample, it loses energy by two process: (i) repeated random scattering and (ii) absorption inside a volume of the specimen, known as the interaction volume, which resembles a balloon, that, depending on the electron energy, has a depth of 1–5 μm into the surface. At this point, various signals are originated from different depths of the interaction volume, and secondary electrons are emitted from the top 5–10 nm of the sample's surface, containing topographical information. Specialized detectors detect the emitted signals. Then, these signals are amplified and displayed on a cathode ray tube (CRT), which is synchronized by the rastering of the electron beam. This results in an image that represents an intensity map of signals emitted within the scanned area. The image replicates exactly the surface features of the sample.

The secondary electrons are originated from a few nanometers of sample's surface, due to their low energy (<50 eV). The brightness of the signal depends on the number of secondary electrons reaching the detector and is sensitive to the sample surface topography. Backscattered electrons are high-energy electrons reflected from the specimen interaction volume by elastic scattering with the substrate atoms. Heavy elements (high atomic number) backscatter electrons are easily detected than light elements (low atomic number), whereby the signal is higher and the spots are brighter in the image. Thus, backscattered electrons are usually used to manipulate the contrast among areas with different chemical compositions.

In this study, the FSP membranes were cut into 10 x 10 mm, mounted over a stub and, then, were sputter-coated with gold (108A, Cressington) for 1 minutes at 15 mA. The samples were analyzed by scanning electron microscopy (JSM-6010 LV, Jeol, Japan). Micrographs were recorded at 10 kV with magnifications ranging from 100 to 5000 times.

### 2.2.4.2 Tensile tests

The performance of a biomaterial scaffold is crucially affected by its mechanical behavior. In a tissue engineering approach, it is important to know the stress necessary to cause plastic deformation or the maximum stress that a biomaterial can resist. Mechanical properties are measured by the response (deformation) of a biomaterial to an applied stress (load).

It is important that the specimen be simple and reproducible, and it should represent the scaffold material composition as a whole. Only proper preparation of the sample gives accurate results. The specimens must be prepared carefully with attention to several details. For example, multiple specimens are tested, all of them with the same dimensions. The specimen axis must be properly aligned with the grips [24].

The typical tensile specimen, shown in Figure 2.7, has enlarged ends which allows gripping. The reduce cross-sectional area of the specimen is named gauge section. It is reduced to ensure that the deformation and the failure will be localized within this region. The gauge length, centered within the gauge section, is where measurements are made. The machine will record the tensile force as a function of the increasing in gauge length.

Force *(F)* acts on a specimen and are expressed in newton *(N)*. Stress ($\sigma$) is defined as the tensile force *(F)* acting on a cross-sectional area *(A)* of the gauge section (equation 2.1). Stress is expressed in force per unit area or in Pascal *(Pa)*.

$$\sigma = \frac{F}{A} \tag{2.1}$$

Elongation ($\epsilon$) is the total amount of stretch ($\Delta L$) of the specimen, in gauge length, per the initial gauge length ($L_0$) during a tensile test. Strain ($\varepsilon$) is defined as the change in the gauge length ($\Delta L$) – deformation – relatively to initial gauge length ($L_0$) (equation 2.2), due to the Stress applied. The units of Strain are millimeter per millimeter. However, commonly no units are shown, because Strain is the ratio of lengths, or can be presented as unit percentage (mm/mm x 100). The Elongation and the Strain are similar concepts, while the first definition is the total amount of extension [24, 25].

$$\epsilon = \frac{\Delta L}{L_0} = \frac{(L - L_0)}{L_0} \tag{2.2}$$

During a tensile test, the force applied *(F)* to a specimen and the elongation of the specimen are measured and recorded at the same time in regular intervals. When force-elongation data are converted to Stress and Strain, it results in a stress-strain curve (Figure 2.8). This representation is more accessible, because the stress-strain curve is independent of specimen dimensions [24-26].

When the specimen is loaded with an uniaxial tension, the stress-strain curve shows three typical regimes of deformation. The specimen is submitted to a small stress and the bonds between the atoms are stretched. Upon unloading, the specimen returns to its original shape and size because of the bonds relax. This reversible deformation comprises the elastic region, where the stress is proportional to the strain. By increasing the Stress, until the yield point *(y)*, atoms slide over each other. After removing the load, the specimen does not recover the original shape, resulting in a plastic deformation, which means that the deformation is permanent. When the specimen reaches the ultimate point *(u)*, deformation becomes unstable because the cross-sectional area is reduced and the deformation starts to be localized, forming a neck. The fracture *(f)* occurs immediately [24-26].

The Stiffness of a biomaterial (binding forces between atoms) corresponds to the slope of the linear elastic region of the stress-strain curve ($\Delta\sigma/\Delta\varepsilon$) and is called elastic modulus or Young's Modulus *(E)*. The higher the elastic modulus, the smaller the elastic strain resulting from the application of a given Stress. Elastic modulus is a basic physical property of each biomaterial. The yield strength ($\sigma_y$) is the Stress at the yield point *(y)*. Due to the gradual transition from the elastic to the plastic deformation, the yield point *(y)* is not easy to identify. For this, a line parallel to the measured elastic modulus is drawn with an offset of 0.2%, intersecting the stress-strain curve, which becomes the yield stress more accurate and reproducible. The higher value of stress at the ultimate point *(u)* is designed by ultimate strength or ultimate tensile strength ($\sigma_u$ or UTS). The tensile strength measures the maximum load that a material can support under specific conditions

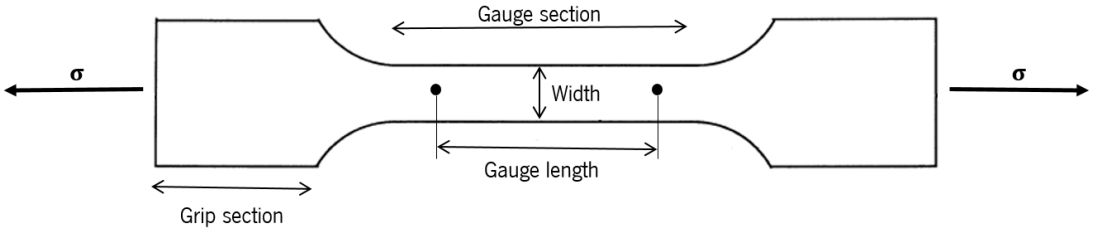


**Figure 2.7 -** Typical tensile specimen with a reduced gauge section and enlarged ends. Adapted from [24, 26].

of uniaxial loading. Until this point, the deformation should be uniform throughout the gauge section. The fracture strength ($\sigma_f$) is the stress at the point of fracture *(f)*. The corresponding strains measured at the yield strength, ultimate strength, and fracture strength are named the yield strain ($\varepsilon_y$), ultimate strain ($\varepsilon_u$), and strain-to-failure ($\varepsilon_f$), respectively [24-27].

There are many loading modes, used for different purposes. In this work, it was used a uniaxial tensile test for the characterization of FSP membranes mechanical properties. Uniaxial tension, whose curve is represented in Figure 2.8, is a tensile test where the specimen cross-section experiences uniform Stresses and Strain. The specimen is fixed by gripping opposite ends, within the load frame of a test machine [26, 27].

To evaluate the mechanical properties, such as elastic modulus, yield strength and fracture strength of FSP membranes, a tensile test was performed. Ten rectangular specimens (30 x 6 mm) with different orientations, as shown in Figure 2.9, were cut with a blade from membranes produced from the three FSP batches. The thickness of each specimen was measured at three points, as Figure 2.9 represents, with a micrometer (Mitutoyo, Japan).

To ensure that the deformation and failure will be localized within the gauge length region, a paper frame (36 mm x 20 mm) with 12 mm square window was used (Figure 2.10). This preparation method allows better handling of specimens during their grippig. Each specimen was placed in the central square window of two paper frames. The paper frames were glued from both

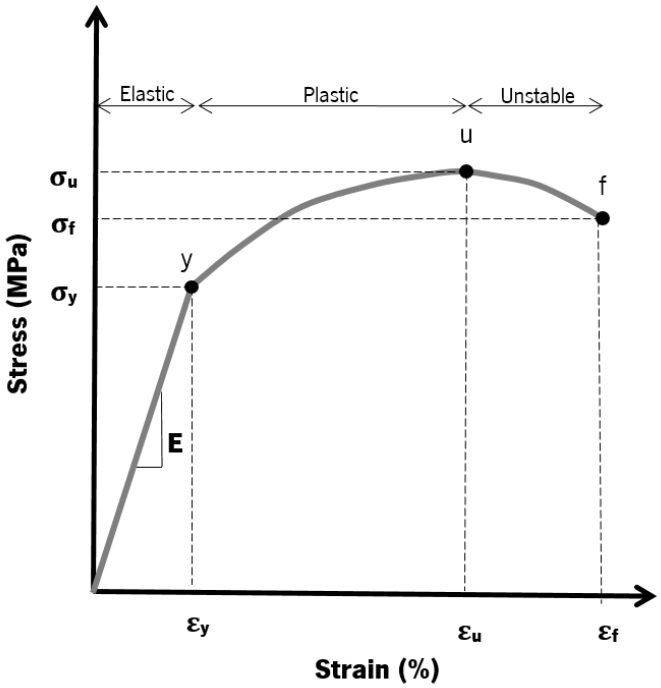


**Figure 2.8 -** Schematic stress-strain curve for a specimen loaded in uniaxial tension. Adapted from [24, 26].

sides with a doubled-sided Tesafilm.

A universal mechanical testing equipment (Model 5543, INSTRON, UK) with a 1 kN load cell was used. The speed rate was selected at 1 mm/min and provided the value of 12 mm gauge length to the tensile tests. Each paper frame was fixed by wedge action grips and grips were manually closed. The thickness of each specimen was provided to the tensile test. The lateral sides of the paper frames were cut and the tensile test was initiated. Tests were made at room temperature and humidity. The test was ended when the specimen fracture. Data were collected by the software Bluehill 2 and the stress-strain curves were drawn. The Young's Modulus was calculated with a linear regression from the linear region of the stress-strain graph, between 0.5% and 1% strain. The yield point was determined by the intersection of a line drawn parallels to the *yy* axis with an off-set of 2% strain after the deflection of the linear region. Facture strength was determined when the load decayed immediately to zero. The values reported are the average of at least twenty specimens.

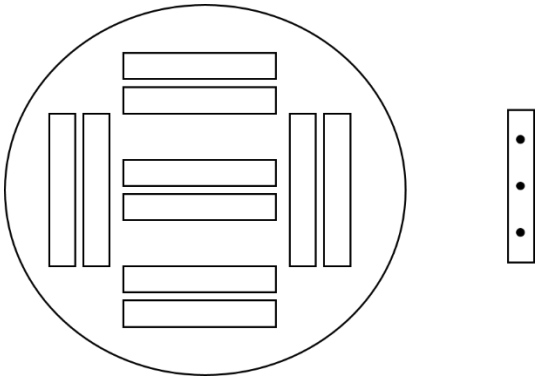

**Figure 2.9 -** Specimens areas for tensile testing (left) and the three points of the specimen thickness measurement (right).

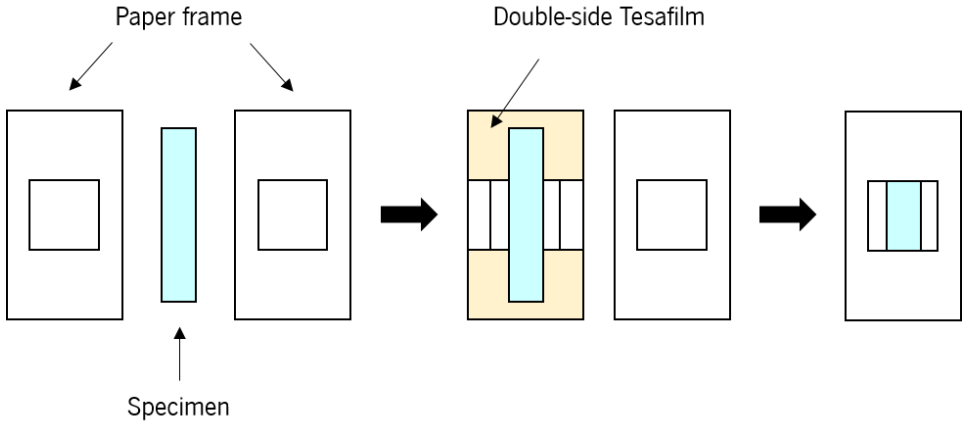


**Figure 2.10 -** Steps of specimen's preparation for tensile testing.

### 2.2.4.3 Differential scanning calorimetry

Proteins are polypeptides that assume a compact, ordered and highly complex structure. The proteins have two states: a native (or folded) state and a denatured (or unfolding) state. This transition is characterized by a change in the protein properties due to extrinsic conditions such as high temperature, which results in thermal melting. These structural rearrangements result in the absorption of heat caused by the redistribution of non-covalent bonds governed by thermodynamic events [28, 29].

Differential scanning calorimetry (DSC) can be used to evaluate quantitatively and qualitatively the stability of the folded conformations of proteins, providing a fundamental thermodynamics of protein stability [28-30]. DSC can measure heat capacity differences ($\Delta Cp$) between the folding an unfolding states of proteins. DSC is a method that can be used for solutions and solids. Heating and measurements are performed through constant heat flux, where a single furnace heat simultaneously the reference pan (empty) and sample pan (protein of interest). The furnace maintains the two pans at the same temperature and the differences in heat uptake are compensated by the DSC instrument. Heating the protein sample initially produces a slightly increase of the baseline, but as heating continues, heat is absorbed by the protein, causing thermal unfold over a temperature range characteristic for that protein. The transition from folding to unfolding conformations results in an endothermic peak. Once unfolding is complete, heat absorption decreases and a new baseline is established.

Figure 2.11 represents a typical plot of a DSC from a protein, named thermogram (heat flow vs. temperature). The thermal unfolding transition, point B on Figure 2.11, represents the temperature where 50% of the protein is folded and 50% is unfolded. The calorimetric enthalpy ($\Delta Hcal$) of the unfolding reaction is the integration of the area under the unfolding transition, between point A and C, which is due to the endothermic events such as the breaking of hydrogen bonds. A biomolecule is in equilibrium between its native (folded) and denatured (unfolded) conformations. The protein is more thermodynamically stable, as higher the thermal unfolding transition [28, 30].

Usually, proteins unfold irreversibly during or after denaturation at high temperatures. However, a fully thermodynamic characterization of the unfolding event requires that the reversibility of the unfolding transition be observed. Reversibility can be measured by cooling the unfolded protein to a temperature where it should refold and then heating the protein again under

identical conditions, in order to obtain a second endothermic event that is observed in the first scan. Irreversibility is observed when this endothermic event is null [28, 30].

As the development, production and storage of stable proteins with full functionality is one of the goal in protein engineering and biopharmaceutical formulation, the thermal stability and structural integrity of FSP extracts and FSP membranes were studied by differential scanning calorimetry. A DSC Q100 equipment (TA Instruments) was used in this study. Both temperature and heat flux were calibrated with indium at a scanning rate of 10°C/min. An empty pan was used as reference. Nitrogen, at a flow rate of 50 mL/min, was used a carrier gas. Samples of approximately 2.5 mg were weighed and sealed into aluminum pans. Samples were scanned from 0 to 150°C at a constant heating rate of 2°C/min. DSC scans were performed two times for the same sample into the aluminum pan, named first and second runs, to check the reversibility of the unfolding transition. Each batch, both FSP extracts and membranes, was run. TA Instruments Universal Analysis software (2000) was used to analyze the experimental data. The residual denaturation enthalpy ($\Delta H$) was calculated using the derivative curve of heat flow. The start point of the area under endothermic peak was the slope of the heat flow curve changed; the end point was defined by the local minimum of the heat flow curve where the derivative curve again reaches a constant value [31]. Data presented is an average value of the thermal unfolding transition temperatures.

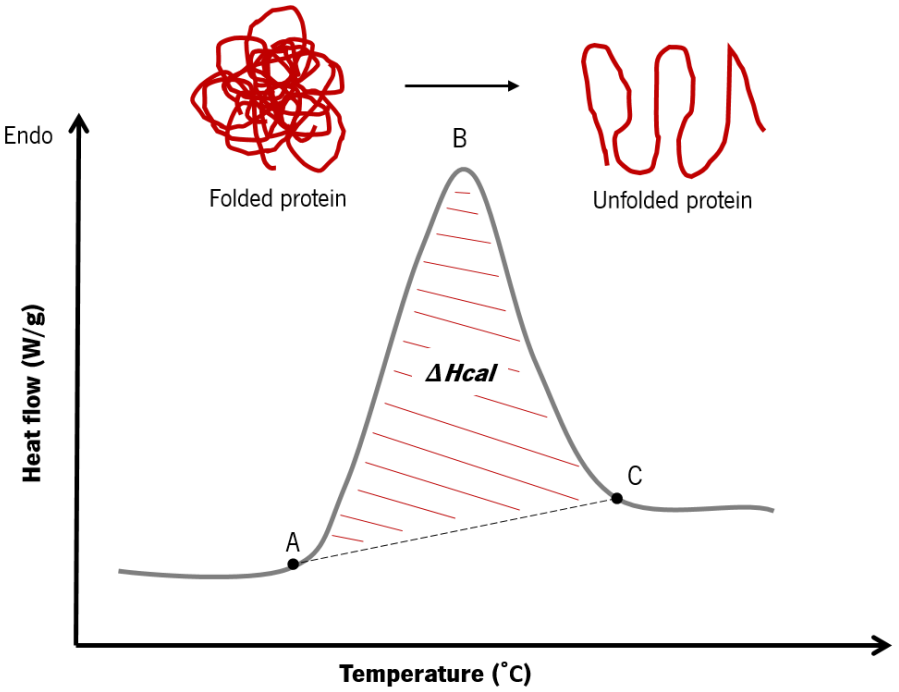


**Figure 2.11 -** DSC thermogram from a protein. Adapted from [28].

#### 2.2.4.4 Thermogravimetric analysis

Thermogravimetric analysis (TGA), also known as thermogravimetry (TG), is a precise quantitative method that measures alterations in the sample mass, resulting in physical (sublimation, evaporation, condensation) or chemical (degradation, decomposition, oxidation) change, that occur while the sample temperature varies T (t), according to a controlled temperature program [35]. The program can be isothermal, when the temperature increase is linear, or nonisothermal. The TGA comprises a thermobalance that combines a sensitive analytical balance with an electronically programmed furnace that measures the loss of sample mass. A TGA is conducted under controlled gaseous atmosphere, in a dynamic or static fashion. Usually, it is used a dynamic atmosphere, which is accomplished by running a gas around the sample at a certain flow rate (50-100 mL/min). This gas can be inert, such as nitrogen (commonly used), or reactive, like oxygen. The sample size is generally between 1-100 mg. Sample holders used in TGA are cylindrical pans (crucibles) made of thermally and chemically resistant materials with good thermal conductivity such as aluminum. TGA runs are normally performed in open pans, to not lead to the pressure rising due to gaseous products accumulations inside the pan. The sample should be in contact with the pan to secure a good thermal contact between both.

As the samples are heated or cooled, they can experience various changes accompanied by a loss or a gain of mass [35]. Degradation and/or decomposition, vaporization of bulk liquids or liquids adsorbed by solids, sublimation, and desorption of gases are mass loss processes. A mass gain includes the adsorption of gases, as well as in reactions of solids with reactive gases (oxygen, chlorine, and carbon monoxide).

TGA measurements results in a thermogravimetric curve, illustrated in Figure 2.12, which is represented in an integral or differential form. The integral form is the TG curve where mass (absolute in gram or relative in % to the initial mass) is plotted against the time or temperature. The shape and position of the TG curve is determined by the mechanism and kinetics of the process associated with the mass change. The differential form (DTG curve) is the derivate of the TG curve with respect to time that is plotted against the temperature. A DTG curve allows identify individual steps; downward peaks represent mass loss and upward peaks represents a mass gain, indicating the temperature range where these particular event occurs. By decreasing the heating rate, a better resolution of TGA is obtained, however the experiment takes longer.

The TGA is applied to evaluate the composition of the materials and their relative thermal stability. When this method is applied to proteins, the goal is to determine the sample moisture

content, hydration level, and decomposition temperature [36]. Normally, materials are modified to be more or less thermally stable in relation to the original materials [35]. This effect is proven by running TGA on modified and original materials under similar conditions, such as heating rate, flow of inert gas, pan type, and sample mass, and it is observed a shift of the TG curve for modified material to higher or lower temperatures.

In the present work, the mass loss of FSP extracts and FSP membranes during a linear increase of temperature was performed in a Simultaneous Thermal Analyzer (STA7200, Hitachi). The initial samples weight was about 3 mg. The samples were scanned from 35 to 700°C, at a heating rate of 10°C/min in crucibles of platinum as a support. Nitrogen was used as the purge gas, at a flow rate of 100 mL/min.

### 2.2.5 Chemical characterization

#### 2.2.5.1 Water contact angle

The biological interactions, such as cell adhesion and spreading, are strongly correlated with the surface energy of a biomaterial scaffold surface. Contact angle measurements allows quantifying concepts of surface tension and surface energy. The contact angle values give a

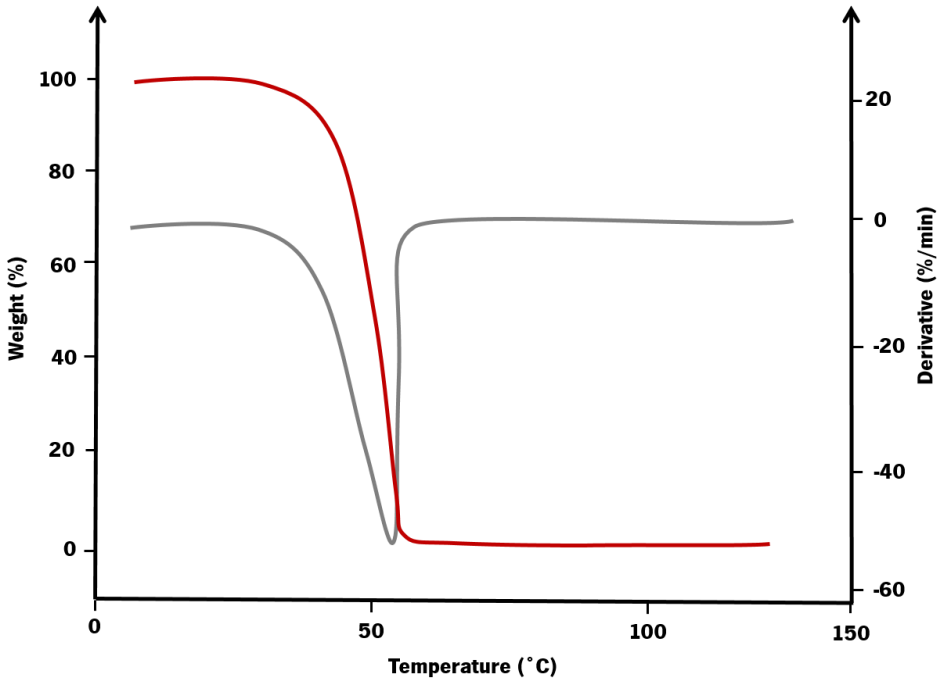


**Figure 2.12 -** TG curve (red) and its derivative, DTG (gray). Adapted from [32].

measure of the chemical bonding of the uppermost surface layers of the biomaterial scaffolds, determining its wettability and adhesion. Contact angle is a simple, sensitive, reliable and inexpensive method that allows the characterization of the biomaterial scaffold surface, named the physical properties of membranes [33]. It not requires special preparation of the sample, although the samples should be clean enough and do not swell or dissolve during the test.

Contact angle ($\theta$) is geometrically defined as the angle formed by the intersection of the liquid/solid interface and the liquid/gas interface[33, 34]. Figure 2.13 shows an illustration of the phenomenon occurred and how contact angle is measured. Experimentally, $\theta$ is measured by drawing a tangent at the contact interface between the liquid and solid phases. Contact angle is a quantitative measure of the wetting of a solid by a liquid, that characterizes the surface hydrophilicity/hydrophobicity of a biomaterials scaffold. For low contact angles ($\theta<90^\circ$, hydrophilic surface), the liquid spreads well over the surface, meaning the liquid has a strong affinity with the solid subtract; whereas high contact angles ($\theta>90^\circ$, hydrophobic surface) indicate poor wetting conditions, so the fluid will minimize its contact with the surface and form a compact liquid droplet. Thus, contact angle gives a direct evolution of interactions that occurs between the liquid, gas and solid phases.

The shape of a liquid droplet is determined by the surface tension of the liquid. In a pure liquid, the net force is equal to zero, because neighboring liquid molecules pulls equally in all directions [34]. However, the molecules in contact with the surface have not neighboring molecules in all directions to provide a balanced net force. As an alternative, they are pulled inward by neighboring molecules, creating an internal pressure. As a result, the surface area of a liquid is

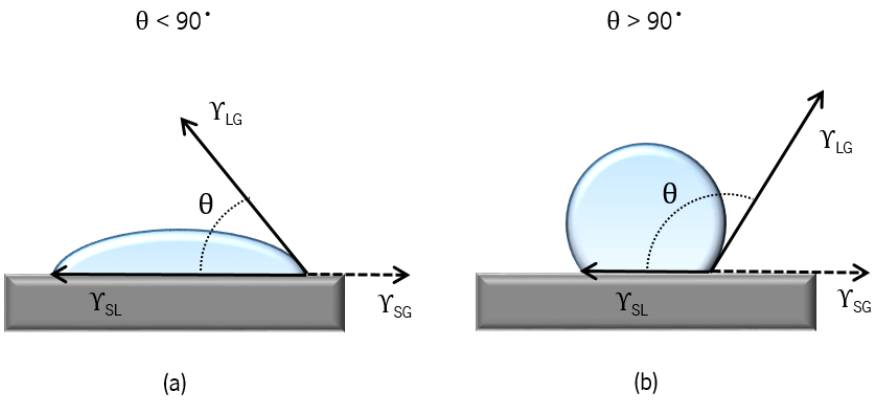


**Figure 2.13 -** Illustration of the sessile drop method by a solid hydrophobic (a) and hydrophilic (b) substrate. θ is the liquid contact angle, and $\Upsilon_{SL}$, $\Upsilon_{SG}$, and $\Upsilon_{LG}$ represents the solid/liquid, solid/gas, and liquid/gas interfaces, respectively. Adapted from [34].

contracted to maintain the lowest free energy. Figure 2.14 elucidates this phenomenon. The surface tension is the intermolecular force that contract the surface, which is responsible for the shape of the liquid droplet. The contact angle is determined by a combination of surface tension and external tension, such as gravity.

There are several types of contact angle measurement method, being the most usually used the Wilhelmy method, sessile drop method, and captive method [23, 33]. In this work sessile drop method was used. This static method is based on the vertical deposition of a drop of pure liquid onto the membrane surface and the contact angle was measured by a goniometer, using an optical sub-system. The angle measure is defined between the baseline of the drop and the tangent at the drop boundary, i.e., the angle formed between the solid/liquid interface and liquid/gas interface.

The water contact angles (sessile drop method) of the FSP membranes were determined at room temperature by a contact angle instrument - goinometer (OCA 15PLUS, DataPhysics). Contact angles were measured in the center and extremity, as well as in top and bottom of the FSP membrane. This conditions were performed in three independents membranes (each from different FSP batch). 1 µL of ultra-pure water was applied by a syringe at a rate of 3 µL/s at three different points of each membrane and the measurement was performed. The images of the water spreading over the sample's surface were recorded by a camera and then analyzed by using the software supplied by the manufacture. The presented data are averaged values those measurements.

#### 2.2.5.2 Surface zeta potential

Interactions between biomaterials' scaffolds and their surrounding tissues are mediated by their physicochemical surface properties. One of the main physical properties of a scaffold involved in the biological development of a tissue is the electric charge onto the material surface [35].

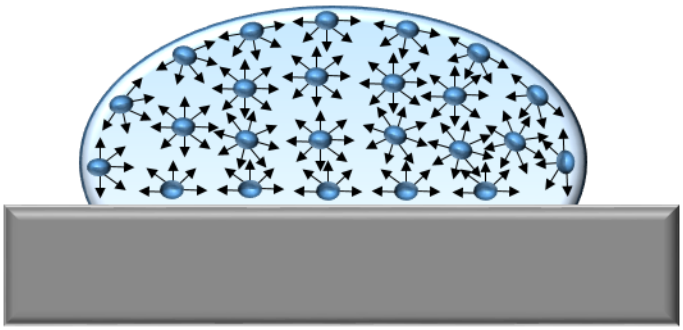

**Figure 2.14 -** Unbalanced forces of liquid molecules at the sample's surface, causing dg surface tension. Adapted from [34].

Zeta potential provides useful information about the surface charge of a material in an ionic solution, specifically at the boundary between the stern layer and the diffuse layer, named the shear plane (Figure 2.15). When a solid surface enters in contact with an aqueous solution, greater amount of materials will acquire a surface charge due to the dissociation of surface ionic groups [36, 37]. The electrostatic charge on the solid surface will attract counterions and repel co-ions presents in the solution. This electric double layer (EDL) is defined as a region close to the charged surface, where exists an excess of counterions that neutralize the surface charge. The stern layer is the liquid layer adjacent to the solid surface, where the ions are strongly attracted. These ions are temporarily bound and immobile at the charged surface. Beyond this layer, there is a diffusion layer where the ions are less affected by the electrostatic interactions of the solid surface, and the net charge density gradually decreases. The diffuse layer flows between the shears planes. The zeta potential ($\zeta$) is thus the electrical potential at the shear plane, characterizing the double-layer properties. Surface composition and solution properties (nature of the ions, ionic strength, and pH) influence the zeta potential.

Experimentally, zeta potential is generated when a liquid is forced to flow directly through a small gap formed between two flat sample surfaces under pressure (Figure 2.15) [36, 37]. In the streaming potential technique, between the ends of channels containing electrolyte, a pressure differential $(\Delta P)$ is applied to induce hydrodynamic flow. An electrical current - streaming current $(I_s)$ – results from the carriage of the ions presents in the diffuse layer of the EDL in direction of the flow. The streaming current is measured when the electrical potential difference between the two ends of the channel is zero, generated by the hydrodynamic flow of the electrolyte in an open circuit. This creates a conduction current $(I_c)$ that induces a flow of ions in the opposite direction of the flow. When the flow reaches a steady state and the conduction current is equal the streaming current, the streaming potential can be measured. A correct value of zeta potential is calculated from the measured streaming current and the dimensions of the cross section of the channel. Positive values of the zeta potential at fixed pH indicates a positive charge of the material surface, which would attract negatively charged entities, such as anions or charged proteins. On the other hand, negative values of the zeta potential at a fixed pH indicates a negative charge of the material surface, that attracts positively charged particles.

In this work, a electrokinetic analyzer (SurPASS, Anton Paar GmbH, Austria) was used to measure the zeta potential of the three different FSP membranes, applied in the channel, across a range of pH values between 6-8. The spit-type channel was 20 mm in length and 10 mm in

width, and had a variable cell height that was set to approximately 130 μm for all experiments. A 1 mM KCl solution was used as the electrolyte, and HCl (0.1 M) and NaOH (0.1 M) solutions were used to adjust the pH. The mean value of these data was present.

### 2.2.5.3 Circular dichroism spectroscopy

Circular dichroism (CD) is an optical spectroscopy method that allows determining the conformational changes and absolute configurations of active molecules, characterizing and quantifying their secondary structure, such as α-helix, β-sheet, or unordered structure [38, 39]. This spectroscopic technique can be applied to particular proteins in solution [39], as well as in thin amorphous dry films [40, 41].

CD measurements are relatively quick and allows an easy spectroscopic determination of the secondary structure content of proteins [39]. It uses small amounts of material and proteins of any size, and can be analyzed in solution, under specific conditions. Far UV CD spectroscopy is

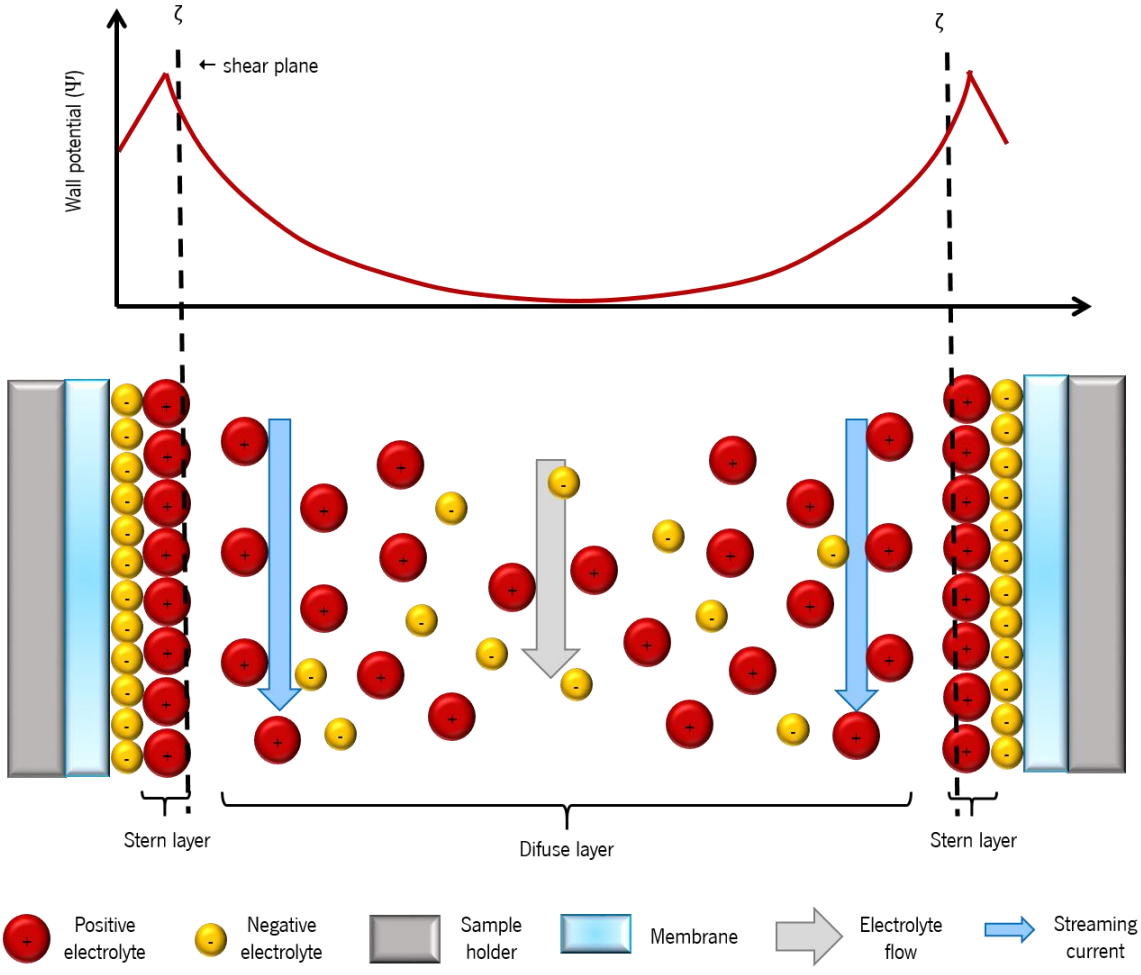


**Figure 2.15 -** Schematic diagram of the zeta potential measurement and illustration of the streaming current generated by electrolyte flow through the channel. Adapted from [36, 37].

also used to provide information on ligand-protein interactions and to monitor protein folding and unfolding. The tertiary structural information can be obtained from the CD spectra of protein aromatic residues in the near UV (from 250 to 300 nm) wavelength range.

Linear polarized light is composed of two circularly polarized components of equal magnitude: one rotating counter-clockwise (left handed, L) and the other clockwise (right handed, R) [42]. When the light passes through an optically active sample, a differential absorbance of the two circularly polarized components will be observed and the resulting radiation elliptically polarized. Thus, the CD is the differential absorption of left- and right-handed circular polarized light ($\Delta A = A_L - A_R$) after passage through the sample. This data is collected by a spectropolarimeter. When R and L components are not absorbed or are absorbed in an equal extent, the recombination of R and L would regenerate radiation polarized in the original plane. When the R and L components are absorbed at different extents, the resulting radiation will have elliptical polarization. A CD signal is observed when radiation strikes a chromophore, which is chiral (optically active), or have a three dimensional structure that provides a chiral environment, and the absorption occurs if electrons are promoted from a ground state to a higher energy state. The CD spectrum is obtained when the dichroism is measured as a function of the wavelength. CD data are presented in terms of ellipticity ($\theta$), in degrees. The ellipticity is the inverse of tangent, which is $b/a$, where $b$ is the minor axis and $a$ is the major axis of the resulting ellipse.

Spectral bands correspond to distinct structural features of a molecule, once CD signal are only present when absorption of radiation occurs. In proteins, the amide chromophores of interest include the peptide bond, whose absorption is between 240 and 190 nm (far UV absorption) [38, 40, 42, 43]. The peptide bond has two electron transitions responsible for the CD signals in this wavelength region: an $n \rightarrow \pi^*$ transition at ≈ 220 nm and a $\pi \rightarrow \pi^*$ transition at ≈ 208 and 190 nm. The characteristics of the CD signal from a single chromophore depends on the local torsion angles of the peptide backbone, i.e., the secondary structure. The CD spectrum represents the sum of signals from all peptide chromophores present in the sample. When a number of chromophores from the same type are in close proximity, the spectra has specific characteristic, because they can behave as a single absorption unit (exciton). The α-helix structure is composed by a negative peak at 222 nm, corresponding to the $n \rightarrow \pi^*$ transition, and in lower wavelengths a negative peak at 208 nm, followed by a positive peak at 192 nm. The β-sheet structure has a $\pi \rightarrow \pi^*$ transition with magnitudes that are normally three to five times smaller than those of α-helix. The β-sheet structure reveals variations in sheet-twist and the relative direction of the individual β-

standard, that is parallel and antiparallel. β-sheet proteins can have variations in the positions and intensities of the coupled $\pi \rightarrow \pi^*$ transition. Unordered structure is characterized by a single negative peak at ≈ 200 nm. The random (or disordered) conformation has a strong negative band at 196 nm, a weak positive band at 217 nm and a very weak negative band at 238 nm. The turn structure is composed by a weak negative peak between 220-230 nm, a positive peak at ≈210 nm, and a strong negative peak at 190 nm. Most proteins contain a mixture of secondary structure types and their spectra are linear combinations of the characteristics spectra. Figure 2.16 shows the different CD spectra for the α-helix, β-sheet and unordered conformations.

There are a wide number of computational algorithms that allows to estimate of the secondary structure composition of an unknown protein, with reference to databases composed of spectra of soluble proteins of known structures. These empirical methods use the data from UV CD spectra [39].

CD spectra (185-260 nm) of the FSP extracts and FSP membranes from all batches were recorded on a CD spectrometer (J-1500, JASCO, Tokio, Japan), at ambient temperature. Each FSP extract was dissolved in HFIP at a concentration of 0.1 mg/mL. HFIP was used as control. A quartz cell of 1 mm was used for spectral measurements of the FSP solution. FSP membranes were analyzed between two quartz cover slip with 25.4 mm diameter and 0.12 mm thickness. The quartz cover slips were used as control. Each spectrum was recorded in far-UV (190-260 nm) and was represented as an average of three consecutive scans measured at 1 nm resolution.

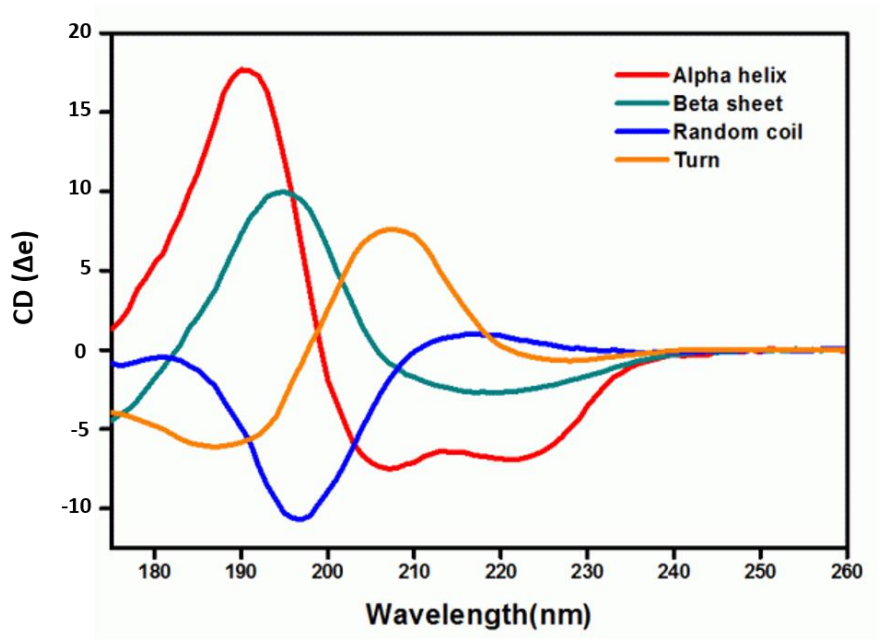


**Figure 2.16 -** Far-UV CD spectra associated with various types of secondary structure. Adapted from [44].

### 2.2.5.4 Infrared spectroscopy

The infrared (IR) spectroscopy is a vibrational spectroscopic technique based on the natural vibrations of chemical bonds, usually between the ground state and the first excitation state, among atoms that compose the material, due to interactions with IR radiation [45]. IR spectroscopy present significant advantages such as a large application range (from small soluble proteins to large membrane proteins), a high time resolution, a short measuring time and the low amount of sample required [46].

The IR spectroscopy uses an interferometer and the Fourier transform algorithm, providing the simultaneous detection of all transmitted energy [45]. Fourier transform IR (FTIR) spectrometer is composed by an IR source, an interferometer and an IR detector. The spectra can be obtained by transmission or reflection method. In the transmission methods, the detector measures the intensity of IR radiation that passes through the sample. In IR spectroscopy, the IR radiation focused on the sample and the changes in the absorption of this radiation by the sample are measured. Upon IR irradiation, when the molecular vibration coincides with the natural vibration, the sample absorbs radiation in the IR region due changes in the dipole moment during vibration (exciting vibration transitions of molecules). The laws of quantum mechanics rule this process, and the total energy of the molecule is increased (absorption) or decreased (emission) by one or more quanta. The total energy of a molecule can be the sum of four contributions: electronic, vibrational, rotational and translational energies, which may be considered separately. Change in the molecular vibration energy after infrared absorption or emission can be given by differences between the final energy and initial energy ($\Delta E = E_f - E_i$).

Vibrational frequency increases with bond strength. Characteristic vibrations of covalent bonds can be classified as *stretching*, when changes the bond length; *bending*, when changes the bond angle[47]. These two changes in vibration motion originate absorption bands in the vibrational spectrum. Certain groups of atoms originate vibrational bands at, or near, the same frequency, independently of the molecule or functional group.

The IR spectrum is plotted against the inverse of the wavelength, the wavenumber ($\tilde{\nu}$), which is directly proportional to the transition energy. The coordinates of the spectrum run from high wavenumbers to low wavenumbers, with the units $cm^{-1}$. The IR region is subdivided into three regions: the near IR (NIR – from 4000 to 14 000 $cm^{-1}$), mid IR (MIR – from 400 – 4000 $cm^{-1}$) and far IR (FIR – from 25–400 $cm^{-1}$). The MIR describes the primary molecular vibrations.

The transparent samples can be analyzed directly. For opaque samples the alkali metal halide pellet method should be used. Potassium bromide (KBr) is mixed with a small amount of the sample considering that this chemical compound is completely transparent in the MIR. Both samples and KBr dices should be dried [33, 45, 46].

IR spectroscopy was used in this work to study the structure of small molecules from the FSP proteins, due the sensitivity of this technique to the chemical composition and architecture of molecules. Thus, IR spectroscopy allows investigating the molecular mechanisms of protein reactions and protein folding, unfolding and misfolding. The chemical structure of a molecule is the dominate effect that determines vibrational frequencies via the strengths of the vibration bonds and the masses of the vibrating atoms. However, the chemical structure of a protein cannot be deduced from the infrared spectrum because this spectrum is composed of many overlapping bands. But, changes in the chemical structure can be detected [46].

The infrared spectrum of proteins contains several relatively strong absorption bands associated to the peptide bond, represented by C=O-NH from amide group (Figure 2.17). The backbone of the molecular mechanism of proteins are the amino acid side chains. Secondary structure analysis of proteins is done using the amide I band, that absorb in NIR region.

The amide I vibration is due the C=O stretching vibrations of the peptide group, absorbing near 1650 $cm^{-1}$. The amide I vibration is hardly affected by the nature of side chain. However, it depends on the secondary structure of the backbone. Due to the sensibility of the secondary structure, the amide I band of can expose the α-helix and β-sheet structures of a protein in a specific region of the amide I. The α-helix presents an absorption band close to 1655 $cm^{-1}$ [48]. With the increasing length of helix, when the helix is bent in coils and is exposed to a solvent, the band position of the helix shifts down. The typical α-helix absorption can be different, i.e. several bands throughout the amide I region, when the α-helix is short (less 6 residues) [49-51]. Antiparallel β-sheets from proteins exhibits a strong band near 1630 $cm^{-1}$ and a weaker band near

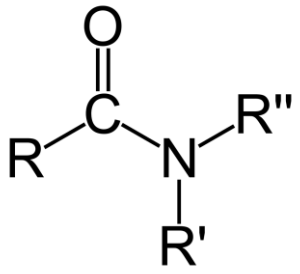


**Figure 2.17 -** Amide group.

1685 $cm^{-1}$ [48]. The number of amide groups in the strands of the sheet affects the position of these bands. Sheets with a larger number of strands have a lower spectral position of a main band. The twist of an antiparallel β-sheets causes a shift the main band to higher wavenumbers. Parallel β-sheets absorbs at higher wavenumber than antiparallel β-sheets, being difference as little as 4 $cm^{-1}$. Experimentally, it is difficult to distinct between parallel and antiparallel β-sheets. On the other hand, the folded protein exhibits a structured amide I spectrum and the unfolded protein shows a larger and featureless amide I band centered near 1650 $cm^{-1}$, which is characteristic of unordered structure. Aggregated protein exhibits a band near or below 1620 $cm^{-1}$, which is characteristic of intermolecular β-sheets [52].

In this study, to qualitatively evaluate the secondary structure of proteins, to determine the α-helix and β-sheet structures, the FTIR analysis was performed. Samples from different batches of FSP extracts and corresponding FSP membranes were dried overnight in an exicator. The FSP extracts were mixed with potassium bromide and processed into pellets and the membranes were analyzed directly with help of a support. Spectra were recorded at 32 scans with a resolution of 4 $cm^{-1}$, from 4400 $cm^{-1}$ to 440 $cm^{-1}$ (IR Prestige 21, Shimadzu, Japan).

### 2.2.6 Biological characterization

Cell culture assays are used to assess the biocompatibility of a material or extract through the use of isolated cells *in vitro*. To evaluate the biological response of mammalian cells to FSP, an *in vitro* cytotoxicity assay was performed. The cytotoxic test provides changes in morphology and in the cell's number. It can directly reflex the impact of testing biomaterial extracts over the culturing cells [53].

#### 2.2.6.1 MRC-5 cell line

According to the ISO 10993-5:2009, cell lines are preferred to test cytotoxicity of biomaterials [54]. Human lung fibroblastic cells, i.e. MRC-5 cell line, were used to perform this test. MRC-5 are human diploid cells derived from normal lung tissue of a 14-week-old male fetus. MRC-5 cells evidence the characteristic fibroblastic morphology (Figure 2.18), i.e., cells are bipolar or multipolar with elongated shapes. They grow attached to a substrate [53].

### 2.2.6.2 Cells seeding

MRC-5 cells were grown in T150 culture flasks (Corning Incorporated, USA), in Dulbecco's modified eagle's medium (DMEM) supplemented with 10% fetal bovine serum (FBS) and 1% antibiotic/antimycotic solution, at 37°C in an atmosphere of 5% $CO_2$. To run the experiment, the cells were previously detached from the culture flask by using TrypLE Express.

i) FSP extracts cytotoxicity

The cytotoxicity of FSP extracts was determined by the extraction test, which detects the rate of toxicity of soluble substances from biomaterial scaffold [53]. For this, a monolayer of cells is exposed to an extract. The reaction of these cells on the presence of the extracts is evaluated over time. If the extracts are not toxic, the cells will proliferate without change the morphology. If the extracts are toxic, the cells will have a growth inhibition, a decrease/increase of the metabolism, an intracellular granulation, a cell death or a change in cell morphology (often caused by adhesion inhibition).

In this study, the MRC-5 cells were seeded at a density of 5 x $10^4$ cell/well of 24-wells culture plate (Corning Incorporated, USA) and incubated for 24h at 37°C, in a humidified atmosphere with 5% $CO_2$. During this culturing time, the cells were allowed to adhere to the surface of the well. FSP extracts at different concentrations (5, 10, 20, 50, 100 mg/mL) were dissolved in DMEM immediately before their addition to the cells in culture. The culture medium was removed from the wells and an identical volume (1mL) of FSP suspension was added. The MRC-5 cells in culture

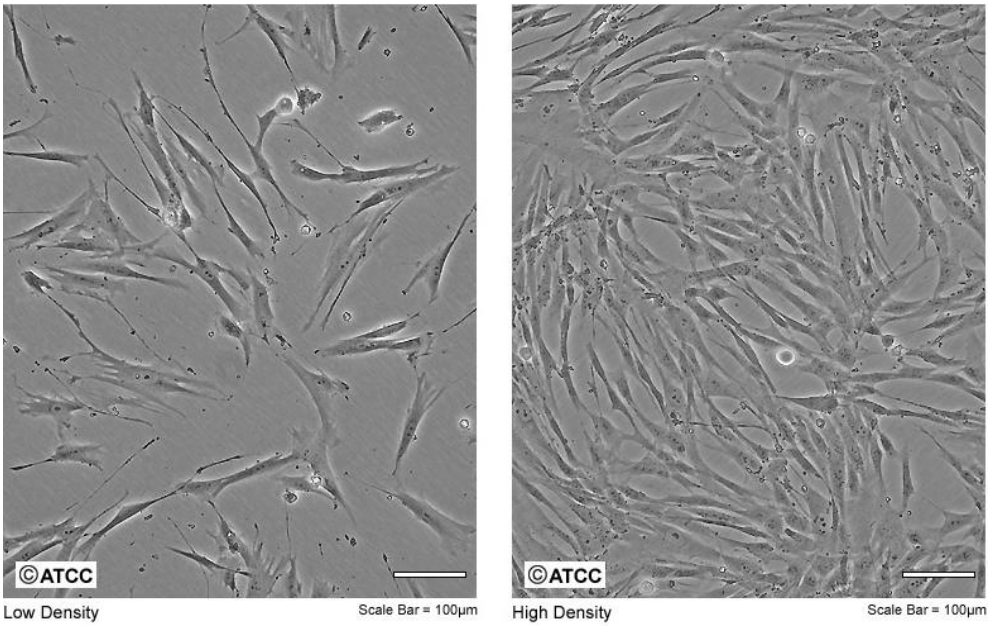


**Figure 2.18 -** MRC-5 cell micrographs showing the fibroblastic morphology.

were incubated with the different concentrations of FSP extracts for 24h, 48h and 72h. The negative control comprises MRC-5 cells just in culture medium.

ii) FSP membranes cytotoxicity

The cytotoxicity of FSP membranes was determined by the direct contact method, which consists in the direct seeding and culturing of mammalian cells onto FSP membranes [53]. The cells are then incubated and during this time, leachables in the FSP membranes can diffuse into the culture medium and contact the cell layer. The biomaterial scaffold is toxic when the cells show malformation, degeneration and lysis. If the biomaterial scaffold is not toxic, during the *in vitro* culture period, the seeded cells proliferate and secrete tissue specific extracellular matrix (ECM). For that, FSP membranes were cut into 10 x 10 mm pieces and they were sterilized by UV irradiation during 30 minutes in each side. Then, they were placed into 24-wells culture plate. Tissue culture polystyrene (TCPS) coverslips were used as a negative controls of cells proliferation. A 100 µL cell suspension containing 5 x $10^4$ cell was seeded over FSP membranes and controls (n=3). After 5h the remain culture medium (900 µL) was added to each well. Cells viability was determined after 24h, 48h, and 72h of direct contact.

### 2.2.6.3 Cells metabolic activity

To evaluate if the FSP extracts or membranes have effects on MRC-5 cells or show direct cytotoxic effects that lead probably to cell death, a cell-viability assay was used [55, 56]. There are several methods that can be used to estimate the number of viability eukaryotic cells. These methods measure the general cells metabolism or an enzymatic activity of a marker of viable cells, such as tetrazolium reduction, resazurin reduction, protease markers, and ATP detection. All these procedures are used in multi-well formats and need the incubation of a reagent with a population of viable cells, allowing to convert a reacting substance to a colored or fluorescent product that can be detected using a microplate reader. This signal is proportional to the number of viable cells. When cells die, they lose the ability to convert the substance to its product.

Focusing on tetrazolium compounds to determine viable cells, MTT, MTS, XTT, and WST-1 are the compounds mostly used. The compounds can be positively charged, which quickly penetrate into viable cells (e.g. MTT), or negatively charged, which do not quickly penetrate cells (e.g. MTS, XTT, WST-1). The negative charged compounds do not penetrate into viable cells, whereby are used with an intermediate electron acceptor, such as phenazine methyl sulfate (PMS) or phenazine ethyl sulfate (PES), which can be introduced into viable cells. Intermediate electron

acceptor is reduced in the cytoplasm or in the plasmatic membrane, transferring electrons to facilitate the reduction of the tetrazolium reagent into colored formazan product by viable cells, that is soluble in cell culture medium. These electrons come from metabolically active cells where dehydrogenase enzymes produced NADPH or NADH. This reaction scheme for tetrazolium reagent is shown in Figure 2.19.

The cells viability was determined by the dehydrogenase activity of MRC-5 cells using MTS assay (CellTiter 96® $AQ_{ueous}$ One Solution Cell Proliferation Assay, Promega). This calorimetric method contains MTS (3-(4,5-dimethylthiazol-2-yl)-5-(3-carboxymethoxyphenyl)-2-(4-sulfophenyl)-2H-tetrazolium) as tetrazolium compound and PES as electron coupling reagent. After 24, 48 and 72 hours of MRC-5 cells culture, the medium with FSP extracts or membranes was removed and gently washed twice with sterilize phosphate buffer solution (PBS). Serum-free culture medium without phenol red and MTS reagent was added to each well at a ratio of 5:1. Cells were incubated at 37°C for 3h in a humidified atmosphere contain 5% $CO_2$. All conditions were performed in triplicate. After this incubation time, a volume of 100 µL of the solution was transferred to a 96-well plate and the absorbance was recorded in triplicate at 490 nm on a microplate reader (SYNERGY HT, BIO-TEK, USA).

Many variables can contribute to the background 490 nm absorbance, such as the type of culture medium, type of serum, pH and exposure to light. Background absorbance may result from the chemical interference of certain compounds with tetrazolium reduction reactions. Strong reducing substances, such as ascorbic acid or sulfhydryl-containing compounds, can reduce tetrazolium salts non enzymatically and lead to increased background absorbance values. For this reason, it was prepared a set of control wells without cells, with the same culture medium/MTS

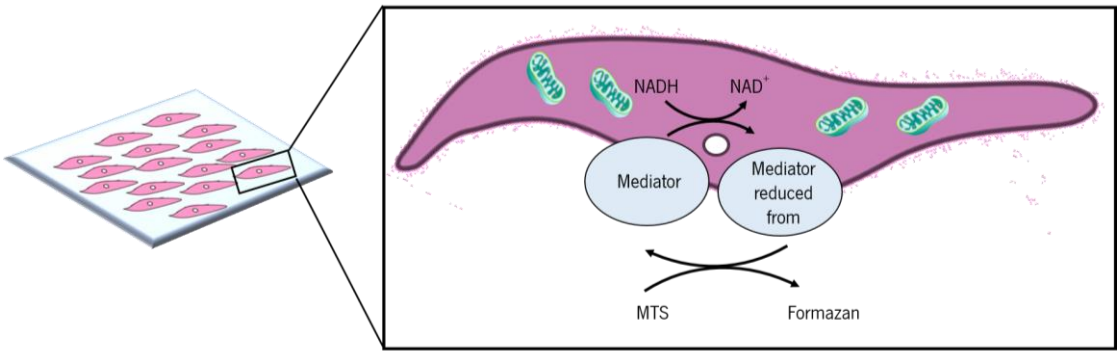


**Figure 2.19 -** Intermediate electron acceptor pheazine ethyl sylfate (PES) transfers electrons from NADH in the cytoplasm, to reduce MTS, in the culture medium, to an aqueous soluble formazan. Adapted from [55].

ratio and incubated in the same conditions. The average 490 nm absorbance from these background wells was subtracted to all other absorbance values to obtain corrected absorbances. It is important to highlight that the plate should be protected from light, since MTS reagent is light-sensitive and discoloration may occur, causing difference at 490 nm absorbance readings.

#### 2.2.6.4 Cells morphology

To observe cells adhering and morphology, as well as their distribution on the surface of TCPs and FSP membranes SEM was used. Biological samples are hydrated and non-conductive. Therefore, before they are observed into the SEM, a series of pre-treatments such as structure fixing, sample drying, and deposition of a conductive coating are required.

At the established times points, the medium was removed and the cells were washed with sterile PBS. A 2.5% glutaraldehyde in PBS solution were added to the samples to fixed cells to the substracts. The plates were paced at 4°C. Then, the samples were dehydrated with graded series of ethanol, ranging from 10 to 100%, and let to dry over night at room temperature. Cells adhered to FSP membranes and cells submitted to FSP extracts were observed by SEM (JSM-6010 LV, Jeol, Japan). The samples were sputter-coated with gold to be conductive. Micrographs were recorded at 10 kV with magnifications ranging from 100 to 1000 times.

#### 2.2.6.5 Statistical analysis

Statistical analysis was performed using Graph Pad Prism Software. Differences between the different conditions of the cellular assays were analyzed using non-parametric test (Kruskal-Wallis test for FSP extracts and Man-Whitney test for FSP membranes assays) and a $p<0.01$ was considered significant. Data were presented as mean ± standard deviations.

## 2.3 REFERENCES

[1] D.M. Cohen, T. Inada, T. Iwamoto, N. Scialabba, FAO species catalogue. Vol. 10. Gadiform fishes of the world (Order Gadiformes). An annotated and illustrated catalogue of cods, hakes, grenadiers and other gadiform fishes known to date., FAO, Rome, 1990.

[2] J. Oehlenschläger, H. Rehbein, Basic Facts and Figures, Fishery Products, Wiley-Blackwell2009, pp. 1-18.

[3] R. Tahergorabi, S.V. Hosseini, J. Jaczynski, Seafood proteins, in: G.O.P.a.P.A. Williams (Ed.), Handbook of Food Proteins, Woodhead Publishing2011, pp. 116-149.

[4] Chemours, Hexafluoroisopropanol, Technical Information, DuPont Chemicals and Fluoroproducts, 2012.

[5] A. Apffel, J.A. Chakel, S. Fischer, K. Lichtenwalter, W.S. Hancock, Analysis of oligonucleotides by HPLC-electrospray ionization mass spectrometry, Analytical Chemistry 69(7) (1997) 1320-1325.
[6] K. Stephansen, I.S. Chronakis, F. Jessen, Bioactive electrospun fish sarcoplasmic proteins as a drug delivery system, Colloids and Surfaces B: Biointerfaces 122 (2014) 158-165.
[7] Y.J. Choi, S.-K. Jin, Recovery of fish protein using pH shift processing, in: S.-K. Kim (Ed.), Seafood Science: Advances in Chemistry, Technology and Applications, CRC Press., Boca Raton, 2015, pp. 117-131.
[8] K. Hashimoto, S. Watabe, M. Kono, K. Shiro, Muscle protein-composition of sardine and mackerel, Bulletin of the Japanese Society of Scientific Fisheries 45(11) (1979) 1435-1441.
[9] W. Visessanguan, S. Benjakul, S. Riebroy, P. Thepkasikul, Changes in composition and functional properties of proteins and their contributions to Nham characteristics, Meat Science 66(3) (2004) 579-588.
[10] J.Y. Ren, M.M. Zhao, J. Shi, J.S. Wang, Y.M. Jiang, C. Cui, Y. Kakuda, S.J. Xue, Optimization of antioxidant peptide production from grass carp sarcoplasmic protein using response surface methodology, Lwt-Food Science and Technology 41(9) (2008) 1624-1632.
[11] D. Smith, Fish Muscle Proteins: Extraction, Quantitation, and Electrophoresis, in: S.S. Nielsen (Ed.), Food Analysis Laboratory Manual, Springer US2010, pp. 115-122.
[12] T. Hashimoto, T. Suzuki, T. Hagiwara, R. Takai, Study on the glass transition for several processed fish muscles and its protein fractions using differential scanning calorimetry, Fisheries Science 70(6) (2004) 1144-1152.
[13] K. Stephansen, M. Mattebjerg, J. Wattjes, A. Milisavljevic, F. Jessen, K. Qvortrup, F.M. Goycoolea, I.S. Chronakis, Design and characterization of self-assembled fish sarcoplasmic protein–alginate nanocomplexes, International Journal of Biological Macromolecules 76 (2015) 146-152.
[14] Y.S. Kim, J. Yongsawatdigul, J.W. Park, S. Thawornchinsombut, Characteristics of sarcoplasmic proteins and their interaction with myofibrillar proteins, Journal of Food Biochemistry 29(5) (2005) 517-532.
[15] Bio-Rad, A Guide to Polyacrylamide Gel Electrophoresis and Detection, Bio-Rad.
[16] D.P. Birnie, Spin Coating Technique, in: M. Aegerter , M. Mennig (Eds.), Sol-Gel Technologies for Glass Producers and Users, Springer US, New York, 2004.
[17] M.D. Tyona, A theoritical study on spin coating technique, Advances in Material Research 2(4) (2013) 195-208.
[18] N. Sahu, B. Parija, S. Panigrahi, Fundamental understanding and modeling of spin coating process: A review, Indian Journal of Physics 83(4) (2009) 493-502.
[19] M. Mozafari, A. Ramedani, Y.N. Zhang, D.K. Mills, Thin films for tissue engineering applications, in: H.J. Griesser (Ed.), Thin Film Coatings for Biomaterials and Biomedical Applications, Woodhead Publishing2016, pp. 167-195.
[20] A.G. Emslie, F.T. Bonner, L.G. Peck, Flow of a Viscous Liquid on a Rotating Disk, Journal of Applied Physics 29(5) (1958) 858-862.
[21] D. Meyerhofer, Characteristics of resist films produces by spinning, Journal of Applied Physics 49(7) (1978) 3993-3997.
[22] R.T. Dombrowski, Microscopy techniques for analyzing the phase nature and morphology of biomaterials, Characterization of Biomaterials, Woodhead Publishing2013, pp. 1-33.
[23] H. Wang, P.K. Chu, Surface Characterization of Biomaterials, in: S. Bose (Ed.), Characterization of Biomaterials, Academic Press, Oxford, 2013, pp. 105-174.
[24] ASM International, Introduction to Tensile Testing, in: J.R. Davis (Ed.), Tensile Testing United States of America, 2004, pp. 1-12.

[25] ASM International, Mechanical Behavior of Materials under Tensile Loads in: J.R. Davis (Ed.), Tensile Testing, United States of America, 2004, pp. 13-31.
[26] R.K. Roeder, Mechanical Characterization of Biomaterials, in: S. Bose (Ed.), Characterization of Biomaterials, Academic Press, Oxford, 2013, pp. 49-104.
[27] ASM International, Uniaxial Tensile Testing, in: J.R. Davis (Ed.), Tensile Testing2004, pp. 33-63.
[28] S.J. Demarest, V. Frasca, Differential Scanning Calorimetry in the Biopharmaceutical Sciences, in: S.A. Berkowitz (Ed.), Biophysical Characterization of Proteins in Developing Biopharmaceuticals, Elsevier, Amsterdam, 2015, pp. 287-306.
[29] C.M. Johnson, Differential scanning calorimetry as a tool for protein folding and stability, Archives of Biochemistry and Biophysics 531(1–2) (2013) 100-109.
[30] G. Bruylants, J.W.a.C. Michaux, Differential Scanning Calorimetry in Life Science: Thermodynamics, Stability, Molecular Recognition and Application in Drug Design, Current Medicinal Chemistry 12(17) (2005) 2011-2020.
[31] D. Skipnes, I. Van der Plancken, A. Van Loey, M.E. Hendrickx, Kinetics of heat denaturation of proteins from farmed Atlantic cod (*Gadus morhua*), Journal of Food Engineering 85(1) (2008) 51-58.
[32] S. Vyazovkin, Thermogravimetric Analysis, in: E.N. Kaufmann (Ed.), Characterization of Materials2012, pp. 1–12.
[33] T.S.S. Kumar, Physical and Chemical Characterization of Biomaterials, in: S. Bose (Ed.), Characterization of Biomaterials, Academic Press, Oxford, 2013, pp. 11-47.
[34] Y.L. Yuan, T. R., Contact Angle and Wetting Properties, in: B.H. Gianangelo Bracco (Ed.), Surface Science Techniques, Springer Berlin Heidelberg2013, pp. 3-34.
[35] A. Krajewski, A. Piancastelli, R. Malavolti, Albumin adhesion on ceramics and correlation with their Z-potential, Biomaterials 19(7) (1998) 637-641.
[36] H. Xie, T. Saito, M.A. Hickner, Zeta Potential of Ion-Conductive Membranes by Streaming Current Measurements, Langmuir 27(8) (2011) 4721-4727.
[37] K. Cai, M. Frant, J. Bossert, G. Hildebrand, K. Liefeith, K.D. Jandt, Surface functionalized titanium thin films: Zeta-potential, protein adsorption and cell proliferation, Colloids and Surfaces B: Biointerfaces 50(1) (2006) 1-8.
[38] A.J. Miles, B.A. Wallace, Circular Dichroism Spectroscopy for Protein Characterization: Biopharmaceutical Applications, in: S.A.B. Damian J. Houde (Ed.), Biophysical Characterization of Proteins in Developing Biopharmaceuticals, Elsevier, Amsterdam, 2015, pp. 109-137.
[39] B.A. Wallace, J.G. Lees, A.J.W. Orry, A. Lobley, R.W. Janes, Analyses of circular dichroism spectra of membrane proteins, Protein Science : A Publication of the Protein Society 12(4) (2003) 875-884.
[40] L. Stevens, R. Townend, S.N. Timasheff, G.D. Fasman, J. Potter, The circular dichroism of polypeptide films, Biochemistry 7(10) (1968) 3717-3720.
[41] G.D. Fasman, H. Hoving, S.N. Timasheff, Circular dichroism of polypeptide and protein conformations. Film studies, Biochemistry 9(17) (1970) 3316-3324.
[42] S.M. Kelly, T.J. Jess, N.C. Price, How to study proteins by circular dichroism, Biochimica et Biophysica Acta (BBA) - Proteins and Proteomics 1751(2) (2005) 119-139.
[43] A.J. Miles, B.A. Wallace, Circular dichroism spectroscopy of membrane proteins, Chemical Society Reviews 45(18) (2016) 4859-4872.
[44] A Method using Match and Linear Regression to Estimate Protein Secondary Structure from Circular Dichroism Spectra. 2016).

[45] J.L.R. Arrondo, A. Muga, J. Castresana, F.M. Goñi, Quantitative studies of the structure of proteins in solution by fourier-transform infrared spectroscopy, Progress in Biophysics and Molecular Biology 59(1) (1993) 23-56.
[46] A. Barth, Infrared spectroscopy of proteins, Biochimica et Biophysica Acta (BBA) - Bioenergetics 1767(9) (2007) 1073-1101.
[47] L.J. Bellamy, The Infrared Spectra of Complex Molecules, Springer Netherlands1980.
[48] V. Cabiaux, R. Brasseur, R. Wattiez, P. Falmagne, J.M. Ruysschaert, E. Goormaghtigh, Secondary Structure of Diphtheria Toxin and Its Fragments Interacting with Acidic Liposomes Studied by Polarized Infrared Spectroscopy, Journal of Biological Chemistry 264(9) (1989) 4928-4938.
[49] N.A. Nevskaya, Y.N. Chirgadze, Infrared spectra and resonance interactions of amide-I and II vibrations of α-helix, Biopolymers 15(4) (1976) 637-648.
[50] T. Heimburg, J. Schuenemann, K. Weber, N. Geisler, Specific Recognition of Coiled Coils by Infrared Spectroscopy: Analysis of the Three Structural Domains of Type III Intermediate Filament Proteins, Biochemistry 35(5) (1996) 1375-1382.
[51] W.C. Reisdorf, S. Krimm, Infrared Amide I' Band of the Coiled Coil, Biochemistry 35(5) (1996) 1383-1386.
[52] J. Kubelka, T.A. Keiderling, Differentiation of β-Sheet-Forming Structures: Ab Initio-Based Simulations of IR Absorption and Vibrational CD for Model Peptide and Protein β-Sheets, Journal of the American Chemical Society 123(48) (2001) 12048-12058.
[53] W. Li, J. Zhou, Y. Xu, Study of the in vitro cytotoxicity testing of medical devices, Biomedical Reports 3(5) (2015) 617-620.
[54] I.O.f. Standardization, Biological evaluation of medical devices, Part 5: Tests for in vitro cytotoxicity, 2009.
[55] T.L. Riss, R.A. Moravec , A.L. Niles , S. Duellman , H.A. Benink , T.J. Worzella , L. Minor, Cell Viability Assays, in: C.N.P. Sittampalam G.S., Nelson H. et al. (Ed.), ssay Guidance Manual [Internet], Bethesda (MD): Eli Lilly & Company and the National Center for Advancing Translational Sciences2013.
[56] Promega, CellTiter 96 Aqueous One Solution Cell Proliferation Assay, Technical Bulletin No. 245, USA.

# CHAPTER 3

Research Article

# FISH SARCOPLASMIC PROTEINS AS A MARINE-ORIGIN MATERIAL WITH POTENTIAL FOR TISSUE ENGINEERING AND REGENERATIVE MEDICINE

Sara Vieira [1,2], Albina R. Franco [1,2], Emanuel M. Fernandes [1,2], Sara Amorim [1,2], Helena Ferreira [1,2], Ricardo A. Pires [1,2], Rui L. Reis [1,2], Albino Martins [1,2], Nuno M. Neves [1,2]

[1] 3B's Research Group – Biomaterials, Biodegradables and Biomimetics, University of Minho, Campus de Gualtar, 4710-057 Braga, Portugal [2] ICVS/3B's, PT Government Associate Laboratory, Braga/Guimarães, Portugal

## Abstract

Fish sarcoplasmic proteins (FSP) constitute around 25–30% of the total fish muscle protein, comprising enzymes and heme proteins. As the FSP are water soluble, large quantities are discarded as part of waste water from fish surimi preparation. Therefore, the development of new applications for this marine waste products has critical importance. Herein, fresh codfish (*Gadus morhua*) was centrifuged and the supernatant was freeze-dried to isolate the FSP. By SDS-PAGE, it was possible to define the composition of FSP extracts. Different batches from different individuals provided similar protein compositions. The FSP denature at 44.12 ± 2.34˚C as characterized by differential scanning calorimetry thermograms (DSC). The thermal degradation was observed at 329˚C by thermogravimetric analysis (TGA). The secondary structure of FSP is mainly composed by α-helix structure, as determined by circular dichroism (CD) and conformed by FTIR. The cytocompatibility of FSP extracts, at concentrations ranging from 5 to 20 mg/mL, was investigated with human lung fibroblasts (MRC-5 cell line). For concentrations lower than 10 mg/mL, no cytotoxicity was observed over 72h of culture. FSP membranes were produced by spin coating technique to evaluate its properties. FSP membranes had uniform surface as analyzed by SEM, and the amount of α-helix structure increased when compared with the FSP extracts. The FSP membranes are more stable than the FSP extracts, since they presented a denaturation temperature of 58.88 ± 3.36˚C, according to the DSC thermogram, and two stages of thermal degradation. FSP membranes were hydrophobic, with a surface zeta potential of -33.4 mV, showing distinctive mechanical properties, with a stiffness of 16.57 ± 3.95 MPa and a yield strength of 23.85 ± 5.97 MPa. Human fibroblasts cultured in direct contact with FSP membranes demonstrate their cytocompatibility until 48h, but its stability affected negatively the cytocompatibility at 72h of culture. Based on these results, FSP can be considered a potential biomaterial recovered from the waste water of fish.

**Keywords:** cytocompatibility, codfish, membranes, physico-chemical characterization, sarcoplasmic proteins, spin coater.

## 3.1 Introduction

The ocean is a vast and rich repository of natural resources. In the past five decades, the growth in the supply of fish for human consumption has outpaced the population growth [1]. In 2014, capture fisheries and aquaculture supplied about 167 million tonnes of fish, of which about 146 million tonnes were used as food for people. The remaining 21 million tonnes was destined for non-food products, where 76% was reduced to fishmeal and fish oil, and the rest being largely used for a variety of purposes, including as raw material for direct feeding in aquaculture. This reduces the fish-derived waste.

Fish has long been recognized as a health promoting food [1]. Evidences suggest that the benefits of fish consumption are not limited to the well-appreciated effects of omega-3 fatty acids. Fish proteins are associated with a risk reduction of type 2 diabetes [2-5]. Dietary cod protein suppresses the non-esterified fatty acid and triacylglycerol contents in serum, and decreases the hepatic triacylglycerol and fatty acid desaturase indices [6]. Fish protein, when compared with casein, was reported to lower blood pressure and allows lowering liver cholesterol and phospholipid concentrations [7-9]. It was also demonstrated a beneficial metabolic effect of cod-scallop in diet, namely in the reduction of aorta atherosclerosis, body weight, visceral adipose tissue, serum glucose and leptin levels [10].

The proteins of fish muscle can be divided into three major classes based on their solubility in aqueous solutions: connective tissue (stroma) proteins (3%), myofibrillar proteins (MPs) (70-80%) or sarcoplasmic proteins (SPs) (25-30%) [11]. The MPs and the stroma proteins are water insoluble, whereas the SPs are soluble in water. Fish sarcoplasmic proteins (FSP) have relatively low molecular weights, globular- or rod-like conformation and low viscosity [12]. FSP comprise several types of proteins, including heme proteins [13] (hemoglobin and myoglobin) and enzymes, such as creatine kinase [14], aldolase [14], glyceraldehyde-3-phosphate dehydrogenase (GAPDH) [14], phosphorylase [15], proteinase inhibitors [16], proteases A and C [17], phospholipase [18], peroxidase [19], transglutaminase (TGase) [20], fructose-bisphosphate aldolase A [21], glycogen phosphorylase [21], beta-enolase [21], triosephosphate isomerase B [21], phosphoglucomutase [21], phosphoglycerate kinase [21], parvalbumins and calmodulins [11, 22].

Over the last years, fish proteins have been proposed as biopolymer films to protect and preserve food, pharmaceuticals and other products, mainly due to their advantages over synthetic polymers, such as biodegradability and environmental characteristics. Only few studies with FSP

demonstrated the film-forming potential due to the poor functional properties [23]. Iowata *et al.* (2000) and Tanaka *et al.* (2001) demonstrated that SPs from blue marlin (*Makaira mazara*), despite their low molecular weight, are able to form flexible films [23, 24]. As the SPs also have the capacity to form a continuous matrix, Paschoalick *et al.* (2003) hypothesized that edible films can be produced by the mixture of SPs with MPs [25]. Other studies also reported the development of homogeneous, colorless, resistant and workable films by casting technique of myofibrillar and sarcoplasmic fraction from Thai and Nile Tilapia muscle [26-28]. The possibility to substitute petroleum-derived synthetic polymers, which cause severe environmental pollution and toxicity, and degrade slowly under environmental conditions, is highly appealing. Recently, Sett *et al.* (2016) proposed a mixture of FSP from codfish (*Gadus morhua*) with nylon 6 as a substitute of traditional synthetic polymers [29]. In the biomedical approach, Stephansen *et al.* (2014) developed and characterized a bioactive electrospun nano-microfiber mesh based on FSP from codfish (*Gadus morhua*) [30], proposing the gastrointestinal delivery of insulin from FSP nanofibers [31]. , Stephansen *et al.* (2015) also reposted a nanocomplexes obtained by electrostatic self-assembling complexation, formed between SPs isolated from codfish and alginate (FSP-Alg) [32].

As the FSP are water soluble, they become part of the waste water of surimi preparation from fish (e.g. hake, cod and Alaska Pollock), which is discarded [13, 33, 34]. In fact, the amount of total FSP being lost is estimated to be at least 5000 tons as a dry base per year [35]. Although these proteins are nutritionally equivalent to the myofibrillar proteins of the muscle, and have been considered a potential source of enzymes, there has been little incentive to recover them [36].

In the present study, FSP from codfish (*Gadus morhua*) were isolated and processed into FSP membranes, by the spin coating technique, as a substrate. Both FSP extracts and membranes were physicochemically characterized to evaluate their secondary structure, the denaturation and the thermal degradation. The morphology, the surface charge density and the mechanical properties of FSP membranes were also analyzed. Cytocompatibility assays with human lung fibroblasts (MRC-5 cell line) were conducted for FSP extracts and membranes (in direct contact).

## 3.2 Materials and Methods

### 3.2.1 Materials

Codfish (*Gadus morhua*) from the Norway Sea (Northeast Atlantic) was purchased from MAKRO, Braga. 1,1,1,3,3,3-Hexafluoro-2-propanol (HFIP) was obtained from Sigma-Aldrich

Company, St. Louis, USA. Biotech Cellulose Ester Dialysis Tubing (cutoff 3.5-5 kDa) was purchased from Spectrum Labs and kept at 4°C until further use.

### 3.2.2 FSP extraction

Fish sarcoplasmic proteins were extracted according to the procedure described by Stephansen *et al.* (2014) with some alterations [30]. Codfish muscle was filleted and frozen at -20°C until further use. The frozen fillet was cut into small pieces and centrifuged at 18000 g during 20 minutes and at 3°C (5810R, Eppendorf, Germany). The supernatants were collected and transferred to dialysis tubes with a cutoff of 3.5-5 kDa. The pH of codfish muscle pieces and of the supernatant was monitored with a pH meter (PHS-3BW, SCANSCI). The dialysis was performed against ultra-pure water at 4°C under stirring. The dialyzed supernatant was freeze dried (CryoDos -80, Telstar, London) and the resulting product, which were the fish sarcoplasmic proteins (FSP), was stored at -20°C. This procedure was repeated for two cod fishes to assure the reproducibility of the method, resulting in three bathes.

### 3.2.3 SDS-PAGE

Detergent sodium dodecyl sulfate polyacrylamide gel electrophoresis (SDS-PAGE) was performed for the three batches of FSP extracts to analyze their protein composition. It was used a handcast gel composed of 4% acrylamide, as stacking gel, and 9% acrylamide, as separation gel. The three batches of FSP extracts at 1 mg/mL were dissolved in ultra-pure water. The protein samples and standards were prepared as follow: 6 µL of each protein sample was mixed with 24 µL of loading buffer (15 mM Tris-HCl pH 6.8, 2.5% -SDS, 25% glycerol, 0.1% bromophenol blue, 5% DTT); 5 µL of protein standard were mixed with 24 µL of loading buffer and 1 µL of ultra-pure water; as blank, 24 µL of loading buffer and 6 µL of ultra-pure water were mixed and load on each free well. All mix samples were heated for 30 minutes at 65°C, following denaturation step of 5 minutes at 95°C. The electrophoresis system was assembled with the polyacrylamide gel and the running buffer (250 Mm Tris, 1.92M glycine and 1% SDS) was added to reservoirs. 30 µL of each protein, protein standards, and the marker were loaded. A constant voltage of 150 V was applied until the bromophenol blue reached the bottom of the gel. The gel was stained with coomassie blue (0.125% coomassie blue R-250, 50% methanol, 10% acetic acid) during overnight. The gel was placed into distaining solution I (29% methanol, 5% acetic acid) during 24h. The distaining

solution I was removed and the distaining solution II (5% methanol, 7% acetic acid) was added to gel overnight. In this point, the gel could be visualized.

### 3.2.4 Production of FSP membranes by the spin coating technique

Spin coating technique was used to produces FSP membrane as a substrate to cell culture. Spin coated FSP membranes were prepared from 100 mg/mL solutions of FSP dissolved in HFIP, stirring overnight. Solution puddles ranging between 0.5 and 1.5 mL were dispensed in the coater of a polystyrene petri dish (85 mm diameter), previously placed on the stage of a spin coater (WS-650Hzb-23NPPB-UD-3, Laurell Technologies). The substrate was then spun at 1000 rpm for 5 seconds. The FSP membranes were dried at room temperature. Then, the FSP membranes were detached and stored until further characterization. For each batch of FSP extracts was produced the respective FSP membranes.

### 3.2.5 Scanning electron microscopy

The analysis of FSP membranes surface in detail was conducted with a scanning electron microscopy (SEM). The FSP membranes were cut into 10 x 10 mm, mounted over a stub and, then, sputter-coated with gold-palladium (108A, Cressington) for 1 minute at 15 mA. The samples were analyzed in a SEM (JSM-6010 LV, Jeol, Japan) and the micrographs obtained at 10 kV with magnifications ranging from 100 to 5000 times.

### 3.2.6 Circular dichroism spectroscopy

Circular dichroism (CD) spectra (185-260 nm) of the FSP extracts and membranes from all batches were recorded on a CD spectrometer (J-1500, JASCO, Tokio, Japan), at ambient temperature. Each FSP extract was dissolved in HFIP at a concentration of 0.1 mg/mL. HFIP was used as control. A quartz cell of 1 mm was used for spectral measurements of FSP solution. FSP membranes were analyzed between two quartz cover slip with 25.4 mm diameter and 0.12 mm thickness. Empty quartz cover slips were used as control. Each spectrum was recorded in far-UV (190-260 nm) and represented as an average of the three consecutive scans measured at 1 nm resolution.

### 3.2.7 FT-IR spectroscopy

To qualitatively evaluate the secondary structure of proteins a Fourier transform infrared (FTIR) analysis was performed. Samples from different batches of FSP extracts and membranes were dried overnight in an exicator. The FSP extracts were mixed with potassium bromide and processed into pellets, whereas the FSP membranes were analyzed directly with the help of a support. Spectra were recorded from 4400 $cm^{-1}$ to 440 $cm^{-1}$, with a resolution of 4 $cm^{-1}$, at 32 scans $^{-1}$ (IR Prestige 21, Shimadzu, Japan). The present spectra are representative of the three FSP batches.

### 3.2.8 Differential scanning calorimetry

The thermal stability and structural integrity of FSP extracts and membranes were studied by differential scanning calorimetry (DSC) (Q100, TA Instruments). Both temperature and heat flux were calibrated with indium at a scanning rate of 10°C/min. An empty pan was used as reference. Nitrogen, at a flow rate of 50 mL/min, was used as carrier gas. Samples of approximately 2.5 mg were weighed and sealed into aluminum pans. Samples were scanned from 0 to 150°C, at a constant heating rate of 2°C/min. DSC scans were performed two times for each sample, named first and second runs, to check the reversibility of the unfolding transition. Each batch, for both FSP extracts and membranes, was run. TA Instruments Universal Analysis software (2000) was used to analyze the experimental data. The residual denaturation enthalpy ($\Delta H$) was calculated using the derivative curve of the heat flow. The starting point of the area under the endothermic peak corresponds to the slope of the heat flow curve when it starts changing; the end point was defined by the local minimum value of the heat flow curve, where the derivative curve again reaches a constant value [37]. Data presented is an average value of the thermal unfolding transition temperatures.

### 3.2.9 Thermogravimetric analysis

The mass loss of FSP extracts and membranes during a linear increase of temperature was performed in a Simultaneous Thermal Analyzer (STA7200, Hitachi). The initial samples weight was about 3 mg. The samples were scanned from 35 to 700°C, at a heating rate of 10°C/min and using crucibles of platinum as a support. Nitrogen was used as the purge gas, at a flow rate of 100 mL/min. The presented data are average values of the three FSP batches.

### 3.2.10 Surface zeta potential

To measure the surface zeta potential of the three batches of FSP membranes, across a range of pH values between 6-8, a electrokinetic analyzer (SurPASS, Anton Paar GmbH, Austria) was used. The FSP membranes were applied in a spit-type channel with 20 mm in length and 10 mm in width, and a variable cell height that was set to approximately 130 μm for all experiments. A 1 mM KCl solution was used as electrolyte, and HCl (0.1 M) and NaOH (0.1 M) solutions were used to adjust the pH. The mean value of these data was present.

### 3.2.11 Water contact angle

The water contact angles (sessile drop method) of FSP membranes were determined at room temperature by goinometer (OCA 15PLUS, DataPhysics). Contact angles were measured in the center and in the extremities, as well as on the top and the bottom sides of FSP membrane. Three independent membranes (each from each FSP batch) were used. 1 μL of ultra-pure water was applied by a controllable syringe at a rate of 3 μL/s at three distinct points of each membrane and the measurement was performed. The images of water spreading over the sample's surface were recorded by a camera and then analyzed by the software supplied by the manufacture. The presented data are average values of those measurements.

### 3.2.12 Tensile tests

To evaluate the mechanical properties of FSP membranes, such as the elastic modulus, the yield strength and the fracture strength, a tensile test was performed. Ten rectangular specimens (30 x 6 mm) were cut with a blade from membranes produced from the three FSP batches. The thickness of each specimen was measured at three distinct points with a micrometer (Mitutoyo, Japan). A universal mechanical testing equipment (Model 5543, INSTRON, UK) with a 1 kN load cell was used. The speed rate was defined at 1 mm/min and a 12 mm gauge length was used in the tensile tests. Tests were conducted at room temperature and humidity. The tests were ended when the specimens fracture. Data were collected by the software Bluehill 2 and the stress-strain curves were drawn. The Young's Modulus was calculated the slope of the linear region of the stress-strain graph, between 0.5% and 1% strain. The yield point was determined by the intersection of a line drawn parallelly to the $yy$ axis with an off-set of 2% strain after the deflection of the linear region. Facture strength was determined when the load decayed immediately to zero. The values reported are the average of at least twenty specimens.

### 3.2.13 Cytocompatibility assays

Human lung fibroblasts (MRC-5 cell line) were grown in Dulbecco's modified eagle's medium (DMEM) supplemented with 10% fetal bovine serum (FBS) and 1% antibiotic/antimycotic solution, at 37°C in an atmosphere of 5% $CO_2$. Before performing the seeding, the cells were detached from the culture flask by using TrypLE Express.

The cytotoxicity of FSP extracts was determined by the extraction test, according to the ISO 10993-5:2009 [38]. The MRC-5 cells were seeded at a density of 5 x $10^4$ cells/well of 24-wells culture plate (Corning Incorporated, USA) and incubated for 24h at 37˚C, in a humidified atmosphere with 5% $CO_2$. FSP extracts at different concentrations (5, 10, 20 mg/mL) were dissolved in DMEM immediately before their addition to the cells in culture. All conditions were performed in triplicate. The culture medium was removed and the same volume (1mL) of FSP suspension was added. The MRC-5 cells in culture were incubated with the different concentrations of FSP extracts for 24h, 48h and 72h, and cells viability determined. The negative control comprises MRC-5 cells just in culture medium.

The cytotoxicity of FSP membranes was determined by the direct contact method, according to the ISO 10993-5:2009 [38]. FSP membranes were cut into 10 x 10 mm specimens sterilized by UV irradiation during 30 minutes in each side and placed into 24-wells culture plate. Tissue culture polystyrene (TCPS) coverslips were used as a negative controls of cells toxicity. A 100 µL cell suspension containing 5 x $10^4$ cells was seeded over FSP membranes and controls. All conditions were performed in triplicate. After 5h the remain culture medium (900 µL) was added to each well. Cells viability was determined after 24h, 48h and 72h of direct contact.

### 3.2.14 Cells metabolic activity

The cells viability was determined by the dehydrogenase activity of MRC-5 cells using the MTS assay (CellTiter 96® $AQ_{ueous}$ One Solution Cell Proliferation Assay, Promega). This calorimetric method contains MTS (3-(4,5-dimethylthiazol-2-yl)-5-(3-carboxymethoxyphenyl)-2-(4-sulfophenyl)-2H-tetrazolium) as tetrazolium compound and PES as electron coupling reagent. After 24, 48 and 72 hours of culture, the medium with FSP extracts or membranes was removed and the MRC-5 cells gently washed twice with sterilize phosphate buffer solution (PBS). Serum-free culture medium without phenol red and MTS reagent was added to each well at a ratio of 5:1. Cells were incubated at 37°C for 3h in a humidified atmosphere contain 5% $CO_2$. After this incubation time,

the absorbance was recorded in triplicate at 490 nm on a microplate reader (SYNERGY HT, BIO-TEK, USA).

### 3.2.15 Cells morphology

At the established times points, the medium was removed and the cells were washed with sterile PBS. The constructs were observed under an inverted microscope (Zeiss). After, a 2.5% glutaraldehyde in PBS solution were added to the samples to fixed cells to the substracts. Then, the samples were dehydrated with graded series of ethanol, ranging from 10 to 100%, and let to dry over night at room temperature. MRC-5 cells submitted to FSP extracts were analyzed by SEM (JSM-6010 LV, Jeol, Japan). The samples were sputter-coated with gold-palladium and the micrographs recorded at 10 kV, at magnifications ranging from 100 to 1000 times.

### 3.2.16 Statistical analysis

Statistical analysis was performed using Graph Pad Prism Software. Differences between the different conditions of the cellular assays were analyzed using non-parametric test (Kruskal-Wallis test for FSP extracts and Man-Whitney test for FSP membranes assays) and a $p<0.01$ was considered significant. Data were presented as mean ± standard deviations.

## 3.3 Results and discussion

### 3.3.1 Isolation of FSP

The FSP from codfish were extracted using fish's own water as solvent. No buffer was used in the extraction process, because it is described that, when sarcoplasmic proteins are subjected to pH shift, they unfolded and exposed the buried thiol groups (SH) [39], which subsequently affect its functional properties. The pH of *Gadus morhua* fillets and pieces was 6.78 ± 0.02, which is in accordance to the literature [37, 40]. The pH of the supernatant was 6.61 ± 0.02. After dialysis, the FSP solution had a pH of 6.78, which is in accordance to Iwata *et. al* (2000) that reported a natural pH of FSP solution around 6.7 [23]. Freeze dried FSP were completely white, without smell, remaining cotton-like.

### 3.3.2 Protein composition of FSP extracts

The protein components of FSP extracts from codfish comprise 11 bands shown in Figure 3.1. The dialysis process contributed to the purification of FSP extracts, as demonstrated by the individualization of the bands without smearing. In general, the band patterns of each FSP extract were alike, suggesting that the extraction method performed from different individuals did not affect the FSP composition.

According to the literature, it can be possible to hypothesized the constituents of proteins that constitute our FSP extracts. Enzymes such as parvalbumins (12 kDa) [11], protease A (15 kDa) [17], protease C (35.6 kDa) [17], aldolase (40 kDa) [14, 41], creatine kinase (43 kDa) [14, 41] and proteinase inhibitors (52 kDa) [16], and proteins such as hemoglobin (65 kDa) [26] are possible to be identified FSP fraction. Other unidentified proteins were also observed with molecular weights around 25, 38, 98, and 110 kDa. FSP from catfish distinctively exhibited molecular weights of 11, 13, 27, 31, 36, 38, 43, 50, 61 and 97 kDa [39]. Nakagawa *et al.* (1988) reported 10 bands from FSP for carp with the molecular weights of 23, 25, 26, 33, 35, 40, 43, 49-51, 60 and 94 kDa [41]. By its side, FSP from pacific mackerel were composed by 11 proteins with molecular weights of 25, 26, 33, 35, 40, 43, 55, 63, 64, 65, and 94 kDa [42]. The different results can be

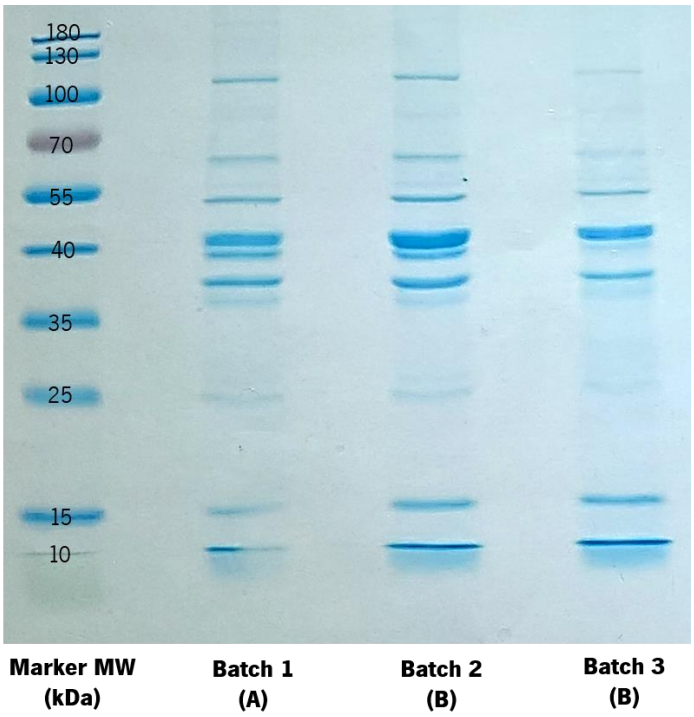


**Figure 3.1 -** SDS-PAGE showing the protein composition of FSP from different batches. (A) codfish 1 and (B) codfish 2.

related with the fishes' species and the isolation methods, once the extraction of FSP using buffers leads to a shift in the pH, and, consequently, to different FSP compositions. Proteins with molecular weights around 35–40 kDa were the most frequent ones, as described by Hemung and Chin (2013) for FSP isolated from red sea bream (*Pargrus major*) [43]. In contrast, proteins with molecular weights of 25, 38, and 94 kDa were present in lower amounts.

Analyzing the bands pattern from each FSP batch, it was possible to observe that between batch 1 (codfish 1) and batch 2 (codfish 2), no significant differences were present. However, in batch 3 (codfish 2) bands corresponding to products with 26, 40, 65 and 110 kDa had lower intensity, corresponding to lower amount of those proteins. This fact could be related with the time that the codfish has been frozen. LeBlanc and LeBlanc (1989) analyzed the changes in sarcoplasmic proteins from frozen stored cod fillets (Gadus morhua) subjected to various storage temperatures and concluded that the frozen storage decreased the sarcoplasmic protein content [45]. The major change observed from the different chromatograms was the loss of high molecular weight proteins, which it is consistent with the bands of 110, 94 and 65 kDa.

### 3.3.3 FSP membranes

Herein, FSP membranes were evaluated as subtracts, being also produced by the spin coating technique. With low volumes of polymeric solution, at concentrations ranging from 0.5 to 1 mL, the FSP membranes showed defects, namely uncoated areas. With a spinning of 1000 rpm, a FSP concentration of 100 mg/mL and a volume of 1.5 mL it was possible to fabricate uniform thin membranes. The membranes were transparent, smelless, without imperfections and easy workable. The average thickness, measured in 30 distinct points of each membrane, was 9.06 ± 1.72 μm.

Spin coating has been used for the production of thin films. Focusing on tissue engineering, these films are biodegradable and used as coatings. Thin films will not only increase bioactivity and biocompatibility, but also protect the surface of biomedical implants against wear and corrosion when implanted into the body. Raphel *et al.* (2016) have been developing elastin-like protein thin films as direct coatings over metallic implants (cp-Ti and Ti6Al4V) for orthopedic and dental applications, because the main failure of these implants is the aseptic loosening of the implant from the surrounding bone tissue [44]. The authors reported that elastin-like protein coatings improve osteoblastic adhesion and mineralization (*in vitro*) and osseointegration and bone formation (*in vivo*). Other example is the study of Mozafari *et al.* (2014) that reported the use of a

coating to cover a bioactive glass-zirconium titate composite [45]. The thin coatings can act as a physical protective barrier to prevent electrolyte access to the metal surface and, thereby, electrochemical process.

### 3.3.4 Morphology of FSP membranes

The SEM micrographs of the FSP membranes showed an uniform surface topography, as expected due to the implemented processing technique (Figure 3.2). No significant morphological differences were observed between the FSP membranes produced from the different batches. This indicates that different batches do not significantly affect the morphology of the developed FSP membranes. Pores were observed on top side of the FSP membranes, with an average diameter of 169.81 ± 73.29 nm (Figure 3.2. A). The pores formation is correlated with the last stage of the membranes production, which is related with the solvent evaporation. In contrast, on the bottom of membrane (Figure 3.2. B), the surface appeared completely smooth. This occurs, because this side of the FSP membrane was in contact with the polystyrene substrate.

### 3.3.5 Secondary structure of FSP extracts and membranes

The secondary structure of FSP extracts dissolved in ultra-pure water and HFIP, as well as of FSP membranes, was examined by CD spectroscopy (Figure 3.3). The native structure of FSP extracts (dissolved in ultra-pure water) had a shape similar to the α-helix conformation: negative bands at approximately 224 and 207 nm, and positive bands at ≈ 190 nm. They were characterized by a high contribution of α-helix conformation (45.63%), followed by a random conformation (27.37%), β-sheets (17%) and β-turns (9.97%). The β-sheets conformation had influence in the shape of the α-helix conformation, since the negative peaks were not well defined.

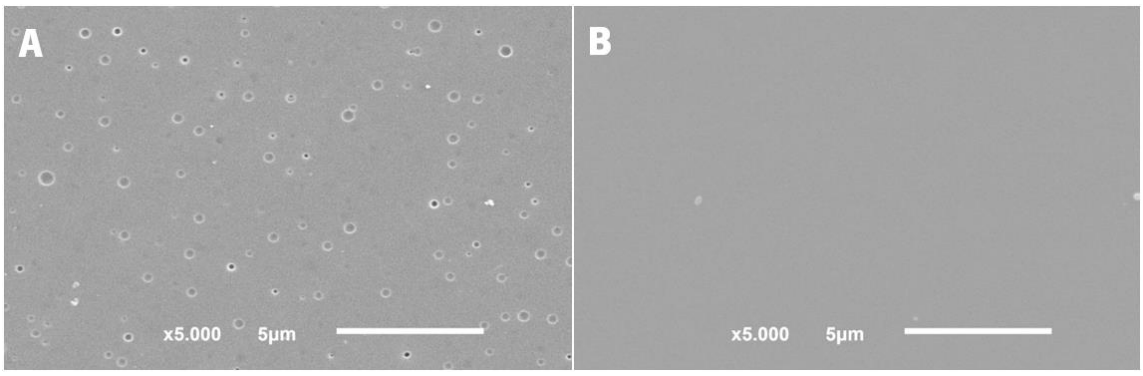


**Figure 3.2 -** SEM micrographs of FSP membrane surface: (A) top and (B) bottom sides.

The dominance of α-helix conformation was in agreement with the results of Villamonte *et al.* (2016) for FSP from hake [46]. The mainly secondary structure of FSP extracts was not altered when they were dissolved in HFIP (53.83% of α-helix conformation, 37.03% of random conformation, and 9.10% of β-turns). The differences observed in the relative intensities of the bands depend mainly on the side chains, which may be related with differences in polarity of the peptide bond environment caused by various side-chain conformations [47].

When FSP extracts dissolved in HFIP were processed into membranes by the spin coating technique, the proteins exhibited a conformational transition, which promoted the formation of 100% α-helix structures. The FSP lost the random coil structure, since in a dried state the polypeptide chain is not able to undergoing the random flight structural fluctuations [47]. In case, the CD spectrum of FSP membranes did not have the characteristic shape of α-helix conformation, which makes impossible the association of the spectrum to any known polypeptide conformation. It became negative, with a deep band between 254 and 231 nm, and a minimum negative at ≈ 241 nm. Fasman *et al.* (1965) also observed a peak at 276 nm in spectrum of L-Tryptophan [48]. The authors explained that the spectrum represented a superposition of the α-helix bands, which must be present and the strong aromatic chromophores bands which are present in the near UV region. Accordingly, herein the difference between peaks can be explained by the use of HFIP as solvent. HFIP has influence on the appearance of molecular structures, which produces the peak shifts, indicating a strong presence of ordered helical contents [49]. On the other hand, HFIP does not destroy the structure of native protein. Thus, the FSP extracts after

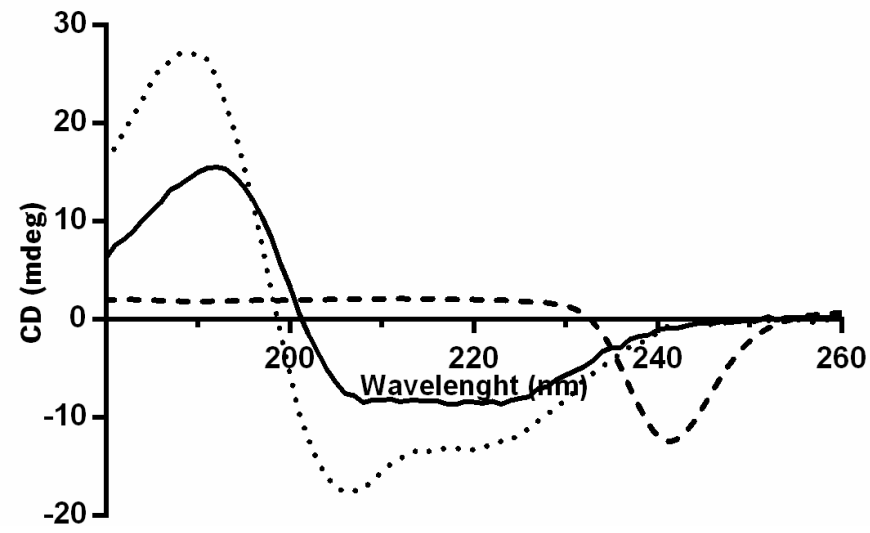


**Figure 3.3 -** Circular dichroism spectrum of FSP extracts dissolved in ultra-pure water (full line) and in HFIP (dotted line), and FSP membranes (dashed line).

being processed change from a α-helix conformation to an unordered structure composed by α-helix components.

FTIR analysis was performed to confirm the secondary structure of FSP extracts and membranes. The amine I spectral region (1600 to 1700 $cm^{-1}$) and the C=O stretching vibration of polypeptide groups can provide information on the secondary structure of proteins [50]. The amide I band of proteins consists of many overlapping component bands that represent α-helix, β-sheet, turns and non-ordered or irregular structures. The β-sheet conformation has a band in the region of 1620-1640 $cm^{-1}$. Anti-parallel β-sheet structure can be identified by the presence of another band near to the region 1670–1695 $cm^{-1}$. α-helix presents an absorption band close to 1656-1658 $cm^{-1}$ [51]. FTIR spectra of FSP extracts and membranes are present in Figure 3.4. As the FSP membranes were analyzed directly, the spectra was more pronounced than the FSP extracts were analyzed according to the KBr method. FSP extracts were found to be in the α-helix conformation, once the IR spectra has a peak at 1655 $cm^{-1}$. The FSP membranes shown the same peak, which indicates that they are also corresponding to the in α-helix structure. Therefore, these FTIR results are in agreement with the previously described CD data.

### 3.3.6 Thermal characterization of FSP extracts and membranes

FSP extracts and membranes were subjected to thermal degradation. Figure 3.5 represents a typical endothermic peak that represents the thermal denaturation of the FSP proteins. All FSP batches shown similar behavior. The FSP extracts thermogram had one defined endothermic

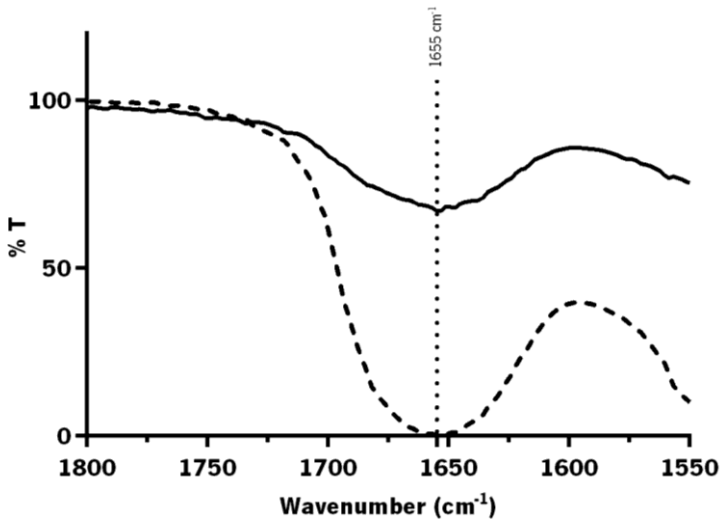


**Figure 3.4 -** FTIR spectra of FSP extracts (full line) and membranes (dashed line

thermal transition at approximately 44.12 ± 2.34 ˚C, corresponding to the denaturation of FSP extracts due to heat. Monterrey-Quintero and Sobral (2000) studied the denaturation of Nile tilapia muscle proteins by DSC and determined that the sarcoplasmic proteins of these fish denatured at 41,1˚C [52]. Other denaturation temperatures of FSP can be found in the literature, varying between 42-45˚C [37, 40]. Any difference between denaturation temperatures can be attributed to various fish species and reported values and the methods of extraction.

When the proteins were processed into membranes, the endothermic peak suffer a shift to 58.88 ± 3.36 ˚C. However, the FSP membranes required less amount of heat to be unfolded. For FSP extracts, the heat absorbed during the experiment was calculated to be 283.93 ± 9.91 J/g. In case of FSP membranes, the heat needed to denatured the proteins was 190.07 ± 13.09 J/g. This shift on denaturation temperatures and heat flow can be related with the solvent (HFIP) used, as well as on the processing technique, which can lead to a stabilization of fish protein. After the first run, the samples were reheated and no peaks were observed during the second scan (data not shown). Therefore, these proteins had an irreversible denaturation. Furthermore, the denaturation temperature of FSP membranes above the body temperature, which demonstrate their potential use on the development of implantable biomedical devices.

The protein stability and decomposition was also analyzed by thermogravimetry, as presented in Figure 3.6. From the TGA thermogram it is possible to observe the sample mass decrement during the heating process. Each batch, for both FSP extracts and membranes, showed similar behavior. The two thermograms corresponded to the classical thermal behavior of freeze-

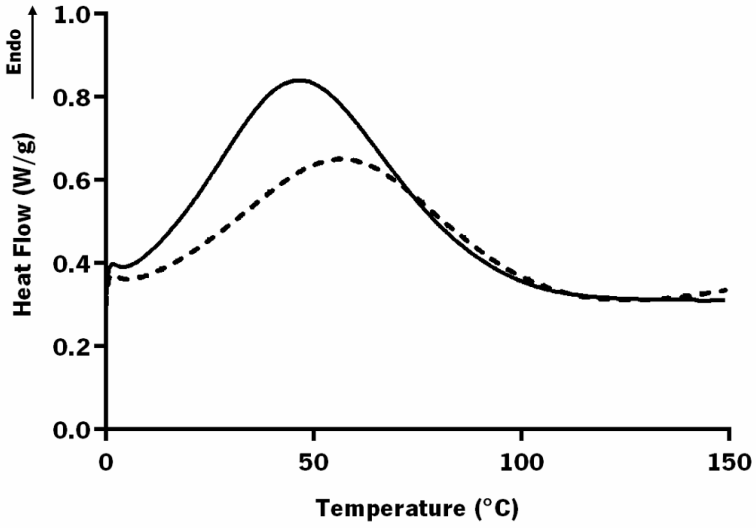


**Figure 3.5 -** DSC thermogram for FSP extracts (full line) and FSP membranes (dashed line).

-dried proteins [53, 54]. For both FSP extracts and membranes, three main stages of weight loss are observed. The first stage (between 39 and 95.7˚C) was related with the evaporation of water absorbed by the FSP extracts and membranes [53, 55], and corresponds to 3.7 and 7% of the total mass for FSPs extracts and membranes, respectively. The second stage (between 175 and 245˚C) was related with the evaporation of the remain structural water bound to proteins from FSP extracts (2.3% of total mass) or membranes (10% of the total mass). The third stage (between 245 and 480˚C) was related with the burn of organic compounds of FSP extracts (65.7% of total mass) or membranes (53.7% of total mass).

The thermal degradation of FSP extracts and membranes consists in two steps, as shown by two maximum temperatures on the DTG curve, at 219˚C and 328˚C. The first maximum temperature is more pronounced for FSP membranes, which means that the FSP extracts were more stable than the FSP membranes. The loss of stability can be related with the increased amount of α-helix content and the loss of β-sheet conformation. At any case, the thermal degradation temperature is not compromise the stability of FSP when used in the development of implantable medical devices

### 3.3.7 Wettability of FSP membranes

Contact angle measurements for the three distinct FSP membranes were performed to determine the surface properties in terms of hydrophobicity or hydrophilicity. The contact angle

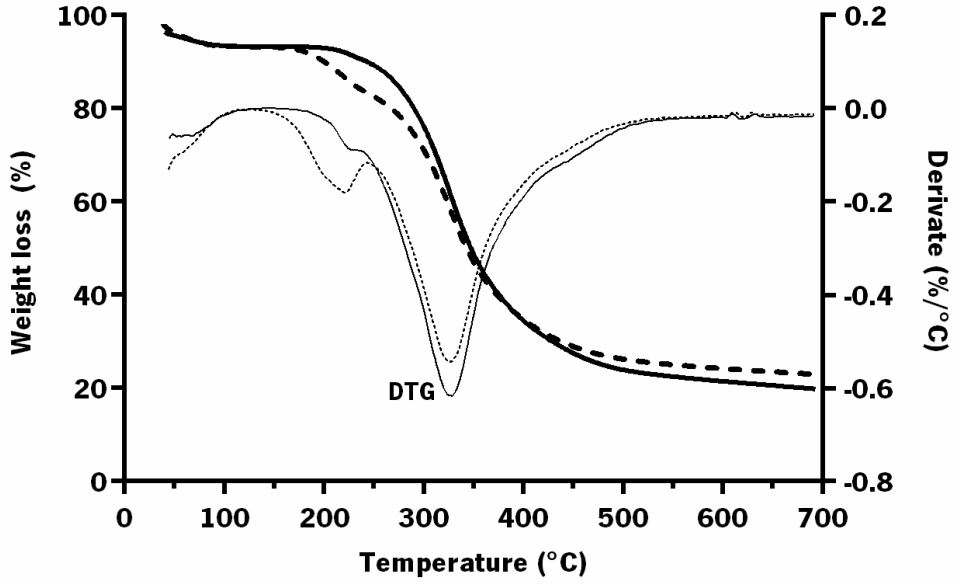


**Figure 3.6 -** TGA thermogram and DTG curves for FSP extracts (full line) and FSP membranes (dashed line).

reflects the first contact of cells with the FSP membranes and, in a further stage, the contact with a body fluid for implantation. The contact angle measurements were performed using ultra-pure water; mean values and corresponding drop snaps are showed in Figure 3.7.

FSP membranes demonstrated a water contact angle of 89.94 ± 13.02˚ on the center of the top side, and 88.11 ± 9.45˚ on the center of the bottom side. In extremity, the water contact angle measurements were 88.43 ± 6.91˚ and 87.33 ± 7.89˚ for the top and the bottom sides, respectively. Measurements were similar for all FSP membranes. There are no significant differences between the top and the bottom sides, as well as between the center and the extremity of different FSP membranes. This results also indicates that the surface properties are uniform throughout the FSP membranes area, which was expected due the processing technique used. As, for all cases, the contact angle is less than 90˚, the FSP membranes are considered hydrophobic. But, it is important to note that they are on the limit of hydrophilicity/hydrophobicity.

### 3.3.8 Surface charge properties of FSP membranes

The electric charge of a biomaterials' surface is considered one of the main physical factors involved in its biological interaction with living systems (cells, tissues) [56]. Figure 3.8 shows mean zeta potential values for FSP membranes immersed in a standard 1 mM KCl solution with pH increasing.

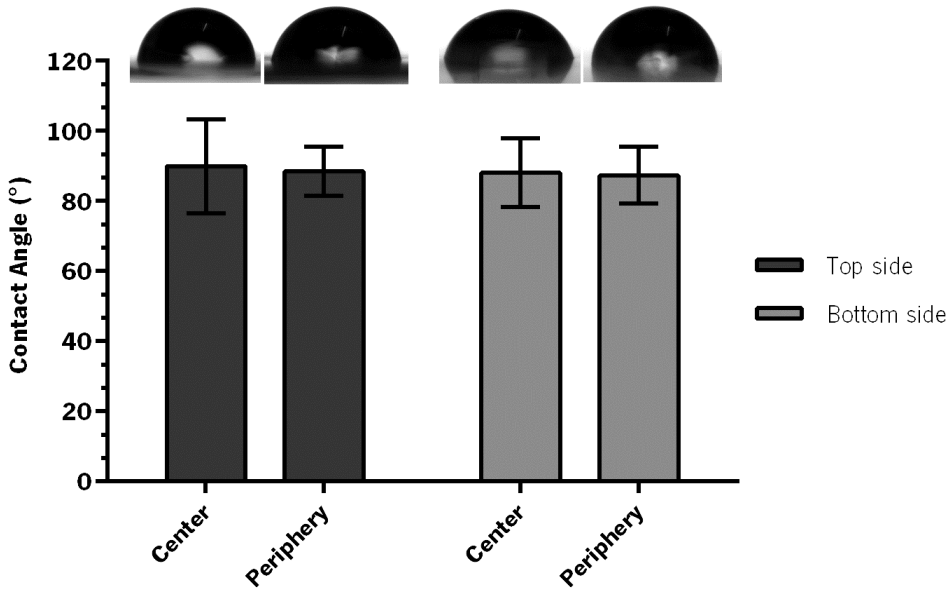


**Figure 3.7 -** Water contact angle values and drop snap of FSP membranes.

All FSP membranes batches showed the same zeta potential/pH curve behavior. The zeta potential of the FSP membranes were negative at pH range between 6 and 8. Often, anion adsorption to hydrophobic surfaces induces them to display a negative zeta potential, because the anions causes the formation of a hydrated shell [57]. FSP membranes are in the limit of the hydrophobicity; therefore the described phenomenon can be also occurring. The surface charge density is almost constant thorough the pH range studied. At pH 7.4 (i.e. physiological conditions) the FSP membranes had a zeta potential of -33.4 mV. Generally, a protein has a characteristic electric charge at physiological conditions. The surface charge properties influence protein adsorption which, by its side, will influence the cell adhesion [56].

### 3.3.9 Mechanical properties

The brittleness of protein films is determined by the strength of protein-protein and protein-water interactions, which can be controlled by the film forming conditions [24]. Three representative stress- strain curves for each batch of FSP membranes are represented in Figure3.9. Initially, the stress varies linearly with the strain, obeying Hooke's law. At higher stresses, this variation becomes non-linear, indicating a shift from elastic to plastic behavior. FSP membranes presented on average yield strength of 23.85 ± 5.97 MPa, an average strain-to-failure of 2.33 ± 0.70%, and an average stiffness of 16.57 ± 3.95± 5.97 MPa, an average strain-to-failure of 2.33 ± 0.70%, and an average stiffness of 16.57 ± 3.95 MPa. The yield strength of FSP membranes was significantly higher than solution-blown FSP/nylon 6 (50:50) fibrous meshes (0.52 MPa) [29],

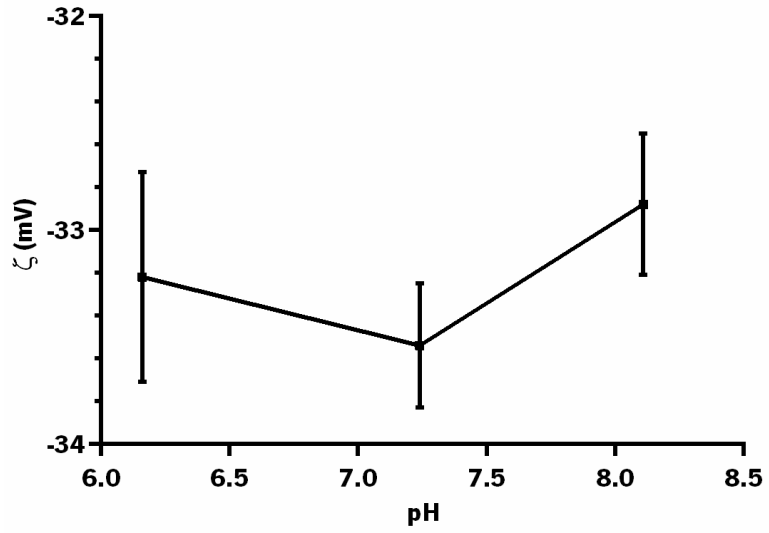


**Figure 3.8 –** Surface zeta potential of FSP membranes, in a electrolyte (KCl) concentration of 1Mm, along increasing pH.

casting films from a FSP solution heated at 70˚C (3-5.5 MPa) [23] and a myofibrillar protein film (17 MPa) [58]. However, FSP membranes had much lower elongation value than the previous films, 14.6, 40-75, and 23%, respectively. This suggests that FSP membranes are more mechanically resistant and less stretchable than other protein films reported in the literature.

### 3.3.10 Cytotoxicity of FSP extracts

The cytocompatibility of FSP extracts, at concentrations ranging from 5 to 20 mg/mL was investigated with human lung fibroblasts (MRC-5 cell line). Figure 3.10 shows fibroblasts metabolic activity when exposed to FSP extracts. For concentrations lower than 10 mg/mL, no cytotoxicity was observed over 72h of culture. Cytotoxicity was present at 20 mg/mL.

The morphology of fibroblasts cultured with the FSP extracts was analyzed by SEM (Figure 3.11). For concentrations lower than 10 mg/mL (Figure 3.11 A-C), SEM micrographs showed high amount of MRC-5 cells, with the typical elongated morphology pronounced philopodium. For high concentrations (Figure 3.11 DF), low number of MRC-5 cells were attached to the subtract and their morphology become more rounded.

### 3.3.11 Cytotoxicity of FSP membranes

The cytocompatibility of FSP membranes was also investigated with human lung fibroblasts (MRC-5) cell line. Figure 3.12 shows the metabolic activity of MRC-5 cells when directly cultured over TCPS and FSP membranes. After 24h of culture, less cells are attached and metabolically

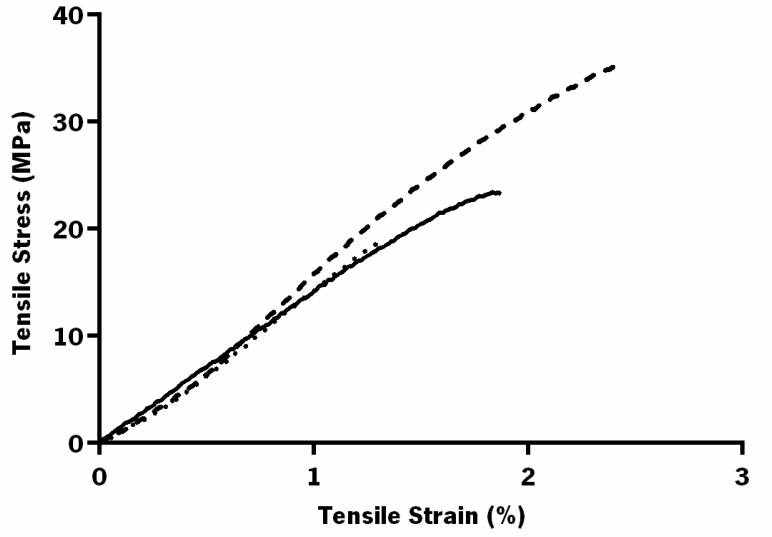


**Figure 3.9 –** Representative stress-strain curves of FSP membranes from batch 1 (full line), 2 (dashed line), and 3 (dotted line) (n=29).

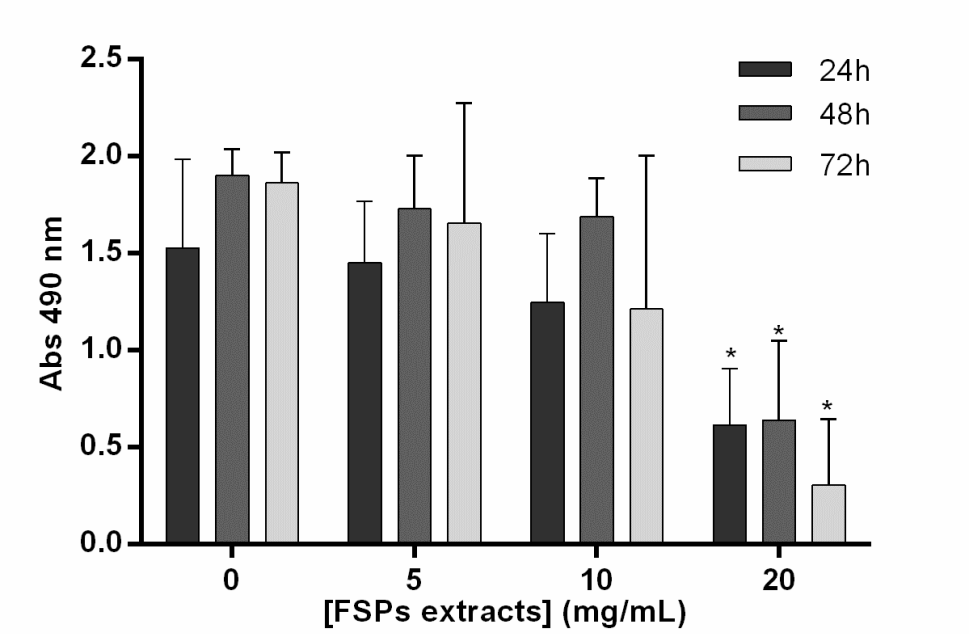


**Figure 3.10 –** Metabolic activity of human lung fibroblasts (MRC-5 cell line), when exposed to FSP extracts. * denotes significant difference compared with the control (0 mg/mL) ($n$=3).

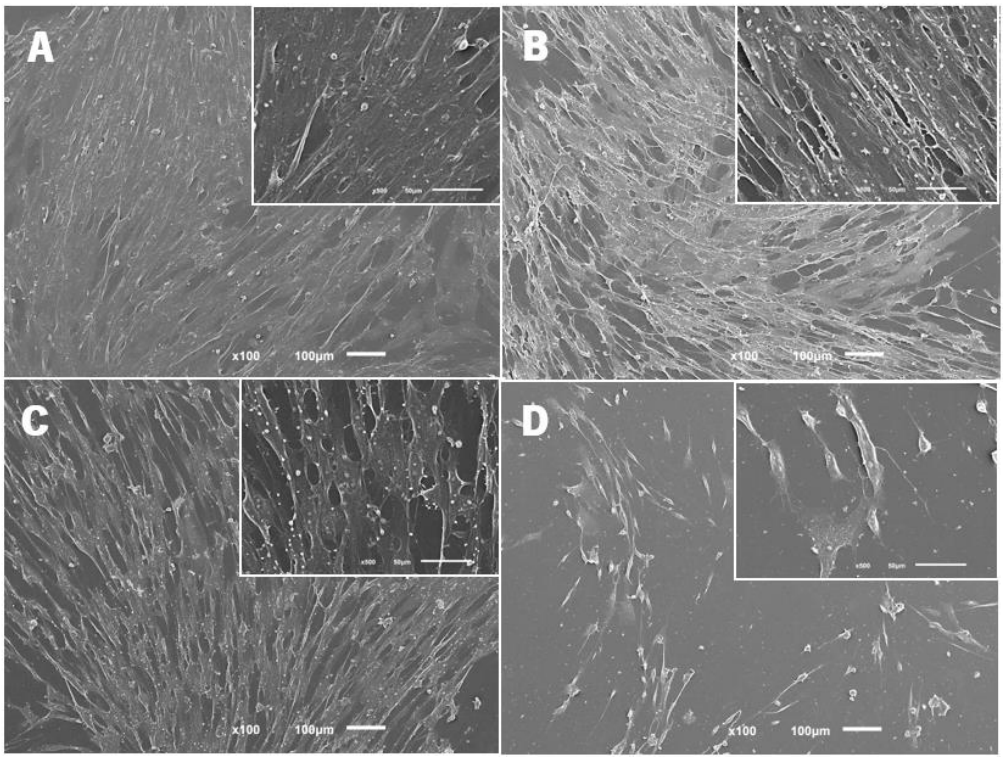


**Figure 3.11 –** SEM micrographs of human lung fibroblasts (MRC-5 cell line) after 48h of culture in the presence of FSP extracts at concentrations: A – 0 mg/mL; B – 5 mg/mL; C – 10 mg/mL; D – 20 mg/mL.

active in the FSP membranes. The fibroblasts present their typical elongated morphology and philopodium, as shown in Figure 3.13. After 48h of culture, the MRC-5 cells have similar metabolic activity as the control, and their morphology remains the same (Figure 3.13). After 72h of culture, the MRC-5 cells shown an elongated morphology when in contact with the FSP membranes. The metabolic activity of fibroblasts decreased drastically. It can be related with the loss of integrity of the membrane, because no crosslinking of FSP membranes was performed.

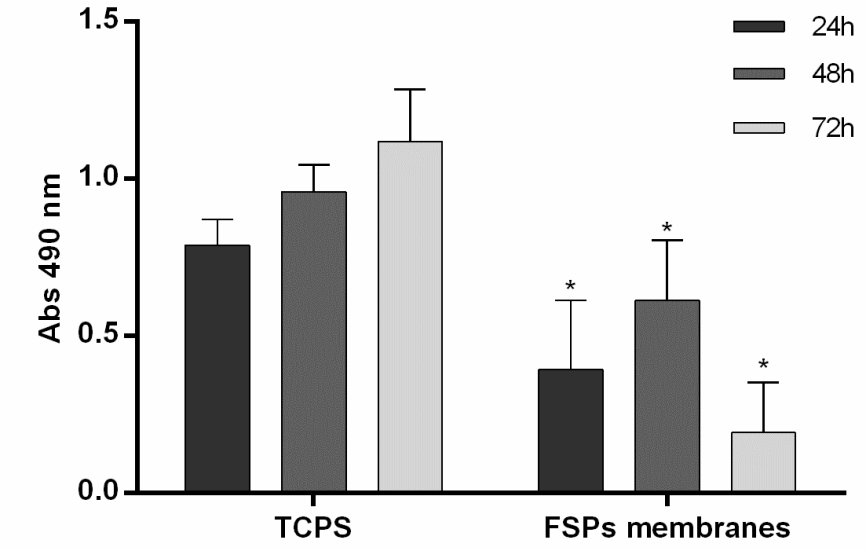


**Figure 3.12 –** Metabolic activity of human lung fibroblasts (MRC-5 cell line) when directly cultured over TCPS and FSP membranes. * denotes significant difference compared with the control (TCPS) (n=3).

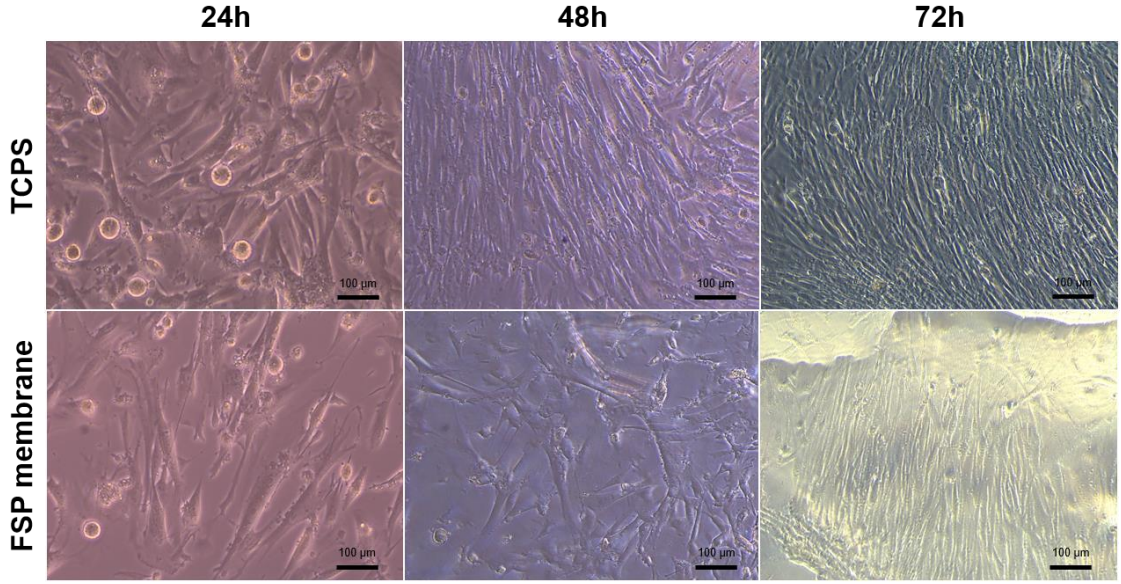


**Figure 3.13 –** Optical images of human lung fibroblasts (MRC-5 cell line) cultured directly over TCPS and FSP membranes during 72h.

## 3.4 Conclusion

FSP were successfully isolated by centrifugation from *Gadus morhua*, a method that did not change their conformation. Different batches, from different individuals, provided similar protein compositions. From the CD spectra was possible to conclude that the secondary structure of FSP extracts was mainly composed by α-helix conformation, as validated by FTIR, but also by random conformation, β-sheet and β-turn. From the DSC thermograms it was possible to determine that FSP extracts were denatured at 44.12 ± 2.34˚C. Viability assays demonstrated that FSP extracts were no cytotoxic for concentration lower than 10 mg/mL, over 72h of culture.

FSP membranes were produced and the surface is smooth throughout the analyzed area, with pores in the submicron range on the top side. The membranes were hydrophobic, with a surface zeta potential of -33.4 mV at physiological pH. FSP membranes had a yield strength of 23.85 MPa, higher than the FSP casting films and the myofibrillar protein films described in the literature. According to the CD spectra, the FSP membranes exhibited a conformation transition to a 100% α-helix structure. The FSP membranes were more stable than FSP extracts, since the thermal denaturation rised to 58.88˚C. Human lung fibroblasts attached to FSP membranes surface exhibit their typical spindle shape. FSP membranes lost their integrity after 72h, as we expected.

Based on these results, FSP can be considered a potential biomaterial recovered from the waste water of fish in applications where the short duration in contact with cells will be an added value.

## 3.5 References

[1] FAO, The State of World Fisheries and Aquaculture. Contributing to food security and nutrition for all, Rome, 2016.

[2] H.O. Bang, J. Dyerberg, A. Nielsen, Plasma lipid and lipoprotein pattern in Greenlandic Wesy-Cast eskimos, The Lancet 297(7710) (1971) 1143-1146.

[3] A.D. Pradhan, J.E. Manson, N. Rifai, J.E. Buring, P.M. Ridker, C-reactive protein, interleukin 6, and risk of developing type 2 diabetes mellitus, Jama-Journal of the American Medical Association 286(3) (2001) 327-334.

[4] V. Ouellet, J. Marois, S.J. Weisnagel, H. Jacques, Dietary cod protein improves insulin sensitivity in insulin-resistant men and women, Diabetes Care 30(11) (2007) 2816-2821.

[5] V. Ouellet, S.J. Weisnagel, J. Marois, J. Bergeron, P. Julien, R. Gougeon, A. Tchernof, B.J. Holub, H. Jacques, Dietary Cod Protein Reduces Plasma C-Reactive Protein in Insulin-Resistant Men and Women, Journal of Nutrition 138(12) (2008) 2386-2391.

[6] H. Maeda, R. Hosomi, M. Koizumi, Y. Toda, M. Mitsui, K. Fukunaga, Dietary cod protein decreases triacylglycerol accumulation and fatty acid desaturase indices in the liver of obese type-2 diabetic KK-Ay mice, Journal of Functional Foods 14 (2015) 87-94.
[7] D. Ait-Yahia, S. Madani, J.-L. Savelli, J. Prost, M. Bouchenak, J. Belleville, Dietary fish protein lowers blood pressure and alters tissue polyunsaturated fatty acid composition in spontaneously hypertensive rats, Nutrition 19(4) (2003) 342-346.
[8] A. Shukla, A. Bettzieche, F. Hirche, C. Brandsch, G.I. Stangl, K. Eder, Dietary fish protein alters blood lipid concentrations and hepatic genes involved in cholesterol homeostasis in the rat model, British Journal of Nutrition 96(4) (2006) 674-682.
[9] X. Zhang, A.C. Beynen, Influence of dietary fish proteins on plasma and liver cholesterol concentrations in rats, British Journal of Nutrition 69(3) (1993) 767-777.
[10] I.-J. Jensen, M. Walquist, B. Liaset, E.O. Elvevoll, K.-E. Eilertsen, Dietary intake of cod and scallop reduces atherosclerotic burden in female apolipoprotein E-deficient mice fed a Western-type high fat diet for 13 weeks, Nutrition & Metabolism 13(1) (2016) 8.
[11] V. Venugopal, F. Shahidi, Structure and composition of fish muscle, Food Reviews International 12(2) (1996) 175-197.
[12] A. Asghar, K. Samejima, T. Yasui, R.L. Henrickson, Functionality of muscle proteins in gelation mechanisms of structured meat products, C R C Critical Reviews in Food Science and Nutrition 22(1) (1985) 27-106.
[13] J. Yongsawatdigul, P. Carvajal, T. Lanier, Surimi Gelation Chemistry, Surimi and Surimi Seafood, Second Edition, CRC Press2005, pp. 435-489.
[14] T. Nakagawa, S. Watabe, K. Hashimoto, Identification of Three Major Components in Fish Sarcoplasmic Proteins, Nippon Suisan Gakkaishi 54(6) (1988) 999-1004.
[15] M. Toyohara, M. Murata, M. Ando, S. Kubota, M. Sakaguchi, H. Toyohara, Texture Changes Associated with Insolubilization of Sarcoplasmic Proteins During Salt-vinegar Curing of Fish, Journal of Food Science 64(5) (1999) 804-807.
[16] S. Siriangkanakun, E.C.Y. Li-Chan, J. Yongsawadigul, Identification and characterization of alpha-I-proteinase inhibitor from common carp sarcoplasmic proteins, Food Chemistry 192 (2016) 1090-1097.
[17] S.T. Jiang, C.Y. Tsao, Y.T. Wang, C.S. Chen, Purification and characterization of proteases from milkfish muscle (*Chanos chanos*), Journal of Agricultural and Food Chemistry 38(7) (1990) 1458-1463.
[18] M.A. Audley, K.J. Shetty, J.E. Kinsella, Isolation and properties of phospholipase a from Pollock muscle, Journal of Food Science 43(6) (1978) 1771-1775.
[19] R.H. Ilgner, A.E. Woods, Purification, physical properties and kinetics of peroxidases from freshwater crayfish (genus Orconectes), Comparative Biochemistry and Physiology Part B: Comparative Biochemistry 82(3) (1985) 433-440.
[20] H. Kishi, H. Nozawa, N. Seki, Reactivity of Muscle Transglutaminase on Carp Myofibrils and Myosin B, Nippon Suisan Gakkaishi 57(6) (1991) 1203-1210.
[21] M. Pazos, L. Méndez, J.M. Gallardo, S.P. Aubourg, Selective-Targeted Effect of High-Pressure Processing on Proteins Related to Quality: a Proteomics Evidence in Atlantic Mackerel (Scomber scombrus), Food and Bioprocess Technology 7(8) (2014) 2342-2353.
[22] N.F. Haard, B.K. Simpson, B.S. Pan, Sarcoplasmic Proteins and Other Nitrogenous Compounds, in: Z.E. Sikorski, B.S. Pan, F. Shahidi (Eds.), Seafood Proteins, Springer US, Boston, MA, 1995, pp. 13-39.
[23] K.I. Iwata, S.H. Ishizaki, A.K. Handa, M.U. Tanaka, Preparation and characterization of edible films from fish water-soluble proteins, Fisheries Science 66(2) (2000) 372-378.

[24] M. Tanaka, K. Iwata, R. Sanguandeekul, A. Handa, S. Ishizaki, Influence of plasticizers on the properties of edible films prepared from fish water-soluble proteins, Fisheries Science 67(2) (2001) 346-351.
[25] T.M. Paschoalick, F.T. Garcia, P.J.A. Sobral, A.M.Q.B. Habitante, Characterization of some functional properties of edible films based on muscle proteins of Nile Tilapia, Food Hydrocolloids 17(4) (2003) 419-427.
[26] P.J.d.A. Sobral, J.S. Santos, F.T. García, Effect of protein and plasticizer concentrations in film forming solutions on physical properties of edible films based on muscle proteins of a Thai Tilapia, Journal of Food Engineering 70(1) (2005) 93-100.
[27] P.J.d.A. Sobral, F.T. García, A.M.Q.B. Habitante, E.S. Monterrey-Quintero, Propriedades de filmes comestíveis produzidos com diferentes concentrações de plastificantes e de proteínas do músculo de tilápia-do-nilo, Pesquisa Agropecuária Brasileira 39 (2004) 255-262.
[28] F.T. García, P.J.d.A. Sobral, Effect of the thermal treatment of the filmogenic solution on the mechanical properties, color and opacity of films based on muscle proteins of two varieties of Tilapia, LWT - Food Science and Technology 38(3) (2005) 289-296.
[29] S. Sett, K. Stephansen, A.L. Yarin, Solution-blown nanofiber mats from fish sarcoplasmic protein, Polymer 93 (2016) 78-87.
[30] K. Stephansen, I.S. Chronakis, F. Jessen, Bioactive electrospun fish sarcoplasmic proteins as a drug delivery system, Colloids and Surfaces B: Biointerfaces 122 (2014) 158-165.
[31] K. Stephansen, M. García-Díaz, F. Jessen, I.S. Chronakis, H.M. Nielsen, Bioactive protein-based nanofibers interact with intestinal biological components resulting in transepithelial permeation of a therapeutic protein, International Journal of Pharmaceutics 495(1) (2015) 58-66.
[32] K. Stephansen, M. Mattebjerg, J. Wattjes, A. Milisavljevic, F. Jessen, K. Qvortrup, F.M. Goycoolea, I.S. Chronakis, Design and characterization of self-assembled fish sarcoplasmic protein–alginate nanocomplexes, International Journal of Biological Macromolecules 76 (2015) 146-152.
[33] G.M. Pigott, Surimi: The “high tech” raw materials from minced fish flesh, Food Reviews International 2(2) (1986) 213-246.
[34] G.M. Hall, N.H. Ahmad, Surimi and fish-mince products, in: G.M. Hall (Ed.), Fish Processing Technology, Springer US, Boston, MA, 1997, pp. 74-92.
[35] E. Okazaki, A study on the recovery and utilization of sarcoplasmic protein of fish meat discharged during the leaching process of surimi processing, Bulletin of the National Research Institute of Fisheries Science 0(6) (1994) 79-160.
[36] T.C. Lanier, Functional Food Protein Ingredients from Fish, in: Z.E. Sikorski, B.S. Pan, F. Shahidi (Eds.), Seafood Proteins, Springer US, Boston, MA, 1995, pp. 127-159.
[37] D. Skipnes, I. Van der Plancken, A. Van Loey, M.E. Hendrickx, Kinetics of heat denaturation of proteins from farmed Atlantic cod (Gadus morhua), Journal of Food Engineering 85(1) (2008) 51-58.
[38] W. Li, J. Zhou, Y. Xu, Study of the in vitro cytotoxicity testing of medical devices, Biomedical Reports 3(5) (2015) 617-620.
[39] P. Tadpitchayangkoon, J.W. Park, J. Yongsawatdigul, Conformational changes and dynamic rheological properties of fish sarcoplasmic proteins treated at various pHs, Food Chemistry 121(4) (2010) 1046-1052.
[40] K.A. Thorarinsdottir, S. Arason, M. Geirsdottir, S.G. Bogason, K. Kristbergsson, Changes in myofibrillar proteins during processing of salted cod (*Gadus morhua*) as determined by

electrophoresis and differential scanning calorimetry, Food Chemistry 77(3) (2002) 377-385.
[41] T. Nakagawa, S. Watabe, K. Hashimoto, Electrophoretic Analysis of Sarcoplasmic Proteins from Fish Muscle on Polyacrylamide Gels, Nippon Suisan Gakkaishi 54(6) (1988) 993-998.
[42] K. Morioka, T. Nishimura, A. Obatake, Y. Shimizu, Relationship between the Myofibrillar Protein Gel Strengthening Effect and the Composition of Sarcoplasmic Proteins from Pacific mackerel, Fisheries science 63(1) (1997) 111-114.
[43] B.-O. Hemung, K.B. Chin, Effects of fish sarcoplasmic proteins on the properties of myofibrillar protein gels mediated by microbial transglutaminase, LWT - Food Science and Technology 53(1) (2013) 184-190.
[44] J. Raphel, J. Karlsson, S. Galli, A. Wennerberg, C. Lindsay, M.G. Haugh, J. Pajarinen, S.B. Goodman, R. Jimbo, M. Andersson, S.C. Heilshorn, Engineered protein coatings to improve the osseointegration of dental and orthopaedic implants, Biomaterials 83 (2016) 269-282.
[45] M. Mozafari, E. Salahinejad, S. Sharifi-Asl, D.D. Macdonald, D. Vashaee, L. Tayebi, Innovative surface modification of orthopaedic implants with positive effects on wettability and in vitro anti-corrosion performance, Surface Engineering 30(9) (2014) 688-692.
[46] G. Villamonte, L. Pottier, M. de Lamballerie, Influence of high-pressure processing on the physicochemical and the emulsifying properties of sarcoplasmic proteins from hake (Merluccius merluccius), European Food Research and Technology 242(5) (2016) 667-675.
[47] L. Stevens, R. Townend, S.N. Timasheff, G.D. Fasman, J. Potter, The circular dichroism of polypeptide films, Biochemistry 7(10) (1968) 3717-3720.
[48] G.D. Fasman, M. Landsberg, M. Buchwald, Conformational studies on synthetic poly-α-amino acids: the helical sense of poly-l-tryptophan: optical rotatory dispersion studies, Canadian Journal of Chemistry 43(5) (1965) 1588-1598.
[49] S.W. Ha, T. Asakura, R. Kishore, Distinctive influence of two hexafluoro solvents on the structural stabilization of Bombyx mori silk fibroin protein and its derived peptides: C-13 NMR and CD studies, Biomacromolecules 7(1) (2006) 18-23.
[50] P.I. Haris, F. Severcan, FTIR spectroscopic characterization of protein structure in aqueous and non-aqueous media, Journal of Molecular Catalysis B: Enzymatic 7(1–4) (1999) 207-221.
[51] V. Cabiaux, R. Brasseur, R. Wattiez, P. Falmagne, J.M. Ruysschaert, E. Goormaghtigh, Secondary Structure of Diphtheria Toxin and Its Fragments Interacting with Acidic Liposomes Studied by Polarized Infrared Spectroscopy, Journal of Biological Chemistry 264(9) (1989) 4928-4938.
[52] E.S. Monterrey-Quintero, P.J.d.A. Sobral, Preparo e caracterização de proteínas miofibrilares de tilápia-do-nilo para elaboração de biofilmes, Pesquisa Agropecuária Brasileira 35(1) (2000) 179-189.
[53] A. Sionkowska, J. Skopinska-Wisniewska, M. Gawron, J. Kozlowska, A. Planecka, Chemical and thermal cross-linking of collagen and elastin hydrolysates, International Journal of Biological Macromolecules 47(4) (2010) 570-577.
[54] S.Y. Cho, Y.S. Yun, S. Lee, D. Jang, K.-Y. Park, J.K. Kim, B.H. Kim, K. Kang, D.L. Kaplan, H.-J. Jin, Carbonization of a stable β-sheet-rich silk protein into a pseudographitic pyroprotein, Nature Communications 6 (2015) 7145.
[55] J. Dandurand, V. Samouillan, M.H. Lacoste-Ferre, C. Lacabanne, B.Bochicchio, A. Pepe, Conformational and thermal characterization of a synthetic peptidic fragment inspired from human tropoelastin: Signature of the amyloid fibers, Pathologie Biologie 62(2) (2014) 100-107.

[56] K. Cai, M. Frant, J. Bossert, G. Hildebrand, K. Liefeith, K.D. Jandt, Surface functionalized titanium thin films: Zeta-potential, protein adsorption and cell proliferation, Colloids and Surfaces B: Biointerfaces 50(1) (2006) 1-8.

[57] H. Xie, T. Saito, M.A. Hickner, Zeta Potential of Ion-Conductive Membranes by Streaming Current Measurements, Langmuir 27(8) (2011) 4721-4727.

[58] B. Cuq, C. Aymard, J.-L. Cuq, S. Guilbert, Edible Packaging Films Based on Fish Myofibrillar Proteins: Formulation and Functional Properties, Journal of Food Science 60(6) (1995) 1369-1374.

# CHAPTER 4

General conclusions and future perspectives

## 4.1 General conclusions

FSP were successfully isolated by centrifugation from *Gadus morhua*, a method that did not change their conformation. Different batches, from different individuals, provided similar protein compositions. From the CD spectrum it was possible to conclude that the secondary structure of FSP extracts was mainly composed by α-helix conformation, as validated by FTIR, but also by random conformation, β-sheet and β-turn. From the DSC thermograms it was possible to determine that FSP extracts were denatured at 44.12 ± 2.34˚C. No cytotoxicity was observed for concentration lower than 10 mg/mL over 72h of culture.

FSP membranes were produced and the surfaces are smooth, with some pores in the submicron range on the top side. The membranes were hydrophobic, with a surface zeta potential of -33.4 mV at physiological pH. FSP membranes had a yield strength of 23.85, higher than the FSP casting films and the myofibrillar protein films described in the literature. According to the CD spectrum, the FSP exhibited a conformation transition to 100% α-helix structure. FTIR spectrum also proved the presence of α-helix structure. The FSP membranes were more stable than FSP extracts, since the thermal denaturation rised to 58.88˚C. However, for high temperatures the FSP membranes became more unstable from 160 to 280˚C. This results were favorable, the denaturation temperature of FSP membranes above the body temperature, which demonstrate their potential use on the development of implantable biomedical devices. No cytotoxicity was observed for FSP membranes for 48h of culture. The human lung fibroblasts (MRC-5 cell line) attached to FSP membranes surface exhibiting their typical spindle shape. FSP membranes lost their integrity after 72h, as we expected. Based on these results, FSP can be considered a potential biomaterial recovered from the waste water of fish in the development of biomedical devices, where a short term stability and being composed for pool of enzymes are partially suited.

## 4.2 Future perspetives

FSP membranes lost their stability after 72h of culture, since no crosslinker was used. With this purpose, we suggest the application in the wound healing. An encapsulation of a drug in the FSP membranes can be performed for the use as a transdermic delivery system (patches) for dermatologic disorders, such as acne, urticarial, dermatitis, or insect venom hypersensitivity. The FSP membranes will release the drug for 24-48h, as the membranes lose their integrity, degrading.